Development of heterogenized catalyst systems for the synthesis of acrylic acid derivatives from carbon dioxide and ethylene

Von der Fakultät Energie-, Verfahrens- und Biotechnik der Universität Stuttgart
zur Erlangung der Würde eines
Doktors der Ingenieurwissenschaften (Dr.-Ing.) genehmigte Abhandlung

Vorgelegt von

Dipl.-Ing. Eko Prasetyo

aus Malang, Indonesia

Hauptberichter:	Prof. Dr.-Ing. Elias Klemm
Mitberichter :	Prof. Dr.-Ing. Ulrich Nieken
Tag der mündlichen Prüfung:	20. April 2015

Institut für Technische Chemie der Universität Stuttgart

2015

Abstract

Use of CO_2 as chemical feedstock represents one of the most sustainable ways for carbon recycling, generating high value products. Current industrial practices include the manufacture of urea, organic (poly)carbonates, and salicylic acid. CO_2 can also be used to produce CO-rich syngas, which can be further processed to olefins, aldehydes, alcohols, or synthetic fuel via the Fischer-Tropsch process.

Direct carboxylation with CO_2 yielding carbonates, carbamates, carboxylates, or lactones is of great importance from the industrial point of view. The route has a high atom efficiency and avoids a complex process with significant amounts of waste, which is common in multi-step conventional processes [1]. The synthesis of sodium acrylate from ethylene and CO_2 represents one of the most attractive carboxylations. Contrary to the current acrylate production process via propene oxidation, the process utilizing ethylene and CO_2 discussed in this work utilizes the cheap and abundantly available CO_2 as C_1 building block.

Current state of the art of sodium acrylate catalytic reaction from ethylene and CO_2 utilizes a molecular nickel complex to form a nickelalactone intermediate and a non-nucleophilic base to cleave nickelalactone, yielding sodium acrylate product. This reaction requires a complex process, with separate nickelalactone formation and cleavage with subsequent sophisticated product separation and base recycling processes. In addition, the alkoxide base may form inactive semicarbonate with CO_2 as well as form conjugate acid which deactivates the nickel complex catalyst. In this work, three different metal catalyst - base combinations are proposed to overcome these limitations.

A combination of molecular nickel complex with CO_2-stable tertiary amine - NaH base system allows the one-pot process reaction with all reactants present during catalytic reaction. The tertiary amine is not

consumed during the catalytic reaction and does not react with the metal complex. Some examples include the combination of triethylamine, phosphazene base, 1,8-diazabicyclo[5.4.0]undec-7-ene (DBU) with NaH, LiH, or KH. The application of hydrophobic tertiary amine simplifies the base recycling step further. Trioctylamine, *N,N*-dimethylaniline, and *N,N*-diethylaniline combined with NaH have been identified as highly effective hydrophobic amine base suitable for this process. Turn Over Number (TON) of up to 16.91 (Turn Over Frequency (TOF) $6.52 \cdot 10^{-5}$ s^{-1}) was achieved with molecular nickel complex as catayst and trioctylamine-NaH base combination.

The second system utilizes a combination of immobilized nickel complex with amine-NaH base system. The immobilized complex was prepared via anchoring of the 1,2-bis(dicyclohexylphosphino)ethane (dcpe) ligand on functionalized silica and polystyrene support. Catalysts with metal complex loading as high as 0.1566 mmol/g and 0.134 mmol/g with silica gel and polystyrene support respectively have been successfully synthesized. MAS NMR investigations also confirmed the presence of covalently anchored active dcpe ligand. The catalytic test of the immobilized metal complex with triethylamine-NaH base system delivered a TON of up to 1.42 (Turn Over Frequency (TOF) $5.48 \cdot 10^{-6}$ s^{-1}), confirming the catalytic nature of the heterogeneously catalyzed reaction. The application of immobilized ligand catalyst system would allow a continuous one-pot process. The process can be designed so that the catalyst remains in the reactor during the whole catalytic reaction, thus minimizing the contact with oxidant or other impurities and improving its lifetime.

The third system employs a combination of a molecular nickel complex with an immobilized base. Four different commercially available immobilized bases of the alkoxide and tertiary amine types have been

identified as effective in the one-pot sodium acrylate reaction. Furthermore, two CO_2-atmosphere tolerant immobilized bases were prepared via direct anchoring on polystyrene support and via copolymerization reaction. A high TON of up to 30.94 (TOF $4.30 \cdot 10^{-4}$ s^{-1}) could be achieved with the combination of (dcpe)-nickelalactone catalyst and immobilized sodium 2-fluorophenolate. In addition, successful recycling experiments of the immobilized base confirmed the versatility and suitability of the immobilized base for the catalytic reaction. A continuous process with two steps-filtration to recycle the immobilized base and isolate the sodium acrylate product is proposed as the most promising concept for an industrial application.

Zusammenfassung

Die Nutzung von CO_2 als chemischer Rohstoff ist eine der nachhaltigsten Wege zur Kohlenstoffwiederverwertung. Dadurch werden Produkte mit hoher Wertschöpfung zugänglich. Die aktuellen industriellen Prozesse sind z. B. die Herstellung von Harnstoff, organische (Poly)Carbonate und Salicylsäure. Des Weiteren kann CO_2 auch in CO-reiches Synthesegas verwandelt werden, das zu Olefinen, Aldehyden, Alkoholen oder synthetischen Kraftstoff (Fischer-Tropsch) verarbeitet werden kann.
Außerdem, direkte Carboxylierung mit CO_2 zu Carbonate, Carbamate, Carbonsäureester oder Lactone ist für die industrielle Anwendung sehr interessant. Die Reaktion hat eine hohe Atomeffizienz, der Prozess wird einfacher, effizienter und es entstehen weniger Abfälle [1]. Die Synthese von Natriumacrylat aus Ethylen und CO_2 ist eine der attraktivsten Carboxylierungsreaktionen. Derzeit wird Natriumacrylat in einer zweistufigen Reaktion aus Propen hergestellt. Der potenzielle Neuprozess unter Verwendung von Ethylen und CO_2 nutzt das billige, in großen Mengen verfügbaren C1-Kohlenstoffquelle, CO_2.
Aktueller Stand der Technik von der katalytischen Reaktion von Natriumacrylat aus Ethylen und CO_2 verwendet ein Nickelkomplex, das ein Nickelalacton-Intermediat bildet, und eine nicht-nukleophile Base, die das Nickelalacton spaltet. Die Reaktion ist sehr komplex, mit einer separaten Bildung und Spaltung von Nickelalacton mit anschließender anspruchsvoller Produkttrennung und Wiederverwertung von Base. Dabei kann die Alkoxide (Base) ein inaktives Semicarbonat und konjugierte Säure bildet, die der Nickelkomplex-Katalysator deaktivieren. In dieser Arbeit werden drei verschiedene Kombinationen von dem Katalysator und der Base untersucht, um die Limitierungen zu überwinden
Eine Kombination von homogenem Nickelkomplex mit CO_2-stabilem

tertiärem Amin – NaH Basesystem ermöglicht den Eintopf-Prozess mit allen Reaktanten anwesend während der katalytischen Reaktion. Während der katalytischen Reaktion wird das tertiäre Amin weder verbraucht noch mit dem Metallkomplex reagiert. Einige Beispiele für Basesystemen sind jede Kombination aus Triethylamin, Phosphazen, 1,8-diazabicyclo[5.4.0]undec-7-ene (DBU) mit NaH, LiH oder KH. Außerdem, der Einsatz von hydrophobem tertiärem Amin vereinfacht die Wiederverwertung von Base. Die Kombinationen aus Trioctylamin, *N,N*-dimethylanilin oder *N,N*-diethylanilin mit NaH waren hocheffektives Basesystem für den Prozess. Turn Over Number (TON) von bis zu 16,91 (Turn Over Frequency (TOF) $6{,}52{\cdot}10^{-5}$ s^{-1}) wurde erreicht mit molekularem Nickelkomplex als Katalysator und eine Kombination von Trioctylamin mit NaH als Base.

Das zweite System ist die Kombination von immobilisiertem Nickelkomplex mit Amin-NaH. Der immobilisierte Komplex wurde durch Verankerung des 1,2-bis(dicyclohexylphosphino)ethane (dcpe) auf funktionalisierte Silica und Polystyrrol Support vorbereitet. Katalysator mit Metallkomplex Beladung von bis zu 0,1566 mmol/g mit Silica Support und 0,134 mmol/g mit Polystyrol Support wurden erfolgreich synthetisiert. MAS-NMR-Untersuchungen bestätigen die Anwesenheit von kovalent-gebundenen dcpe Liganden. Katalytische Untersuchung von diesem System lieferte eine TON von bis zu 1,42 (Turn Over Frequency (TOF) $5{,}48{\cdot}10^{-6}$ s^{-1}). Der Einsatz von immobilisiertem Komplex würde einen kontinuierlichen Eintopf-Prozess ermöglichen. Der Prozess kann so gestaltet werden, dass während der gesamten katalytischen Reaktion der Katalysator im Reaktor bleibt. Dadurch kann der Kontakt mit Oxidationsmittel oder anderen Verunreinigungen vermeidet werden, was zur Verbesserung der Lebensdauer des Katalysators führen kann.

Im dritten System wurden Kombinationen aus Nickelkomplex und immobilisierten Basen verwendet. Vier verschiedene kommerzielle immobilisierte Basen (Alkoxid und tertiäres Amin) waren effektiv in Eintopf-Reaktion von Natriumacrylat. Ferner wurden zwei CO_2 stabile immobilisierte Basen sowohl durch direkte Verankerung auf Polystyrol Support als auch durch Copolymerisationsreaktion vorbereitet. Eine hohe TON von bis zu 30,94 (TOF $4{,}30 \cdot 10^{-4}$ s^{-1}) konnte mit der Kombination von molekularem (dcpe)-Nickelalacton-Katalysator und immobilisiertem Natrium-2-fluorophenolat erreicht werden. Zusätzlich, erfolgreiche Recyclingsversuche von immobilisierten Basen bestätigt die Vielseitigkeit und die Eignung dieser immobilisierten Basen in eine katalytische Reaktion. Ein kontinuierliches Verfahren mit zweistufige Filtration zum Trennen der immobilisierten Base und zur Gewinnung von Natriumacrylat wird als das vielversprechendste Konzept für eine industrielle Anwendung vorgeschlagen.

Acknowledgments

This work would not have been possible without the encouragement and the assistance of others.

I would like to thank my supervisor at hte GmbH, Dr. Stephan A. Schunk, for giving me a chance to work on a very interesting theme and teaching me to push myself, aim high, and never settle for less than my very best.

I thank my supervisor at University of Stuttgart, Prof. Dr.-Ing. Elias Klemm, for his scientific support and fruitful discussions. I would also like to express my gratitude to Prof. Dr.-Ing. Ulrich Nieken for examining my dissertation.

I would like to thank Dr. Michael Lejkowski for sharing his strong scientific experiences and providing ideas and insights into organometallic and organic chemistry. He is always enthusiastic to answer my endless questions.

I am also grateful to Dr. Alvaro Gordillo for his scientific advice, knowledge, and suggestions. I have learned a lot about organometallic chemistry especially hydrosilylation from him.

I owe a particular debt of gratitude to apl. Prof. Dr. Michael Hunger for his assistance and friendly discussion with MAS-NMR measurement.

To the members of liquid phase lab, past and present, especially Jörg Rother, Angelo Brau, Mathias Boesing, Adrien Schmidt, and Daniel Wendt, I would like to express my gratitude for the strong support and help on the screening experiments.

I am very grateful for the great team work at hte GmbH and would like to especially acknowledge synthesis laboratory members, Andreas Strasser, Simon Holz, Michael Bartz, and Robert Müller for their assistance and support during my first half PhD working on heterogeneous catalysis and the members of analytical laboratory, particularly Tamara

Gabriel, Stefanie Wagner and Oliver Laus for their support with GC-MS, X-ray diffraction, BET, DSC, STA-TG, and FTIR measurements.
I thank:

- CaRLa's team: Dr. Michael Limbach, Dr. Nuria Huguet, Dr. Ivana Jevtovikj, and Dr. Ronald Lindner for their assistance and help with my chemistry questions.

- Sandra Weber from University of Stuttgart for her help with NMR measurement.

I would like to thank my friends, especially Thomas Roussiere, Luis Tojil Alvarado Rupflin, and Timo Emmert for the interesting scientific discussion and for the great time during my PhD work.
The financial support from the German Federal Ministry of Education and Research (Chemische Prozesse und stoffliche Nutzung von CO_2: Technologien für Nachhaltigkeit und Klimaschutz) is gratefully acknowledged.
Finally, I would like to thank my dad, my grandma, and my sisters for their support. They always encourage me and help me pursue my dreams. I thank them from the bottom of my heart. This dissertation is dedicated to them.

Eigenständigkeitserklärung

Hiermit erkläre ich, dass ich die Dissertation, abgesehen von den ausdrücklich bezeichneten Hilfsmittel, selbständig verfasst habe.

Stuttgart, den 30.10.2014

Eko Prasetyo

Contents

List of Figures

List of Tables

Nomenclature

Abbreviations

Symbol	Description
AIBN	2,2-Azobis(2-methylpropionitrile)
BEMP	2-*tert*-butylimino-2-diethylamino-1,3-dimethylperhydro-1,3,2-diaza-phosphorane
BTPP	*tert*-butylimino-tri(pyrrolidino)phosphorane
COD	cyclooctadiene
DBU	1,8-diazabicyclo[5.4.0]undec-7-ene
dcpe	1,2-bis(dicyclohexylphosphino)ethane
DMF	dimethylformamide
dppe	1,2-bis(diphenylphosphino)ethane
dppm	1,1-bis(diphenylphosphino)methane
dppp	1,3-bis(diphenylphosphino)propane
dtbpe	1,2-bis(di-*tert*-butylphosphino)ethane

dtbpm	1,1-bis(di-*tert*-butylphosphino)methane
dtbpp	1,3-bis(di-*tert*-butylphosphino)propane
HOMO	highest occupied molecular orbital
LUMO	lowest unoccupied molecular orbital
MAS-NMR	Magic Angle Spinning Nuclear Magnetic Resonance
NA	Normalized Area
NCS	*N*-chlorosuccinimide
NMR	Nuclear Magnetic Resonance
P1	*tert*-butyl-tris(dimethylamino)phosphorane
P2	1-*tert*-butyl-2,2,4,4,4-pentakis(dimethylamino)-$2\lambda^5,4\lambda^5-catenadi(phosphazene)$
P4	1-*tert*-butyl-4,4,4-tris(dimethylamino)-2,2-bis[tris(dimethylamino)-phosphoranylidenamino]-$2\lambda^5,4\lambda^5-catenadi(phosphazene)$
ppm	parts per million
PS	polystyrene
PTA	1,3,5-triaza-7-phosphaadamantane
SBA-15	Santa Barbara mesoporous silica material
STY	Space Time Yield
TBAF	Tetrabutylammonium flouride
TBD	1,5,7-triazabicyclo[4.4.0]dec-5-ene

TEA	triethylamine
THF	tetrahydrofuran
TLC	Thin Liquid Chromatography
tmeda	*N,N,N',N'*-tetramethylethylenediamine
TMS	trimethylsilyl
TOA	trioctylamine

Greek Symbols

Symbol	Description	Dimensions	Units
ρ	Density	ML^{-3}	$kg\,m^{-3}$

Roman Symbols

Symbol	Description	Dimensions	Units
c	Molar concentration	NL^{-3}	$M\ (mol \cdot L^{-1})$
m	Mass	M	kg
n	Amount of substance	N	mol
p	Pressure	$ML^{-1}T^{-2}$	bar
TOF	Turn Over Frequency	T^{-1}	s^{-1}
TON	Turn Over Number	dimensionsless	1
T	Temperature	Θ	°C
t	Time	T	s
V	Volume	L^3	m^3 or L

Chapter 1

Introduction

Acrylic acid and its ester derivates are one of the most important products of the C_3-value-chain of the chemical industry. Currently acrylic esters are the largest application of acrylic acid, which in 2010 consumed about 57% of total crude acrylic acid produced. The esterification products are used mainly in the production of polymers for coatings, paints, adhesives, and binder for leather, paper, and textiles [2]. The other 43% of total crude acrylic acid produced was upgraded to glacial acrylic acid used to produce super absorbent polymers and polyacrylic acid homo-, co- and terpolymers, which find applications in dispersants, flocculants, and thickeners [3].

Super absorbent polymer is the most important product derived from glacial acrylic acid. Currently it consumes about 75% of total glacial acrylic acid production via cross-linking radical co-polymerization of acrylic acid or its salt. Super absorbent polymer has unique ability to absorb up to 1000 times their mass of water through hydrogen bonding with water molecules. When super absorbent polymer comes into contact with water, the sodium ions of the super absorbent polymer interact with water. As sodium ions bind with more water molecules,

the polymer chains with carboxyl moiety become negatively charged and repel each other, making room for more water, which is subsequently absorbed into the molecular structure, causing the polymer to swell. The difference in osmotic pressure between the polymer and the water accelerates the absorption process. Because each polymer chains are connected with each other or crosslinked, the thermodynamically favored expansion of the polymer chains is limited, thus the polymers do not dissolve and retain its solid form during water absorption. The crosslinker plays an important role in determining the swelling property and mechanical stability of the polymers. Due to strong hydrogen bonding and the difference in osmotic pressure between the polymer and water, once absorbed, water remains physically entrapped in the polymer network and can only be released by drying or by impeding the polymer's ability to bond with water molecule (e.g. by adding water soluble salts). Additional cations in the liquid counter the negative charge of the polymer chains, reducing the repulsion force between the polymer chains, and thus limiting the extent of swelling of the polymer and its ability to absorb water [4, 5]. Due to this phenomenon, super absorbent polymer can only absorb up to 100 times their mass of a 0.9 % NaCl solution, which is 10 times less than in case of pure water.
Owing to a very high absorption capacity and strong irreversible absorption, super absorbent polymers have revolutionized the baby diaper and adult incontinence industries since the 1970s and has quickly replaced traditional cellulosic or fiber-based absorbent materials. Recently, super absorbent polymers also find their application in agriculture where they are used to improve water retention in a water-efficient agriculture.
In 2010 super absorbent polymers consumed about 32% of total crude acrylic acid production, which equates to about 2.08 million metric tons global super absorbents capacity. With an estimated annual growth of

about 5.6 % p.a during 2010-2015, super absorbent polymers is the strongest growing application of acrylic acid [3]. The majority of super absorbents is currently produced by Evonik Stockhausen (23.8%), Nippon Shokubai (22.6%), and BASF (19.2%). Together they accounted for 65.7% of global super absorbents capacity [3, 4].

1.1 State of the Art Production of Acrylates

Industrial acrylic acid manufacture was started by Röhm & Haas in 1901 via cyanohydrin process. The starting materials, ethylene oxide and hydrogen cyanide, were reacted in the presence of base to form ethylene cyanohydrin, which was then reacted with alcohol in the presence of diluted sulfuric acid to give the acrylate ester [2, 3, 6]:

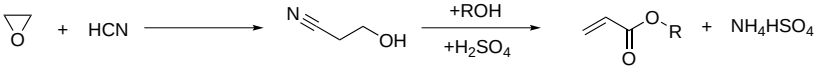

Figure 1-1: Acrylic acid synthesis via cyanohydrin route.

The ethylene cyanohydrin route was abandoned in the early 1970s due to its safety related issues and challenging NH_4HSO_4 waste management. Alternatively, acrylates can also be produced via alcoholysis of acrylonitrile in the presence of sulphuric acid. The process uses two equivalents of sulphuric acid to hydrolyze acrylonitrile at 200 - 300 °C, producing acrylate and acrylamide as byproduct. In 1960s, as the price of acrylonitrile fell, Ciba Specialty Chemicals, Asahi Chemical, and Celanese Mexicana practiced the process. The process was inefficient in that it generates a high amount of waste and requires extensive workup to recycle the excess sulphuric acid contaminated with the byproduct. The process was discontinued in the 1990s with the development of the new

oxidation process [2, 3].

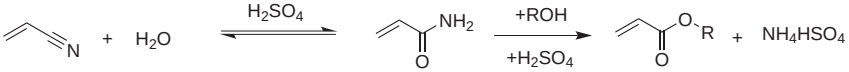

Figure 1-2: Acrylic acid synthesis via acrylonitrile hydrolysis route.

In 1939, Reppe discovered the catalytic carbonylation of acetylene with CO and H_2O using $Ni(CO)_4$ catalyst to give acrylic acid. The reaction takes place at 220-230 °C and 100 bar. Three different modifications exist with different type of catalyst precursor and the quantity of $Ni(CO)_4$:

- process with stoichiometric amount of $Ni(CO)_4$.
- catalytic process with catalytic amount of $Ni(CO)_4$.
- catalytic process with $NiBr_2$ as catalyst and non-carbonyl-forming CuI as cocatalyst.

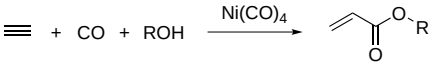

Figure 1-3: Reppe's carbonylation of acetylene.

Due to high selectivities to acrylic acid (up to 90%, based on acetylene) with small amount of catalyst required, the Reppe process became the favored process in the 1960s and was practiced by BASF until 1990s [2, 6–8].

By the late 1970s, the increasing cost and limiting availability of acetylene prompt the development of a more economic and environmentally friendly process. Selective oxidation of propene to acrylic acid quickly gained prominence due to high availability of relatively low cost propene from steam reforming. The acetylene-based process was phased out and currently the acrylic acid production relies on gas-phase

catalytic oxidation of propene with solid catalyst and acrolein as intermediate. The process can be carried out either in single-step direct oxidation or two-steps oxidation in multitubular fixed-bed reactor, with the latter one being the most favored process to maximize the acrylic acid selectivity.

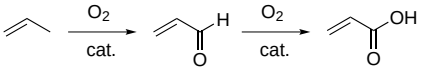

Figure 1-4: Acrylic acid synthesis via two steps oxidation of propene.

In the first step, propene is converted to acrolein in the presence of air at 330 - 380 °C at a pressure of 1 - 2 bar with Mo and Bi based mixed oxides catalyst containing one or more of other elements such as Fe, Co, Ni, Tl, W, Al, Zr, Ti, Te, K, P, Sb, Sn, or Si as promoter to improve the outcome of the reaction [9–12]. In the second step, acrolein is further oxidized to acrylic acid at 250 - 300 °C with Mo and V based mixed oxides containing one or more of W, Cu, Co, Ni, Fe, Pb, Bi, Sn, Sb, or Si [10–12]. Contact time is kept to a minimum, at a few seconds, to avoid over-oxidation. Acrylic acid is isolated from the effluent gas of the second-stage oxidation by contact with water in an absorber column to give an aqueous solution of 20 to 70 wt% [13, 14]. After extraction with an organic solvent, such as ethyl acetate, butyl acetate, ethyl acrylate, 2-butanone or aromatic hydrocarbons, the acrylic acid can be further purified by distillation or re-crystallization before polymerization. To prevent unintentional polymerization of the acrylic acid monomer, distillation is carried out in the presence of polymerization inhibitor, such as hydroquinone or hydroquinone monomethyl ether, at low temperature and reduced pressure [2].

Propene oxidation is currently the most economical process with worldwide production capacity of $5.2 \cdot 10^6$ metric tons in 2010 [3]. However,

since the process is petroleum dependent, volatility and continual increases in propene price are unavoidable and affect the economy of acrylic acid. Thus, it is of great economic interest to secure acrylic acid production and its price stability with an alternative route, e.g. with a process based on renewable resources.

1.2 Alternative Routes to Sodium Acrylate

In the past several years, the development of alternative routes to acrylic acid has been of high economic and academic interest. Several production technologies based on alternative feed stocks are being developed. Bio-based compounds and cheap, abundantly available ethylene are among the feed-stocks of choice. Indeed, acrylic acid producers utilizing both bio-based and petro-based feed stocks would be in better position, to hedge the price volatility of one feed stock with broad spectrum of feed stocks.

This work is a part of BMBF funded project to develop a green novel process for the sodium acrylate production from ethylene and CO_2. The synthesis of acrylates from ethylene and CO_2 would not only utilize the cheap and abundantly available CO_2 as C_1 building block but also, due to its atomic efficiency, it would avoid waste formation. In addition, further utilization of renewable ethylene, e.g. derived from de-hydration of bio-ethanol [16], would further highlight its positive environmental impact.
Contrary to the current acrylate production process via propene oxidation, a process utilizing ethylene and CO_2 discussed in this work

Table 1.1: Emerging Alternative Route to Acrylic Acid [3, 15]

Company	Process
Cargill / Novozymes / BASF	catalytic dehydration of 3-hydroxypropionic acid (microbic fermentation of sugar)
OPX Biotechnologies / DOW Chemical	catalytic dehydration of 3-hydroxypropionic acid (microbic fermentation of dextrose or sucrose)
Arkema	oxidation of acrolein, which is obtained from dehydration of glycerol (byproduct in bio diesel manufacture from rapeseed)
Nippon Shokubai	oxidation of acrolein, obtained from dehydration of glycerol
Mitsubishi Chemical / Genomatica	catalytic cross-metathesis of ethylene and fumaric acid (microbic fermentation of lactic acid)
Novomer	oxidative carbonylation of ethylene oxide to form propiolactone, which is then converted to acrylic acid
Union Oil	oxidative carbonylation of ethylene in the presence of $PdCl_2$ - $CuCl_2$
Röhm & Haas (DOW Chemical), several research institutions	one-step partial oxidation of propane to acrylic acid on vanadium phosphorous oxides, heteropolycompounds, and mixed metal oxide

proceeds in liquid phase and may allow significantly lower capital investment as well as a very flexible and easily scalable plant capacity. Moreover, coupling the new process with a solid catalyst instead of molecular catalyst would allow simpler separation and recycling. The structure and activity of a solid catalyst system containing an active immobilized molecular catalyst capable of facilitating oxidative coupling between ethylene and CO_2 yielding acrylate as well as an alternative system utilizing a combination of molecular catalyst and immobilized base system are investigated in this work.

1.3 CO_2 as Chemical Feedstock

Industrial revolution beginning in the 1800s has contributed to significant increase of greenhouse gases emission, especially CO_2, in the atmosphere. Anthropogenic CO_2 emissions come mainly from extensive use of fossil fuels and irresponsible deforestation. The growing concern about elevated greenhouse gas levels, resulting in global warming, sea level rise or extreme weather events among others, demands improved energy-efficient processes and reduction in CO_2 emissions. Managing and reducing greenhouse gas emissions is becoming more and more relevant today, with several regulations came into force in the last decade. Several climate friendly technologies, such as electric vehicles or energy- and resource-efficient production processes have been investigated and developed in recent years. Moreover, the potential application of the greenhouse gas CO_2 as raw material in the chemical industry is much more advantageous and is becoming increasingly important in academic and industrial research [17, 18].

Generally, CO_2 can be captured either from the atmosphere or more efficiently directly from industrial sources. Although CO_2 is one of the most abundant greenhouse gases, the low concentration in the atmosphere, which is about 400 ppm [19], is far too low for viable industrial application. Until an efficient CO_2 capture technology from the atmosphere is well established, it is more feasible to focus on industrial process streams, capturing CO_2 before it reaches the atmosphere. CO_2 is generated in high concentration in NH_3 production, power plants, steel production plants, cement, and fermentation industries. The purity of the CO_2 stream can be further increased either via absorption, adsorption, membranes application or cryogenic processes [20–23]. Currently, most of CO_2 removal processes are dominated with physical or chemical absorption technologies, for example amine-based scrubbing process, and energy efficient adsorption technologies, for example pressure swing adsorption (PSA) with titanosilicate, activated carbon or aluminosilicate zeolite adsorbents [24–32], which is increasingly implemented in new plants in the recent years. Typically, a PSA process consists of several fixed bed units, sometimes as many as 16 beds [33], which undergo successive pressurization (adsorption) and depressurization (regeneration) steps. When a gas mixture of nitrogen and carbon dioxide is passed under high pressure through an adsorbent bed that binds CO_2 more strongly than nitrogen, part or the entire CO_2 will stay in the bed unit and the gas coming out of the bed will be enriched in nitrogen. After the bed reaches full adsorption capacity, it can be regenerated by reducing the pressure, thus releasing adsorbed CO_2 in high purity. Finally, the bed is ready for the next cycle after purging with nitrogen.

Utilization of CO_2 as chemical feedstock is regarded as the most elegant

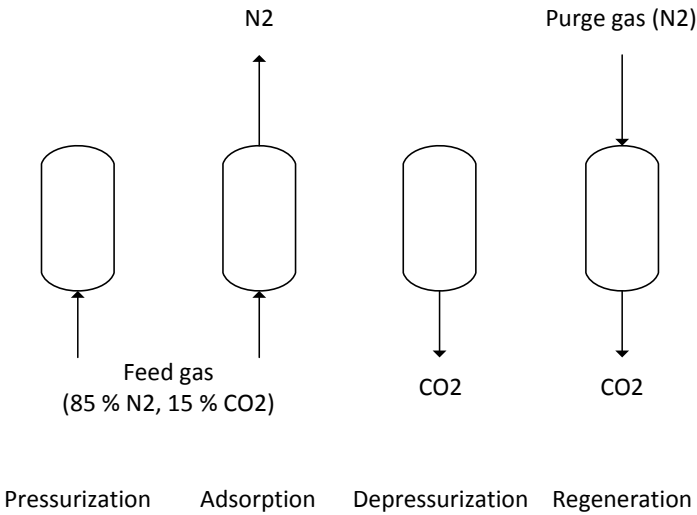

Figure 1-5: Four steps PSA process.

sustainable way for carbon recycling, generating products with high added value. The biggest challenge in chemical utilization of CO_2 is, however, the high thermodynamic energy barrier as the molecule is almost inert (free energy formation of CO_2 ΔG_f° = -393.52 kJ/mol [34]). Thus, energy is necessary to activate stable CO_2. Often the processes requiring CO_2 activation are carried out at elevated temperature and pressure, thus limiting the feasibility of their industrial application. Some possible chemical utilization options of CO_2 are listed in the Figure 1-6. In the chemical industry, CO_2 has been used mainly in the production of urea, methanol, (in)organic (poly)carbonates, or salicylic acid (Figure 1-7 and Table 1.2) [17, 35, 36].

The synthesis of urea is the biggest single industrial application of CO_2, with a production volume of about $150 \cdot 10^6$ t/a in 2010 [37]. The overall

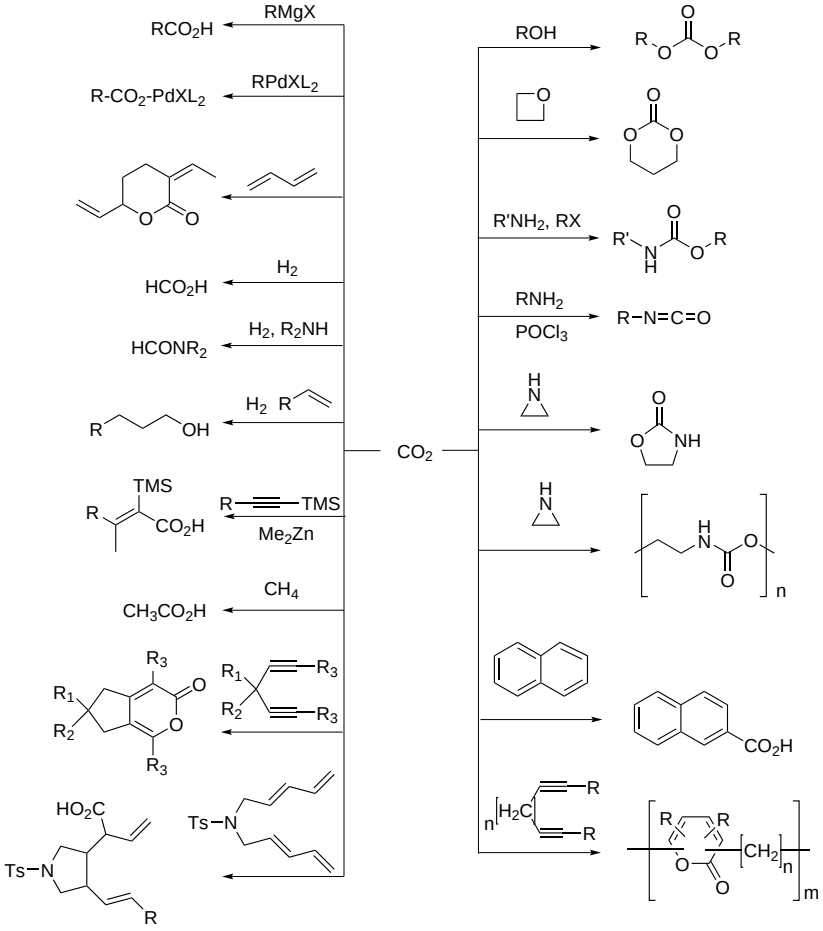

Figure 1-6: Chemical utilization of CO_2 [35].

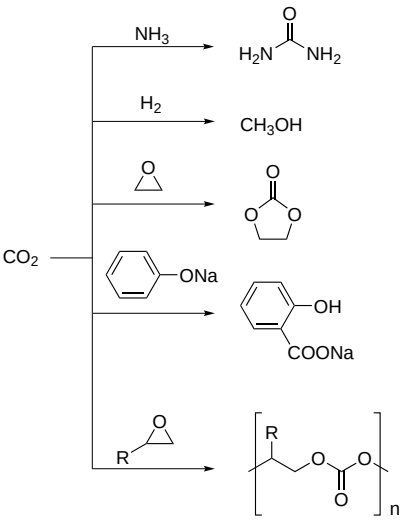

Figure 1-7: Industrial chemical utilization of CO_2.

Table 1.2: Industrial chemical processes with CO_2 as feedstock.

Product	Process
Urea	thermal, 150 - 250 bar, 150 - 200 °C [37]
Methanol	solid catalyst ($Cu/ZnO/Al_2O_3$), 50 - 100 bar, 250 °C [38, 39]
Organic (poly)carbonates	solid catalyst (5 - 200 bar, 100 - 200 °C) and molecular catalyst (1 - 300 bar, 25 - 150 °C) [40–49]
Salicylic acid	Kolbe - Schmitt reaction, 5 bar, 150 - 160 °C [50–53]
Syngas (CO/H_2 mixture)	Mixed-Reforming (Eq. 1.3 - 1.4 combined with Eq. 1.9), solid catalyst (Ni, Fe, Cu, Al, Mg [54–64], 20 - 40 bar, 500 - 950 °C [65]

reaction is highly exothermic [37]: in the first step (Equation 1.1) ammonia and CO_2 are converted to ammonium carbamate; in the second (Equation 1.2), endothermic step, the ammonium carbamate dehydrates to yield urea and water.

$$2NH_3(l) + CO_2(l) \rightleftharpoons NH_2COONH_4 \quad \Delta H^0_{298} = -117kJ/mol \tag{1.1}$$

$$NH_2COONH_4 \rightleftharpoons NH_2CONH_2 + H_2O \quad \Delta H^0_{298} = +15.5kJ/mol \tag{1.2}$$

The process does not require a catalyst and takes place at 150 - 200 °C and 150 - 250 bar. Several industrial processes are known, such as Stamicarbon, Avancore, Snamprogetti, ACES, isobaric double recycle, each with different recycling mechanism of nonconverted ammonia and CO_2. Urea is mainly used in the manufacture of fertilizers and as raw material in the chemical industry (e.g. urea formaldehyde resins).

Methanol is the second largest industrial application of CO_2, with worldwide production of about $42{\cdot}10^6$ t/a in 2008 [38]. Methanol is mainly used in chemical synthesis of formaldehyde, methyl *tert*-butyl ether, acetic acid, methyl methacrylate, and dimethyl terephthalate among others. With increasing fuel price, methanol is also becoming more important for energy production, especially in the methanol to olefins (MTO) or methanol to gasoline (MTG) process. Industrially, methanol is produced from synthesis gas and CO_2 mixture with $Cu/ZnO/Al_2O_3$ catalyst at 50 - 100 bar, 250 °C [38, 39]. Several studies have shown that the reaction may proceed either from carbon monoxide or carbon dioxide [66–69].

Syngas can be produced via numerous processes from liquid and gaseous hydrocarbons, alcohols, carbohydrates [70–72], and even solid feed stocks such as coal [73] or biomass [74]. Depending on the feedstock and process conditions (feed steam/carbon ratio, reaction temperature, or pressure), reforming generates syngas with various H_2/CO ratio. On the technical scale, the syngas production is represented by the following reactions [70]:

- Steam reforming takes place at high temperature around 500 - 900 °C and a pressure of about 20 - 40 bar with a steam/carbon ratio of around 2.5 - 3 to ensure coke-free operation, generating a syngas with H_2/CO ratio in the range of about 2.2 to 4.8 [65, 70]. Steam reforming often uses widely available and cheap natural gas as feed stock [75–77]. Part of the hydrocarbon feed is burnt with air to provide the heat necessary for the endothermic steam reforming reaction. The heat at the reformer outlet can be reclaimed for steam production or to preheat the feed stock.

$$CH_4 + H_2O \rightleftharpoons CO + 3H_2 \qquad \Delta H^0_{298} = 206 kJ/mol \tag{1.3}$$

$$C_mH_n + mH_2O \rightleftharpoons mCO + \left(m + \frac{n}{2}\right)H_2 \tag{1.4}$$

- Partial oxidation. Contrary to the endothermic steam reforming, (catalytic) partial oxidation is an exothermic process. Industrial non-catalyzed reforming takes place over a temperature range of 1150 - 1500 °C and a pressure range of 25 - 80 bar [78]. There are three main process types, which represent more than 320 plants worldwide [79]: Texaco process, which uses gaseous and liquid hydrocarbons feed stocks, Shell process, which uses heavy

oils, and Lurgi process, which uses a broad range of feed stock including gasification of tars, oils, and slurries formed as by-products from fixed bed gasification. Partial oxidation generates a syngas with H_2/CO ratio close to 2, which is highly attractive for direct methanol synthesis [80] or Fischer Tropsch synthesis [81, 82].

$$CH_4 + \frac{1}{2}O_2 \rightleftharpoons CO + 2H_2 \qquad \Delta H^0_{298} = -36kJ/mol \tag{1.5}$$

$$C_mH_n + \frac{m}{2}O_2 \rightleftharpoons mCO + \frac{n}{2}H_2 \tag{1.6}$$

- Autothermal reforming (ATR) or oxidative steam reforming combines steam reforming and partial oxidation, resulting in a net reaction enthalpy close to zero. The autothermal reforming is typically performed between 900 - 1500 °C and a pressure in the range of 1 - 80 bar [78]. Depending on the amount of steam, oxygen, and fuel used in the process, ATR generates a syngas with variable H_2/CO ratio [83].

$$CH_4 + \frac{1}{4}O_2 + \frac{1}{2}H_2O \rightleftharpoons CO + \frac{5}{2}H_2 \tag{1.7}$$

$$C_mH_n + \frac{m}{4}O_2 + \frac{m}{2}H_2O \rightleftharpoons mCO + (\frac{m}{2} + \frac{n}{2})H_2 \tag{1.8}$$

- Carbon dioxide reforming. In recent years, there is an increased interest to replace steam commonly used in steam reforming with CO_2. CO_2 can be used either as substitute of steam (dry reforming) or as an additional complement in mixed reforming. CO_2 reforming of methane (Eq. 1.9 yields a syngas with lower residual

CH_4 and H_2/CO ratio lower than 1.7, which is suitable for higher hydrocarbons or alcohols synthesis. CO_2 reforming may be used to convert CO_2 rich natural gas streams into liquid fuels (gas to liquid fuels) or to upgrade the flue gas from fossil-fuel power stations.

$$CO_2 + CH_4 \rightleftharpoons 2CO + 2H_2 \qquad \Delta H^0_{298} = 247 kJ/mol \tag{1.9}$$

- Coal or biomass gasification. Gasification of solid feedstock is a complex process involving the pyrolysis of coal and the subsequent gas phase reactions and heterogeneous reactions of char with gaseous compounds [84]. Gasification is typically carried out in a moving fixed bed, fluidized bed, entrained flow, or molten bath reactor with air, oxygen, steam, or their combinations as gasifying medium.

$$C + H_2O \rightleftharpoons CO + H_2 \qquad \Delta H^0_{298} = 131 kJ/mol \tag{1.10}$$

$$C + O_2 \rightleftharpoons CO_2 \tag{1.11}$$

$$C + \frac{1}{2}O_2 \rightleftharpoons CO \tag{1.12}$$

$$C + CO_2 \rightleftharpoons 2CO \tag{1.13}$$

- Water Gas Shift (WGS) or Reverse Water Gas Shift (RWGS) equilibrium is always involved in the reforming processes.

$$CO + H_2O \rightleftharpoons CO_2 + H_2 \qquad \Delta H^0_{298} = -41 kJ/mol \tag{1.14}$$

Syngas is one of the most important gas mixtures in the energy and chemical industry. It is used in the production of aldehydes, alcohols, or synthetic fuel (Fischer-Tropsch process) [80–82, 85].

Carboxylation processes with CO_2 yielding carbonates, carbamates, carboxylates, or lactones are also of great importance from the industrial point of view. The process has a high atom efficiency and can reduce as well as prevent significant amount of waste, which are usually generated from multi-step conventional processes [1]. Direct carboxylation of olefins or other organic compounds would represent a sustainable process with a huge market potential. Currently, the synthesis of salicylic acid and its derivatives is the only industrial application of direct carboxylation with CO_2. The process starts with dry sodium phenoxide which is carboxylated in the presence of 5 bar CO_2 at 150 - 160 °C. The process is typically carried out in an autoclave with subsequent work up and acid treatment with H_2SO_4 [53].
Several new concepts for carboxylation reactions with CO_2 have been developed and intensively investigated in the academia. The reactions typically utilize catalysis to bypass the energy barrier of the chemically inert CO_2. Current concepts for CO_2 activation and its carboxylation are further discussed in the following section.

1.3.1 Bonding of CO_2 to Metal Centers

The coordination of CO_2 on metal centers reduces the activation energy, allowing CO_2 to react with other molecules. CO_2 is a linear, nonpolar molecule with two sets of orthogonal π orbitals and 16 electrons in its ground state. The LUMO (lowest unoccupied molecular orbital) and HOMO (highest occupied molecular orbital) orbitals of the carbon and oxygens atoms respectively are responsible for the Lewis acid and Lewis base character of the CO_2, resulting in various coordination modes at different metal centers (Figure1-8). Coordination with metal center results in an activated state with increased CO bond distances and a bent OCO moiety. Successful activation can be monitored either with infrared spectroscopy (lower frequency vibration modes) or ^{13}C NMR spectroscopy (low field shifts).

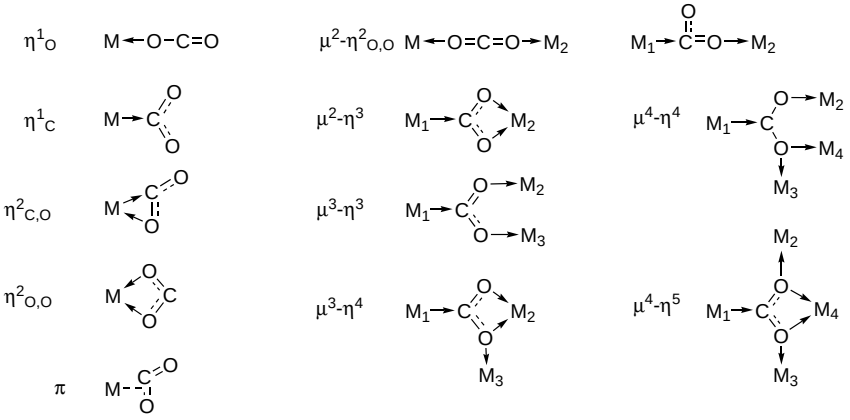

Figure 1-8: Coordination modes of CO_2 to metal centers [36, 86].

1.3.2 Reactivity of Activated CO_2

Generally, the chemically inert CO_2 can be activated via:

- coordination with metal centers (Lewis acid or Lewis base) followed by subsequent reaction with a second substrate to produce carboxylates, carbamates, or carbonates.

- insertion reaction into M-X bonds (X = C, H, O, N) to form carboxylato, formato, carbonato, or carbaminato complexes.

- simultaneous coordination of CO_2 and a substrate by low valent metal complexes, such as Ni(0) or Pd(0), followed with oxidative cycloaddition to afford metalalactones.

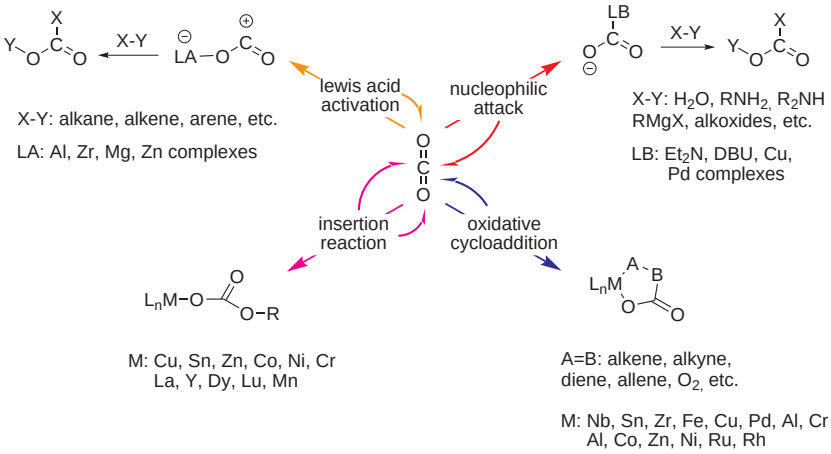

Figure 1-9: Activation modes of CO_2 leading to chemical transformation [35].

The binding of CO_2 and substrate molecules at the metal center is a crucial step in catalytic transformation of CO_2 into organic products. Some examples of direct carboxylation of organic compounds are listed in Table1.3. Despite recent academic achievements, a lot of issues have still to be addressed before catalytic carboxylation reactions with CO_2 is applicable at the industrial level, for example: the activity, life time,

Table 1.3: Direct carboxylation of organic compounds with CO_2.

Process	Catalyst
benzoylacetone to benzoylacetic acid	1,3-dialkylimidazolium-2-carboxylates [87]
ethylene to acrylic acid	Ni [88–91], Ti [92], Fe [93], Mo [94], and Rh [95] complexes
alkyne to pyrones	Ni complex [96–106]
diene to pyrones, lactones, or linear esters	Pd [107–117] and Rh [118–120] complexes
R_2NH to carbamic acid (R = n-butyl, isopropyl, cyclohexyl)	alkyl halides [121], Co [122] complex, organic bases [123–126], titanosilicate molecular sieves [127], β -zeolites [128, 129], Ti-SBA-15 [130, 131]
RNH_3 to alkylammonium N-alkylcarbamates (R = benzyl, allyl, t-butyl, cyclohexyl)	crown ethers [132]
epoxide to polycarbonates	Al-phorphyrin complexes [133] or Zn-compounds [133–137]
epoxide to cyclic carbonates	ionic liquid [138–141], organic bases [142], main group meal halides [143], metal complexes [9], ammonium salts [144, 145], supported bases [146], phosphines [146], metal oxides [147–149], transition metal systems [137, 150, 151]
epoxide to linear carbonates	Sn [152–156] and Nb [157, 158] complexes, ZrO_2 [159–164], CeO_2–ZrO_2 [165–167]

stability, and cost of the transition metal catalyst and cocatalyst.

1.4 Catalysis

Catalysis is an important topic in the chemical industry. Catalyst lowers the activation energy of a chemical reaction, which paves new reaction pathways and thus changes the reaction kinetic. Nowadays, more than

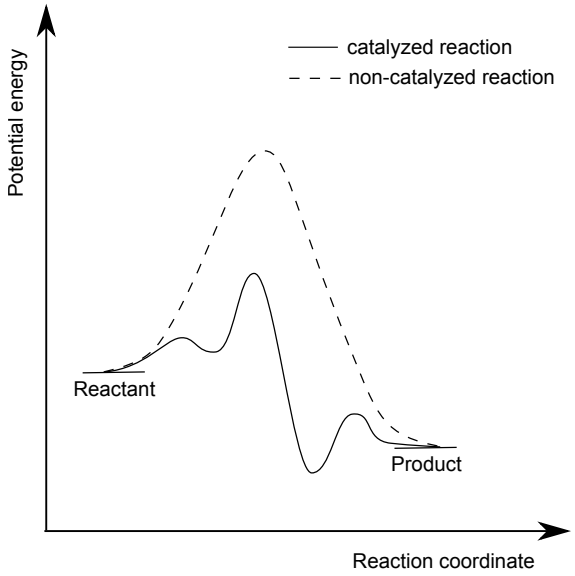

Figure 1-10: Catalyst opens up new reaction pathways with lower activation energies.

75% of all industrial chemical transformation use catalysts to increase process efficiency [168]. Generally, the catalysts can be classified into two groups: molecular catalysts (acid/base catalysts, organocatalysts, biocatalysts, and transition metal complexes) and solid catalysts (bulk or supported catalysts). Of increasing importance are also hybrid catalysts

(immobilized molecular catalysts), which will be further discussed in Chapter 3.
There are some major differences between molecular and solid catalysis as illustrated in Table 1.4.

Process with Molecular Catalyst

In homogeneously catalyzed reactions, the catalysts, the starting materials, and the products are present in the same phase. Each individual catalyst molecule is a catalytically active species. When coupled with a high degree of dispersion or mixing, a molecular catalyst displays a very high activity. Molecular catalysts also allow for high selectivities at mild reaction conditions and low catalyst concentrations. High mobility of each molecule, including the catalyst, during reaction ensures more collisions with substrate molecules. However, due to the low stability of metal complexes, the reactions can only be performed up to temperatures below 250 °C. In addition, laborious catalyst separation from the products, which sometimes demands complex processes such as distillation or liquid-liquid extraction, hinders their industrial application. There are four main types of molecular catalysts:

- Acid and base catalysts
- Organocatalysts
- Biocatalysts (Enzymes, Cells, etc.)
- Transition metal catalysts, i.e. a transition metal atom as the catalytic active centers surrounded by coordinating ligands.

The classical transition metal catalysts (organometallic catalysts) are one of the most important type of molecular catalysts. Some large-scale industrial processes with molecular catalyst are listed in Table 1.5.

Table 1.4: Differences between molecular and solid catalysts [168, 169].

	Molecular catalyst	**Solid catalyst**
Form	Soluble compounds or metal complexes	Bulk or supported metals or metal oxides
Active site	Single active site, all catalyst molecules	Multiple active sites, only surface atoms
Structure	Well defined	Poorly defined
Phase	Same phase as the reactants	Different phase from the reactants
Reaction conditions	Mild (<250 °C)	Harsh, high temperature (>100 °C) and pressure
Activity	High	Low
Selectivity	High	Low
Stability	Low	High
Transport limitations	Practically absent	Present, can be severe
Catalyst separation and regeneration	Complicated	Easy (Fixed-bed: unnecessarry; Suspension: filtration)
Mechanistic understanding	Reasonably well understood	Complicated, require sophisticated investigations
Activity loss	Irreversible reaction with products, poisoning	Sintering, poisoning

Table 1.5: Industrial processes with molecular transition metal catalysts [170].

Unit operation	Process	TON	TOF [h^{-1}]
Dimerization of olefins	IFP-Dimersol, Alphabutol, Difasol: dimerization of monoolefins; DuPont: synthesis of 1,4-hexadiene from butadiene and ethylene	1000 (1,4-hexadiene synthesis) [171]	625,000 [172] - 800,000 (dimerization of monoolefins) [173]
Oligomerization of olefins	Hüls: trimerization of butadiene to cyclododecatriene; SHOP, Idemitsu, IFP-Alphaselect, UOP-Linear-1, Sabic-α-Sablin: oligomerization of ethylene to α-olefins, Chevron-Phillips: trimerization of ethylene to 1-hexene		780 (Hüls Vestamide trimerization) [171]; 82,000 (SHOP) [174, 175]; 156,000 (Chevron-Phillips trimerization) [171]
Polymerization	metallocene-based olefins and dienes polymerization	>100,000 [176]	>10,000,000 [176]

Carbonylation	Reppe reactions; Monsanto: carbonylation of methanol to acetic acid; Ruhrchemie/Rhone-Poulenc: propene to 1-butanol and 2-ethylhexanol	1,400 (methanol carbonylation) [177]	400 (methanol carbonylation) [177]; 10,000 (propene hydroformylation) [178]
Hydrocyanation	DuPont: adiponitrile from butadiene and HCN	644 [179, 180]	215 [179, 180]
Oxidation	cyclohexane oxidation; production of carboxylic acids (adipic and terephthalic acid); Halcon: propylene oxide production; Wacker-Hoechst: selective ethylene oxidation to acetaldehyde	95,000 (cyclohexane oxidation) [181, 182]	18,000 (cyclohexane oxidation) [182]; 20 (ethylene epoxidation) [183]; 3,600 - 350,000 (Wacker ethylene oxidation) [184]
Isomerization	DuPont: Conversion of 1,4-dichloro-2-butene to 3,4-dichloro-1-butene		450 (iron oxide nanoparticle) [185, 186]

Metathesis	Degussa-Hüls: octenenamer from cyclooctene		500 - 700 [187]
Hydrogenation	Monsanto L-Dopa process: asymmetric hydrogenation; Procatalyse: benzene to cyclohexane; Takasago: L-menthol	20,000 (L-dopa) [188]; 400,000 (L-menthol) [170]	1,000 (L-dopa) [188]; 25,000 (L-menthol) [170,188]

The reactivity of molecular transition metal catalysts depends on the characteristics of the central metal atoms (oxidation state, number of d-electrons, coordination number and availability of free coordination sites on the metal) and the attached ligands (steric and electronic properties). The transition metal is usually in low oxidation state with partially filled d and/or f orbitals. Nucleophilic ligands with available electron lone pairs (HOMO) donate electrons to the electrophilic metal (LUMO), forming a σ-bond to the metal center. In addition, the HOMO of transition metal can also donate electrons into an empty π^* antibonding orbital of the ligands (LUMO), a concept called π-backbonding. Some important ligands types in molecular transition metal catalysis are listed in Table 1.6

The total amount of electron in the valence shells of transition metals (both the valence electrons of the metals and electron contribution of the ligands) dictates the stability or reactivity of the complexes, which is described by the 18 valence electron (18-VE) rule. A metal complex that has 18 valence electrons are typically stable, while a complex with fewer than 18 valence electrons, also called coordinatively unsaturated complexes, tend to show enhanced reactivity. There are however some cases in which the 18-VE rule is violated:

- 16 e^- complexes: low spin d^8 metal ions such as Fe(0), Ru(0), Os(0), Co(I), Rh(I), Ir(I), Ni(II), Pd(II), Pt(II), Cu(III) and Au(III).

- complexes with bulky ligands: $Ti(neopentyl)_4$ (8-VE), $Cp_2Ti(C_2H_4)$ (16-VE), $V(CO)_6$ (17-VE), $CpCr(CO)_3$ (17-VE), $Pt(PtBu_3)_2$ (14-VE), $Co(norbornyl)_4$ (13-VE), $[FeCp_2]^+$ (17-VE)

- High spin complexes: $CrCl_3(THF)_3$ (15-VE), $[Mn(H_2O)_6]_2^+$ (17-VE), $[Cu(H_2O)_6]_2^+$ (21-VE), $[CrO_4]_2^-$ (16-VE), $Mo(=NR)_2Cl_2$ (12-VE)

Table 1.6: Ligand types in molecular transition metal catalysts [189].

Ligand types	Examples	Electron contribution
Hydride	H^-	1
Halogenides	Cl^-, Br^-, I^-, F^-	1
Oxygen containing ligands	water, alcohols, ethers	2
Sulfur containing ligands	mercaptans, thioethers	2
Nitrogen containing ligands	amines, nitriles	2
	NO	1 (bent NO) or 3 (linear NO)
Phosphorous containing ligands	phosphines PR_3, phosphites $P(OR)_3$	2
Carbon containing ligands	alkyls, aryls	1
	CO, alkenes, carbenes	2
	allyls	1 (η 1-allyls) or 3 (η 3-allyls)
	carbynes, alkynes	3
	dienes	4
	cyclopentadienyls	5
	aromatics	6

- high VE complexes: Cobaltocene (19-VE), Nickelocene (20-VE), $[Cu(H_2O)_6]_2^+$ (21-VE)

In addition to its ability to coordinate and/or activate a molecule, the transition metal is also able to change the oxidation states and the coordination numbers easily. These three distinctive features allow the transition metal complex to undergo four fundamental reactions in organometallic catalysis:

1.) Association and Dissociation

The metal center can associate or coordinate a ligand or a substrate that enters a certain coordination distance. The ligand or substrate occupies a free coordination site of the metal and forms a coordination bond with the metal. Reversibly, the ligand can leave the coordination site, which is called dissociation. The valence electrons and the coordination number of the metal increase during association and decrease during dissociation. In both cases, the oxidation number of the metal remains constant. A special case of consecutive dissociation of one ligand and association of another is called ligand exchange.

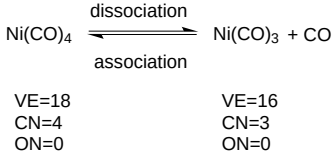

Figure 1-11: Fundamental reaction in organometallic catalysis: Association and Dissociation [190].

2.) Oxidative Addition and Reductive Elimination

Contrary to association and dissociation reactions, oxidative addition and reductive elimination involve a change in oxidation state

of the metal. During oxidative addition, the metal adds atoms or molecules and at the same time undergoes formal oxidation. On the other hand, during reductive elimination, the metal is formally reduced by eliminating ligands. Oxidative addition and reductive elimination are both important steps in the initial and final phase of a catalytic reaction.

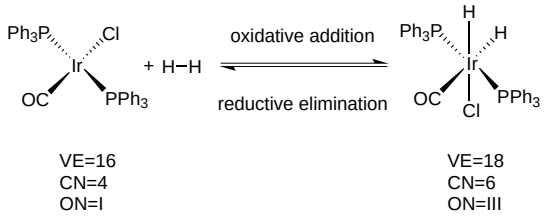

Figure 1-12: Fundamental reaction in organometallic catalysis: Oxidative Addition and Reductive Elimination [190].

3.) Insertion and De-insertion

Insertion is a crucial step to incorporate a certain substrate into another. Insertion demands substrates to be coordinated in *cis* position. On the other hand, de-insertion or extrusion happens when a substrate split off into two molecules. In both cases, the oxidation state of the metal remains constant.

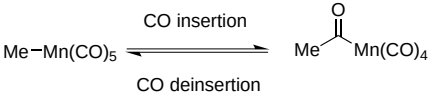

Figure 1-13: Fundamental reaction in organometallic catalysis: Insertion and De-insertion [190].

4.) Oxidative Coupling and Reductive Cleavage

In oxidative coupling, the metal center merges two molecules with

each other, forming a metallacycle, and as a result the oxidation state of the metal increases. The reverse reaction, the reductive cleavage, split off the metallacycle into two molecules while the oxidation state decreases.

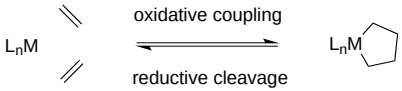

Figure 1-14: Fundamental reaction in organometallic catalysis: Oxidative Coupling and Reductive Cleavage [190].

Different metal-ligand combinations have different preference to facilitate a certain reaction with different selectivities. The electronegativity of transition metals affects their preference to coordinate a certain molecule [189, 191].

Early transition metals groups III and IV are often found in a very high oxidation state, for example Zr(IV) or Ta(V). Due to low amount of d-electrons, early transition metals in their highest oxidation state prefer hard σ-donors (N, O, or F ligands) and will tend to coordinate π acceptor ligands (for example CO, C_6H_6, or C_2H_4) weakly. On the other hand, early transition metals with lower oxidation states, such as d^2 Zr(II) or Ta(III), are very π basic and bind such ligands very strongly. With the exception being Ti, early transition metals display a very limited redox capability. Early transition metal complexes usually show a remarkable activity in polymerization reactions.

Transition metals of the groups V, VI, and VII, bind ligand strongly with not very reactive metal carbon bonds. They prefer ligands with σ-donor and π-acceptor backbonding capabilities, for example CO. Due to many accessible oxidation states, they are especially suitable for redox reactions. Mid transition metal complexes are usually used in the oxidation as well as alkene and alkyne metathesis reactions.

Similar to middle transition metals, late transition metals groups VIII, IX, and X are generally suitable for redox reactions. They exist either as 18-VE or 16-VE (square planar) complex. Late transition metals prefer σ-donor and weak π-acceptor ligands, such as phosphines. π back donation is less pronounced, resulting in positively-charged, coordinated π ligands, which is very susceptible to nucleophilic attack. Coordination with C-ligands results in a weak metal carbon bonds with moderate reactivity, while coordination with O- or N-ligands generates weaker, yet reactive M-O or M-N bonds. Typical catalysis includes hydroformylation, hydrogenation, hydrosilylation, isomerization and oligomerization reactions.

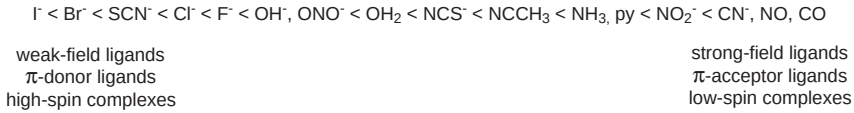

Figure 1-15: Examples of common ligands by field strength [189].

Moreover, 3d transition metals, especially early transition metals with low d-electron counts, bind ligands weaker than 4d and 5d transition metals with high d electron density and usually tend to undergo 1 e^- redox changes instead of 2 e^- redox changes. In addition, 3d transition metals with high oxidation states are generally not very stable with strong oxidizing character. 4d and 5d transition metals with higher oxidation states are more stable and less oxidizing, allowing a more pronounced redox cycle.
Ligands, the second part of a organometallic catalyst, can also affect the reactivity of the complex in two ways:

- Steric effects: depending on whether the ligand is coordinated through a single donor atom (monodentate ligand) or through

multiple donor atoms (chelating ligands), the accessibility of free coordination site for a substrate and its stability can be influenced and thus affecting the metal site to favor a certain reaction. The steric demand of a ligand can be quantified and is known as the Tolman cone angle Θ, for monodentate ligands, or ligand bite angle, for chelating ligands.

- Electronic effects: the nucleophilicity of the ligand affects the ability of the metal to bind substrates. Strong σ-donor ligands increase the electron density of the metal atom, allowing strong π back donation to ligands and vice versa.

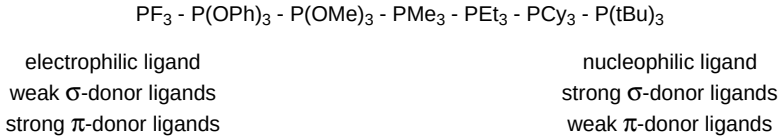

Figure 1-16: Some phosphine ligands with increasing nucleophilicity from left to right.

The combination of metal and ligand results in unique properties of organometallic catalysts in binding and activating the substrates. The valence electrons of the organometallic complex define the strength and mode of bonding of the molecules while the ligand provides the steric hindrance neccessary to direct the selectivity of a reaction.

Process with Solid Catalyst

The most important features of solid catalysts are the stability, easy product separation and catalyst regeneration, which makes their industrial application attractive (Figure 1.7).

Table 1.7: Industrial processes with solid catalysts [170].

Process	Catalyst	Conditions
Steam reforming of methane	Ni/Al_2O_3	750 - 950 °C, 30 - 35 bar
CO conversion	Fe/Cr oxides	350 - 450 °C
Methanization (SNG)	Ni/Al_2O_3	500 - 700 °C, 20 - 40 bar
Ammonia synthesis	Fe_3O_4 (K_2O, Al_2O_3)	450- 500 °C, 250 - 400 bar
Oxidation of SO_2 to SO_3	V_2O_5/support	400 - 500 °C
Oxidation of NH_3 to NO	Pt/Rh nets	900 °C
Claus process (sulfur)	Al_2O_3	300 - 350 °C
Methanol synthesis	ZnO-Cr_2O_3 or CuO-ZnO-Cr_2O_3	250 - 400 °C, 200 - 300 bar or 230 - 280 °C, 60 bar
Fat hardening	Ni/Cu	150 - 200 °C, 5 - 15 bar
Benzene to cyclohexane	Raney Ni or noble metals	liquid phase 200 - 225 °C, 50 bar or gas phase 400 °C, 25 - 30 bar
Aldehydes and ketones to alcohols	Ni, Cu, Pt	100 - 150 °C, up to 30 bar
Esters to alcohols	$CuCr_2O_4$	250 - 300 °C, 250 - 500 bar
Nitriles to amines	Co or Ni on Al_2O_3	100 - 200 °C, 200 - 400 bar

Ethylbenzene to styrene	Fe_3O_4 (Cr, K oxide)	500 - 600 °C, 1.4 bar
Butane to butadiene	Cr_2O_3/{ceAl2O3	500 - 600 °C, 1 bar
Ethylene to ethylene oxide	Ag/support	200 - 250 °C, 10 - 22 bar
Methanol to formaldehyde	Ag cryst.	ca. 600 °C
Benzene or butene to maleic anhydride	V_2O_5/support	400 - 450 °C, 1 - 2 bar
o-Xylene or naphthalene to phthalic anhydride	V_2O_5/TiO_2 or V_2O_5-$K_2S_2O_7/SiO_2$	400 - 450 °C, 1.2 bar
Propene to acrolein	Bi/Mo oxides	350 - 450 °C, 1.5 bar
Propene to acrylonitrile	Bi molybdate (U, Sb oxides)	400 - 450 °C, 10 - 30 bar
Methane to HCN	Pt/Rh nets	800 - 1400 °C, 1 bar
Vinyl chloride from ethylene + HCl/O_2	$CuCl_2/Al_2O_3$	200 - 240 °C, 2 - 5 bar
Cumene from benzene and propene	H_3PO_4/SiO_2	300 °C, 40 - 60 bar
Ethylbenzene from benzene and ethylene	Al_2O_3/SiO_2 or H_3PO_4/SiO_2	300 °C, 40 - 60 bar
Polymerization of ethene (polyethylene)	Cr_2O_3/MoO_3 or Cr_2O_3/SiO_2	50 - 150 °C, 20 - 80 bar

Cracking of kerosene and residues of atmospheric crude oil distillation to produce gasoline	Al_2O_3/SiO_2 or zeolites	500 - 550 °C, 1 - 20 bar
Hydrocracking of vacuum distillates to produce gasoline and other fuels	$MoO_3/CoO/Al_2O_3$ or Ni/SiO_2-Al_2O_3 or Pd zeolites	320 - 420 °C, 100 - 200 bar
Hydrodesulfurization of crude oil fractions	$NiS/WS_2/Al_2O_3$ or $CoS/MoS_2/Al_2O_3$	300 - 450 °C, 100 bar H_2
Catalytic reforming of naphtha (high-octane gasoline, aromatics, LPG)	Pt/Al_2O_3 or bimetal/Al_2O_3	470 - 530 °C, 13 - 40 bar H_2
Isomerization of light gasoline (alkanes) and of *m*-xylene to *o*/*p*-xylene	Pt/Al_2O_3 or $Pt/Al_2O_3/SiO_2$	400 - 500 °C, 20 - 40 bar
Demethylation of toluene to benzene	MoO_3/Al_2O_3	500 - 600 °C, 20 - 40 bar
Disproportionation of toluene to benzene and xylenes	$Pt/Al_2O_3/SiO_2$	420 - 550 °C, 5 - 30 bar
Oligomerization of olefins to produce gasoline	H_3PO_4/kieselguhr or H_3PO_4/activated carbon	200 - 240 °C, 20 - 60 bar

Currently, solid catalysts still dominate 90% of all industrial processes [192]. Solid catalysts are divided into two main types:

- Bulk catalysts, in which the active sites are part of the catalyst structure (e.g. zeolites)
- Supported solid catalysts, in which the active sites are not part of the catalyst structure (e.g. transition metal catalyst supported on silica)

Only surface atoms of a solid catalyst are accessible to the reactants and thus are catalytically active. In general, solid catalyzed reactions consist of several chemical and physical reaction steps (Figure 1-17):

1.) Diffusion of the educts through film diffusion layer to the catalyst surface.

2.) Diffusion of the educts into the pores.

3.) Adsorption of the educts on the inner surface of the pores.

4.) Chemical reaction on the active site.

5.) Desorption of the products from the catalyst surface.

6.) Diffusion of the products out of the pores.

7.) Diffusion of the products away from the catalyst through film diffusion layer and into the fluid phase.

Therefore, in heterogeneously catalyzed reactions, the effective reaction rate is influenced by many parameters, such as the thickness of the film diffusion layer, the bulk density of the catalyst, the pore structure, and the mass transport rate of the reactants in the diffusion layer. Depending on which parameter has the dominating influence on the effective reaction rate, three different cases can be distinguished:

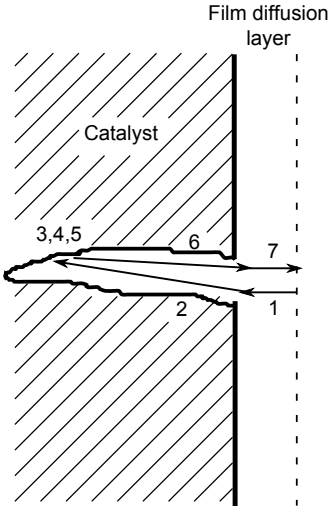

Figure 1-17: Seven steps of heterogeneously catalyzed reaction.

- Film diffusion limitation: the diffusion rate in the fluid film is the slowest and the rate determining step for the reaction rate.
- Pore diffusion limitation: the diffusion rate in the pore is the slowest and rate determining step.
- Kinetic limitation: the chemical reaction rate is the slowest and rate determining step.

Heterogeneously catalyzed processes often require several process improvements to enhance the effective reaction rate. For example, film diffusion limitation can be suppressed by increasing the velocity of the fluid in the reactor. In case of pore diffusion limitation, the ratio of the outer to the inner surface area can be improved by reducing the particle size, thus shortens the pore diffusion path. In addition, all mass transport and kinetic limitation regimes can also be influenced by temperature of the reactions, obeying the Arrhenius law (Figure 1-18).

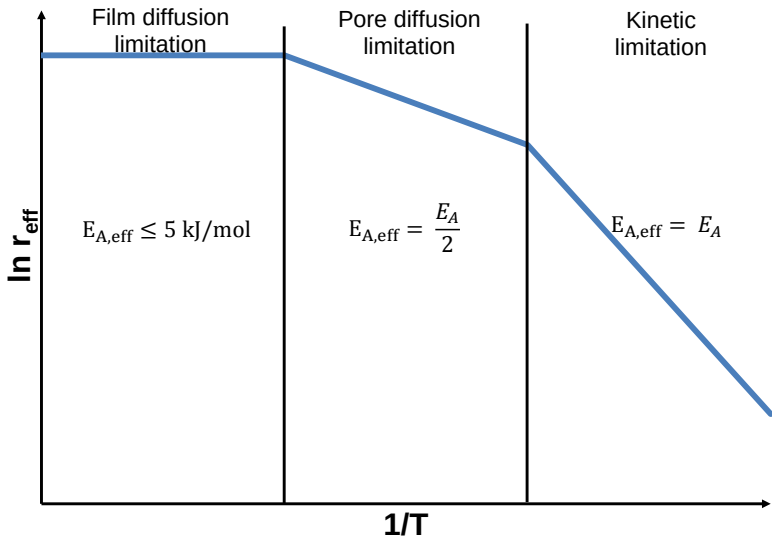

Figure 1-18: Effective reaction rate as a function of reaction temperature.

Heterogeneously catalyzed reactions proceed via chemisorption of the participating molecules at the active sites. There are two important "classical" reaction mechanisms in solid catalysis:

1.) Langmuir-Hinshelwood mechanism
Reactant A and B are adsorbed at different active sites of the catalyst surface. The neighboring chemisorbed reactants A and B react with each other to give product C, which is then desorbed from the catalyst surface.

2.) Eley-Rideal mechanism
Only reactant A is chemisorbed at the catalyst surface. The reactant A reacts directly with B in the fluid phase to give product C, which is then desorbed from the catalyst surface.

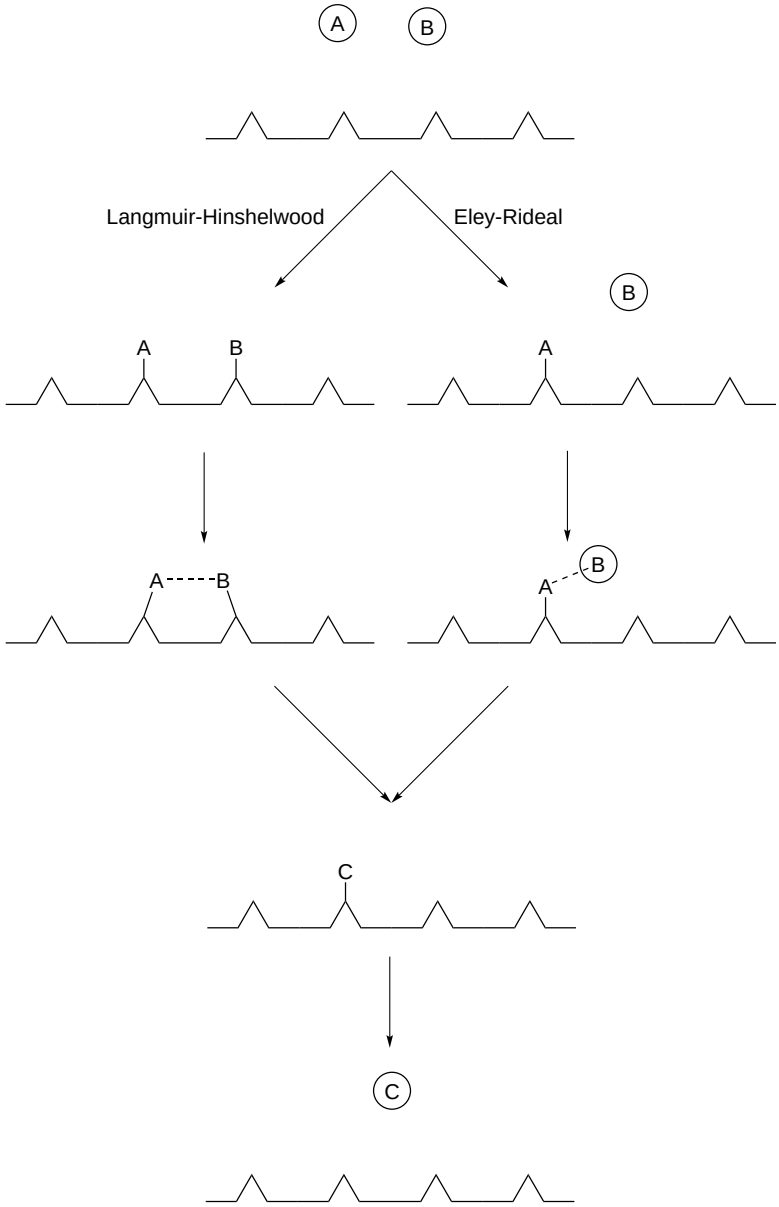

Figure 1-19: Langmuir-Hinshelwood mechanism (left) and Eley-Rideal mechanism (right).

Despite several fundamental differences between molecular and solid catalysis, reactions at solid catalysts can be related to those with organometallic catalystsThe activity of solid catalysts depends on the characteristic of the catalyst surface. Catalyst atoms with low coordination numbers, for example those at crystalline defects, may provide free accessible coordination sites for substrates resulting in enhanced reactivity during catalytic reaction [193]. Moreover, defects generate dangling bonds with different specific electron energy levels, which may affect the coordination and modes of bonding of molecules. A complex synergy between structural and electronic properties of the catalyst surface results in different types of defects (steps or kinks) to favor different reactions to take place. In addition, the electronic property of the catalysts is also determined by long range valence electron sharing over many successive adjacent atoms. The surface of a solid catalyst can donate (n-semiconductors) or accept electrons (p-semiconductors) from adsorbed species, leading to anionic and cationic chemisorption respectively. The donor and acceptor levels of the catalyst can be tailored by introducing dopant. The ability to accept and donate electron allows the catalyst to undergo redox cycle. Lastly, the crystallographic plane of the catalyst influences the geometry and surface density among others, which influence the nature and strength of the interactions with the environment and thus the chemistry of the atoms and molecules forming on the surface. A correctly spaced group of atoms on surface may better accommodate a certain reactant molecules, and thus direct the selectivity of the reaction. While the fundamentals of the solid catalyst and the molecular transition metal catalyst may be similar, direct translation of a homogeneous process with molecular catalyst to heterogeneous one with solid catalyst is not trivial. Finding a solid catalyst system with similar steric and electronic properties of a molecular catalyst transition

metal complex is a trial-and-error process that frequently required high throughput experimentation.

1.5 State of the Art Homogeneously Catalyzed Process: Sodium Acrylate from Ethylene and CO_2

Coupling of ethylene and CO_2 was first reported by Hoberg *et al.* in 1987. The stoichiometric reaction utilized molecular nickel complex yielding a stable nickelalactone species at low temperature [88, 194]. In the following decades, several stable metalalactones have been synthesized either from ethylene and CO_2 coupling or by reacting nickel complex with succinic anhydride [195–199].

In 2006, Walther *et al.* proposed a putative catalytic cycle leading to acrylic acid based on Hoberg's finding [200]. In the first step, a metal complex coordinates ethylene, which forms a stable nickelalactone complex via oxidative coupling with CO_2. In the next step, the nickelalactone transforms into a nickelacrylate complex spontaneously (Figure 1-20). The hypothetical cycle should be completed by subsequent ligand exchange with ethylene, liberating acrylic acid product. However, the catalytic reaction was not experimentally realized as the most challenging step, the cleavage of metalalactone via β-hydride elimination has never been truly understood.

Recently, Rieger *et al.* [197] and Kühn *et al.* [198,201] reported a nickelalactone cleavage step with electrophilic agents, such as methyl iodide or methyl triflate, generating methylpropionate and methylacrylate in low yield. Use of these methylating agents, however, oxidize the metal species irreversibly and thus deactivate the catalyst. Their application in catalytic acrylate reaction is not yet known. This is also due to a

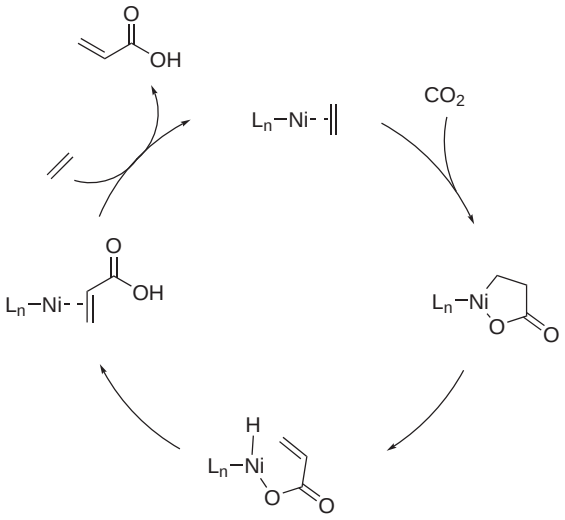

Figure 1-20: Hypothetical catalytic cycle leading to acrylic acid from CO_2 and ethylene according to Walther *et al* [200].

very challenging ethylene mediated liberation of the esters of acrylic acid [197].

In addition, Bernskoetter *et al*. reported nickelalactone cleavage with a combination of Lewis acid and nitrogen-containing base [202]. The Lewis acid promotes ring opening through β-hydride elimination in the nickelalactone species, which readily forms an nickel acrylate complex upon contact with a base, such as *tert*-butylimino-tri(pyrrolidino)phosphorane (BTPP). The application of the finding in catalytic reaction is, however, not yet realized. It can also be expected that a combination of Lewis acid and Lewis base is only possible for a few very unique systems reported as frustrated Lewis pair, which further complicate the development of the catalytic cycle.

Homogeneously catalyzed acrylate synthesis from CO_2 and ethylene

referred in this work will be based on the finding reported by Limbach *et al*. (Figure 1-21) [203, 204]. $Ni(COD)_2$ forms nickel ethylene complex in the presence of a phosphine ligand and ethylene. Under

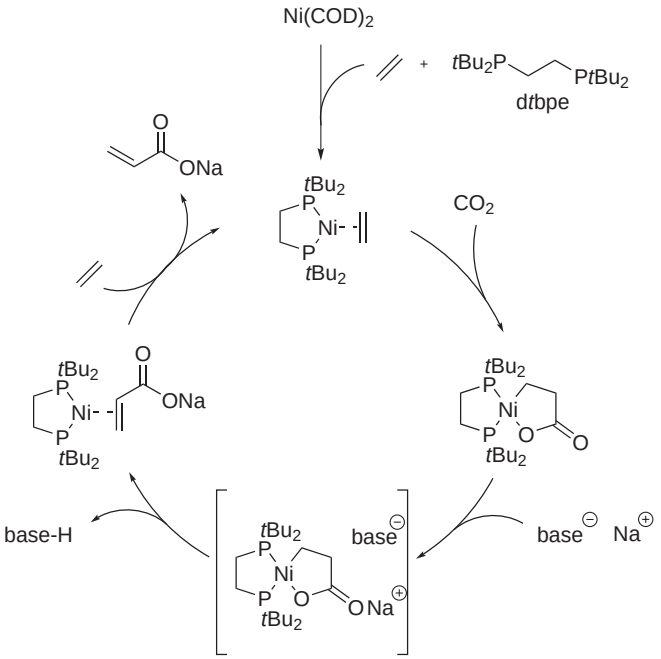

Figure 1-21: Hypothetical catalytic cycle leading to acrylates from CO_2 and ethylene with 1,2-bis(di-*tert*-butylphosphino)-ethane (d*t*bpe) ligand [203].

CO_2 pressure at high temperature, the ethylene complex forms a stable nickelalactone. The optimum pressure and temperature required for nickelalactone formation are greatly influenced by the phosphine ligand (Figure 1-22 and Table 1.8). The following cleavage of nickelalactone to its corresponding acrylate complex is the most challenging step. Contrary to the putative catalytic cycle of Walther *et al*., the nickelalactone cleavage can be achieved by introducing non-nucleophilic base to give

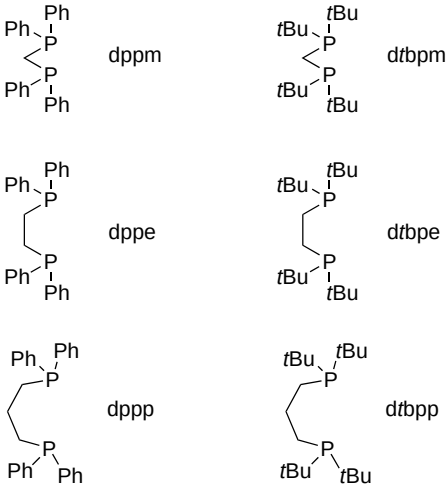

Figure 1-22: List of ligands investigated by Limbach *et al.* for nickelalactone formation [203]. dppm: 1,1-bis(diphenylphosphino)methane, dppe:1,2-bis(diphenylphosphino)ethane, dppp:1,3-bis(diphenylphosphino)propane, d*t*bpm:1,1-bis(di-*tert*-butylphosphino)methane, d*t*bpe:1,2-bis(di-*tert*-butylphosphino)ethane, d*t*bpp:1,3-bis(di-*tert*-butylphosphino)propane

Table 1.8: Nickelalactone formation with various ligands investigated by Limbach *et al*. [203]. Solvent: THF, 2 bar ethylene, 6 bar CO_2, 50 °C, 72 hours.

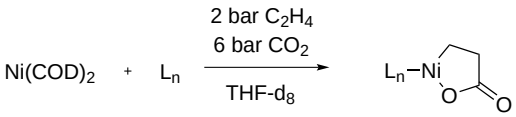

Entry	Ligand	R	Yield Nickelalactone [%]
1	dppm	Ph	0
2	dppe	Ph	0
3	dppp	Ph	0
4	d*t*bpm	*t*Bu	60 (only under ethylene and CO_2 pressure, decomposes upon pressure release)
5	d*t*bpe	*t*Bu	35
6	d*t*bpp	*t*Bu	0

the respective nickel-π-sodium acrylate complex (Table 1.9) [203]. The base was presumed to abstract one of the acidic αproton of the lactone and the sodium cation seems to stabilize the acrylate during the elimination reaction. When the quarternary ammonium salt was used as base (Entry 4 and 5), conversion of the lactone to the respective acrylate was achieved only after the addition of a sodium source, sodium tetrakis[3,5-bis(trifluoromethyl)phenyl]borate ($NaBAr_F$).

Table 1.9: List of bases investigated by Limbach *et al.* for (d*t*bpe)-nickelalactone cleavage [203]. Solvent: Chlorobenzene, 0.025 mmol (dtbpe)-nickelalactone, 0.1 mmol base, optionally 0.05 mol $NaBAr_F$, 30 bar ethylene.

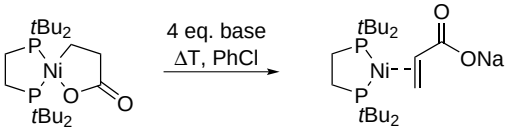

Entry	Base	Additive	Yield [%]
1	NaOtBu	-	90
2	NaHMDS	-	87
3	NaOMe	-	51
4	NBu_4OMe	-	0
5	NBu_4OMe	$NaBAr_F$	47

Exchange of the acrylate species with ethylene closes the catalytic cycle. A DFT calculations of ΔG profile for the acrylate catalytic cycle [203] showed two local maxima corresponding to the energy barrier of nickelalactone formation and cleavage respectively. The catalytic cycle can thus be viewed as a combination of two separate reactions: nickelalactone formation, which is catalyzed by transition metal nickel, and nickelalactone cleavage, which is mediated by a base. Due to a side

reaction of the alkoxide base with CO_2 forming inactive semi-carbonate, Limbach *et al.* proposed a process divided into two separate steps. Nickelalactone is formed in the first step under ethylene and CO_2 rich atmosphere while nickelalactone cleavage step is conducted under CO_2 free atmosphere.

1.6 The Alkoxide Base System - Process Design

The catalytic cycle described by Limbach *et al.* [203] utilized a molecular catalyst, the nickel complex, and an alkoxide as base. A hypothetical process with two separate steps has to be designed to prevent the alkoxide base from forming inactive complexes with CO_2.

Process 1.1 (two steps system according to Limbach *et al.* [203]):

Catalytic reaction

A solution of (d*t*bpe) and $Ni(COD)_2$ (0.025 M) in organic solvent, such as chlorobenzene or THF, is preheated and mixed with gas (ethylene : CO_2 = 1:4) before entering the reactor. The autoclave reactor is further pressurized and heated to reach certain operating pressure (50 bar) and temperature (60 °C). The reactor is run in three different operation modes. In the first mode, the nickel complex forms a nickelalactone complex in the presence of ethylene and CO_2.
Since the formation of nickelalactone from ethylene and CO_2 is strongly affected by the reaction equlibrium, full conversion can hardly be achieved. To maximize the space time yield, after reaching approximately 55 % conversion (2 hours), the reactor is switched to the second operating mode: the reactor is depressurized for the subsequent nickelalactone cleavage. During depressurization, it is important to maintain sufficient

stirring to ensure complete removal of dissolved CO_2 from the solvent. The ethylene-CO_2 gas mixture can be further used to pressurize a second, parallel reactor. The alkoxide base NaO*t*Bu (0.2 eq.) is added into the reactor, which is then immediately pressurized with 20 bar of ethylene, heated at 45 °C, and stirred for 1 hour, during which the base mediated cleavage of the nickelalactone takes place. The operating modes 1 and 2 are repeated up to 18 times, after which, the reactor is completely depressurized (operating mode 3) and the reaction mixture is fed into an extraction module, where the acrylate product is isolated from the reaction mixture via water extraction. To increase efficiency, the heat from the product stream can be recuperated and used to preheat the feed stream. Three different heat exchangers are proposed for the process: two heat exchangers to preheat the feed stream and one heat exchanger to preheat the recycled nickel complex stream.

Product isolation and reactants recycling

The sodium acrylate product is extracted from water with diethyl ether to improve the miscibility gap between the organic and aqueous phases. The liquid-liquid extraction process takes place at 25 °C. The organic phase containing diethyl ether and the nickel complex solution in chlorobenzene is further vacuum distilled to separate the diethyl ether from the nickel complex solution, which can be recycled into the reactor. Diethyl ether is recovered and can be fed into the extraction column. The water phase containing sodium acrylate product and *tert*-butanol, a conjugate acid of the NaOtBu, is further reprocessed by solvent stripping to isolate the sodium acrylate as solid. The conjugate acid of alkoxide base, which forms an azeotrope with water, can be reclaimed, for example

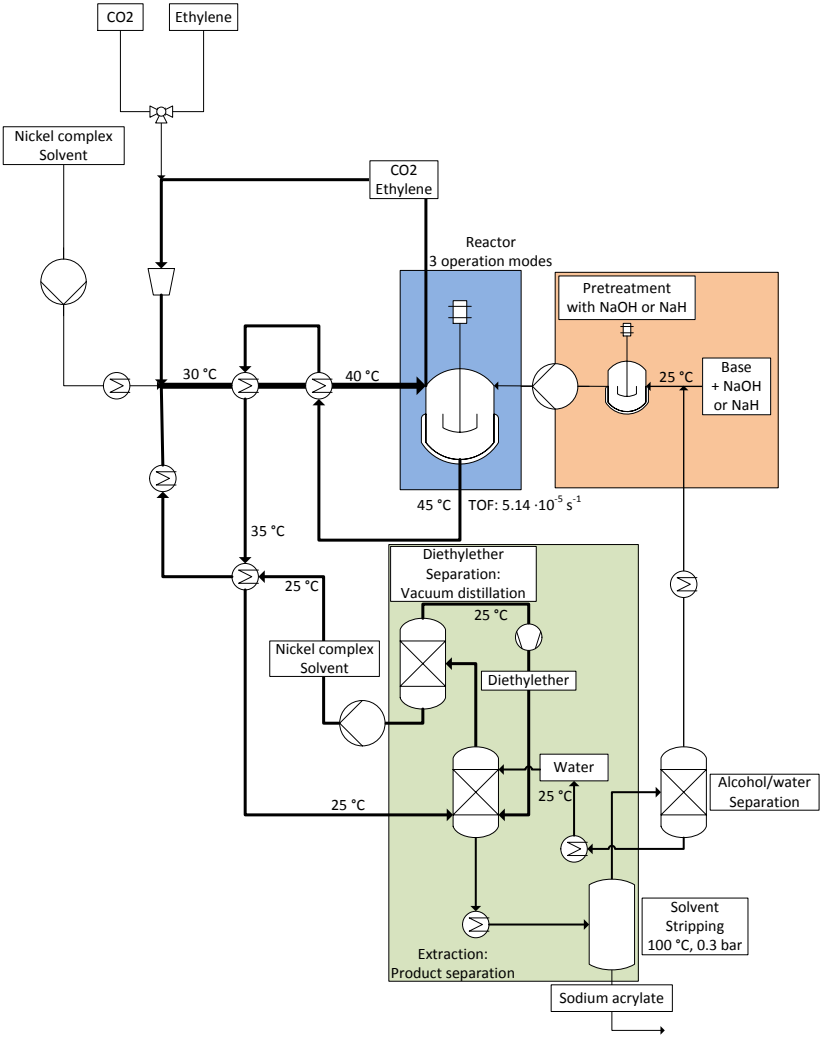

Figure 1-23: Process 1.1: Use of a molecular catalyst nickel complex and CO_2-sensitive alkoxide base in catalytic acrylate reaction.

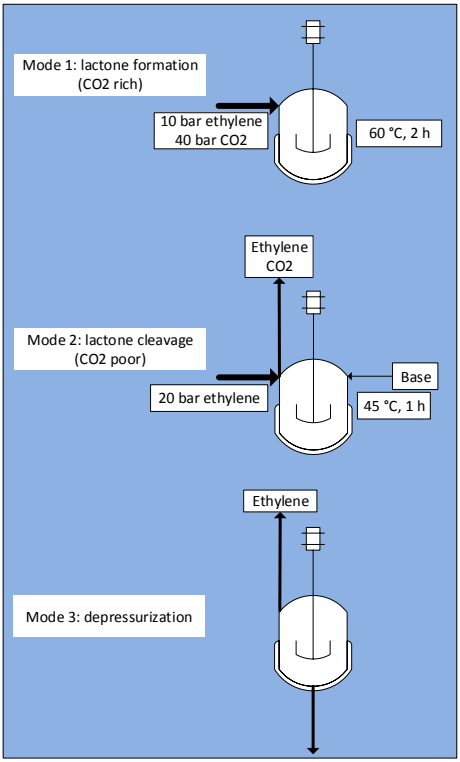

Figure 1-23: (cont.)

via heterogeneous azeotropic batch distillation with cyclohexane as an entrainer [205]. The alkoxide base can be regenerated by reacting its conjugate acid with NaH or NaOH.
The sophisticated process with alternating operation modes and a challenging recycling of the alkoxide base may not be suitable for industrial application. Multi-reactors system operating alternately can be used to maximize the space time yield of the product while recycling the reactants as well as the ethylene and CO_2 gases. Due to the instability of the nickel complex, the process described above has to be carried out strictly oxygen free with low-temperature extraction and recycling steps. All solvents, including water and diethyl ether for product extraction, have to be degassed before use to remove dissolved oxygen.
While the system utilizing a homogeneous nickel complex and an alkoxide base was reported as the only working catalytic reaction of ethylene and CO_2 leading to sodium acrylate [203], the system was limited by several factors:

1.) Side reactions of the alkoxide base with CO_2 yielding the sodium carbonate derivates.

2.) The formation of conjugate acid byproduct of the alkoxide base, which deactivates the Ni catalytic species and can contaminate the sodium acrylate product.

3.) Two-pot process: the formation of nickelalactone with the subsequent, separate nickelalactone cleavage step.

4.) Sophisticated product separation and base recycling processes.

In this work, three different system concepts are proposed to address the limitations of the state-of-the-art process reported by Limbach *et al* [203]:

- Homogeneous process with a molecular nickel complex as catalyst and amine-NaH base systems (Chapter 2).
- Heterogeneous process with an immobilized nickel complex as catalyst and amine-NaH base systems (Chapter 3).
- Heterogeneous process with a molecular nickel complex as catalyst and an immobilized base (Chapter 4).

Chapter 2

Homogeneous Process

2.1 Liquid Base - NaH System

Catalytic acrylate synthesis from CO_2 and ethylene requires an additional electrophilic agent or non-nucleophilic base which can cleave the stable nickelalactone intermediate. Homogeneous process utilizing non-nucleophilic bases have reported a working catalytic cycle. However, most active alkoxide base reported by Limbach *et al*. [203] are limited by their low solubility in reaction solvent and their side reactions with CO_2 yielding their respective sodium carbonate derivates [206]. Additionally, they form conjugate acid byproduct (alcohols), which deactivates the Ni catalyst species and can contaminate the sodium acrylate product. Moreover, due to the high degree of solubility of the alcohols in water, a sophisticated recycling of the base is required after the extraction process. Liquid or readily-soluble non-nucleophilic bases, which do not react with CO_2 or other reactants, are of huge interest and would benefit the catalytic process. Furthermore, high mobility of liquid bases would improve the collision probability of the base with the nickelalactone intermediate, which will be important especially in

processes utilizing solid catalyst. In the preliminary experiments, the combination of a liquid, non-nucleophilic base namely a phosphazene with NaH as cation (Na^+) source were tested and displayed activity in nickelalactone cleavage. It was also found that tertiary amine bases work in combination with NaH. Interestingly this base system work also in the presence of CO_2 pressure, which paves a way to a much better process described in the following subchapter. Some bases with amine functionality investigated in this work are illustrated in Figure 2-2.

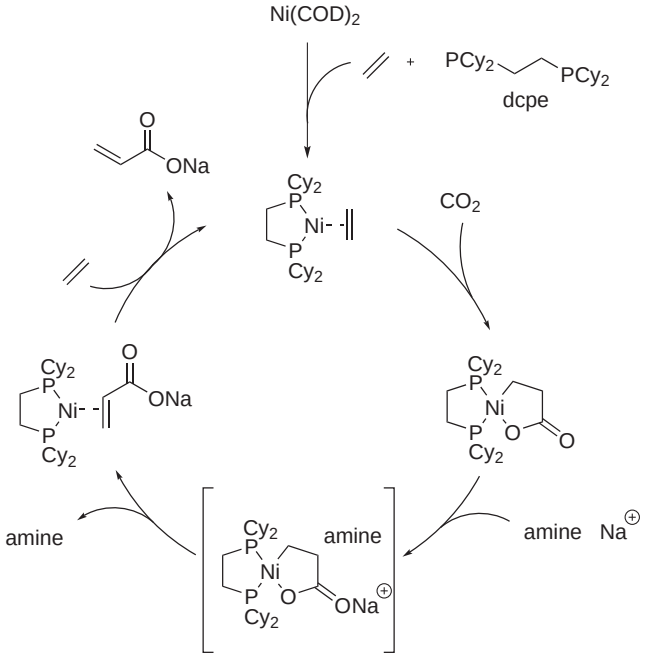

Figure 2-1: Hypothetical catalytic cycle leading to acrylates from CO_2 and ethylene with 1,2-bis(dicyclohexylphosphino)-ethane (dcpe) ligand and amine-NaH base system.

In this work, 1,2-bis(dicyclohexylphosphino)-ethane (dcpe) will be the main ligand investigated (Figure 2-1). The commercially available dcpe,

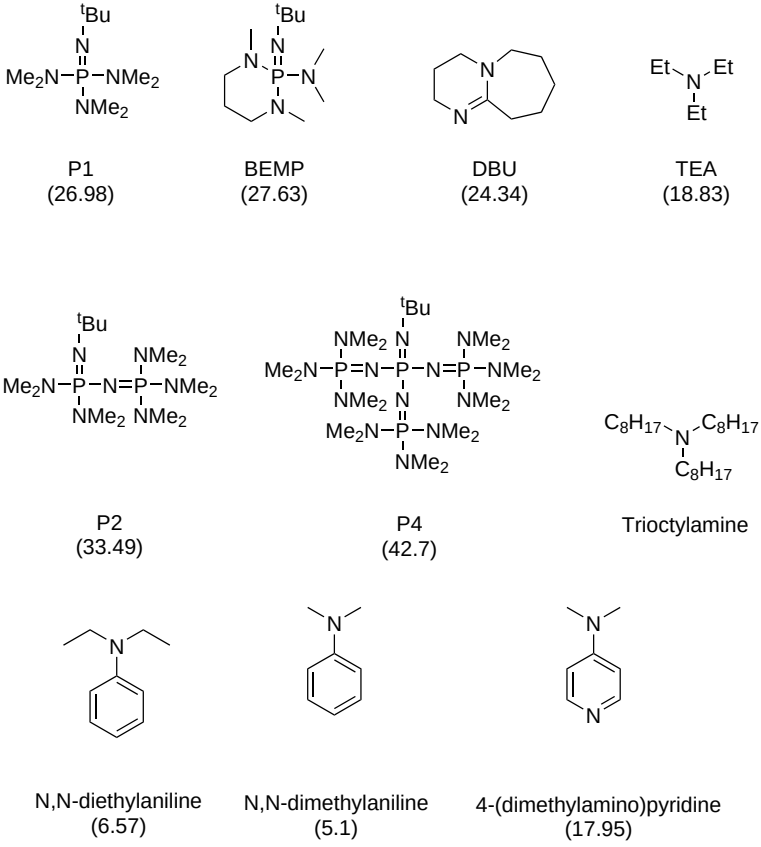

Figure 2-2: Active bases investigated in this work. pK_A values in acetonitrile in parentheses. Exception: *N,N*-dimethylaniline and *N,N*-diethylamine pK_A values in water [207–209].
P1:*tert*-butyl-tris(dimethylamino)phosphorane,
P2:1-*tert*-butyl-2,2,4,4,4-pentakis(dimethylamino)-$2\lambda^5,4\lambda^5-catenadi(phosphazene)$,
P4:1-*tert*-butyl-4,4,4-tris(dimethylamino)-2,2-bis[tris(dimethylamino)-phosphoranylidenamino]-$2\lambda^5,4\lambda^5-catenadi(phosphazene)$,
BEMP:2-*tert*-butylimino-2-diethylamino-1,3-dimethylperhydro-1,3,2-diazaphosphorine,
DBU:1,8-diazabicyclo[5.4.0]undec-7-ene, TEA:triethylamine.

which was reported to readily form a stable (dcpe)-nickelalactone from ethylene and CO_2 [91, 203], is currently the most cost-efficient ligand. Control experiments with dcpe ligand and alkoxide base confirmed the formation of sodium acrylate, justifying its application as a model ligand for the catalytic investigations.

2.1.1 Process Design Options

A process with amine-NaH base system would simplify the process 1.1 described before (Figure 1-23).

Process 1.2 (the lactone formation and cleavage in one reaction step Figure 2-3): Use of an amine-NaH base system, which is active under CO_2, allows both the formation and cleavage of the nickelalactone to be carried out in one-pot process. The process design is based on the experimental data discussed in the next section (Subchapter 2.1.2), with 0.2 mmol $Ni(COD)_2$, 0.2 mmol dcpe ligand, 50 eq. triethylamine as base, 500 eq. NaH as cation (Na^+) source, and 50 mL THF as solvent at 100 °C and 5 bar ethylene and 10 bar CO_2, yielding 101.75 mg sodium acrylate (TON = 5.41, Entry 21 Table 2.1). Contrary to process 1.1 (based on the publication of Limbach *et al*. [203]) described before, the process with amine-NaH base system was run with ethylene : CO_2 ratio of 1:2 and THF as solvent. These parameters was obtained from the reaction optimization carried out at CaRLa with several ligands [210] and are used in this work for easy comparison between project partners.

Catalytic reaction

Dissolved nickel complex in organic solvent THF is preheated and mixed with gas (ethylene : CO_2 = 1:2), triethylamine and NaH before entering the reactor. The autoclave reactor is further pressurized and heated to reach certain operating pressure (15 bar) and temperature (100

°C). Contrary to the process described before (Figure 1-23), the reactor with amine-NaH system is run with all components present in the one-pot reaction. The nickel complex forms a nickelalactone complex in the presence of ethylene and CO_2, which is subsequently cleaved with the amine-NaH combination. The amine-NaH base system is stable during the catalytic reaction, without any side reaction with CO_2. The catalytic cycle proceeds until the process is stopped. The reactor is depressurized, after which, the mixture is fed into an extraction module, where the acrylate product is isolated via water extraction. To increase efficiency, the heat from the product stream can be recuperated and used to preheat the feed stream. Three different heat exchangers are proposed for the process: two heat exchangers to preheat the feed stream and one heat exchanger to preheat the recycled nickel complex stream.

Product isolation and reactants recycling

The sodium acrylate product is extracted from water with diethyl ether to improve the miscibility gap. The liquid-liquid extraction process takes place at 25 °C. The organic phase containing diethyl ether and nickel complex solution is further vacuum distilled to separate the diethyl ether from the nickel complex solution in THF, which can be recycled into the reactor. The diethyl ether is recovered and can be fed into the extraction column. The water phase containing sodium acrylate product and triethylamine, is further reprocessed by evaporating the solvent to isolate the sodium acrylate as solid. Triethylamine can be reclaimed via distillation. Compared to the process described before, the process with amine-NaH system significantly reduces several steps and makes base recycling more efficient. Multi-reactors system operating alternately can be used to maximize the space time yield of the product while recycling the reactants as well as the ethylene and CO_2 gases.

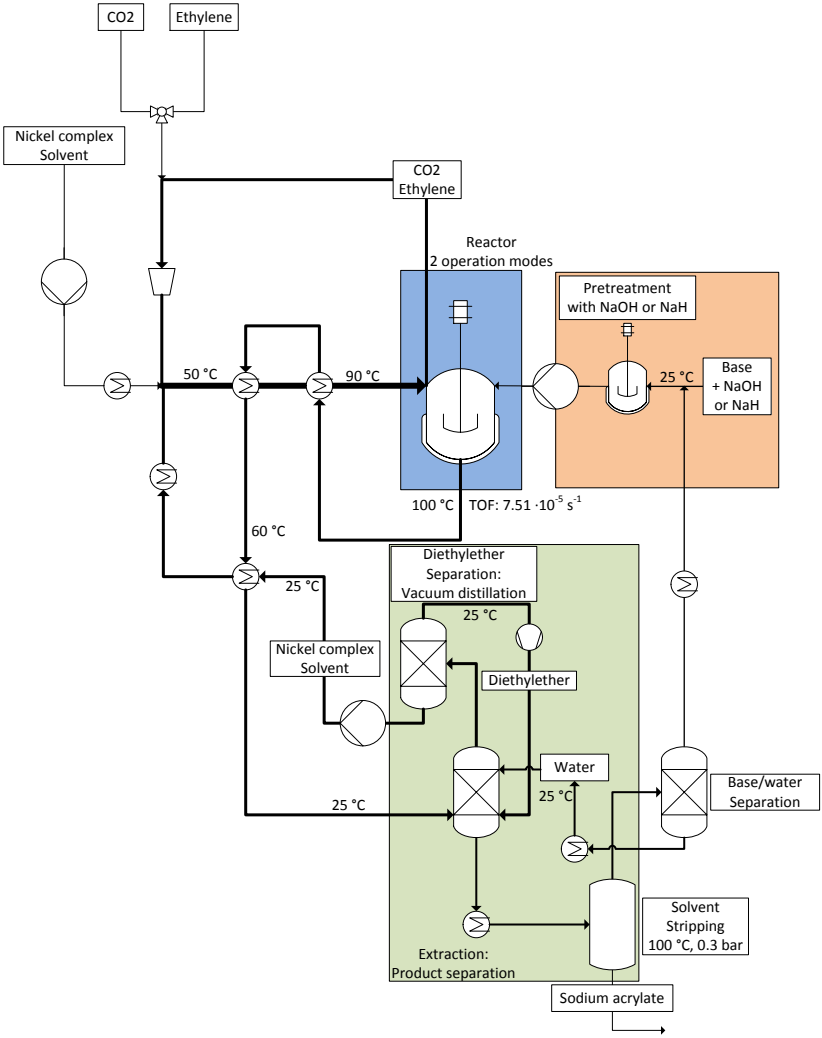

Figure 2-3: Process 1.2: Use of a molecular catalyst nickel complex and CO_2-stable amine-NaH base in catalytic acrylate reaction.

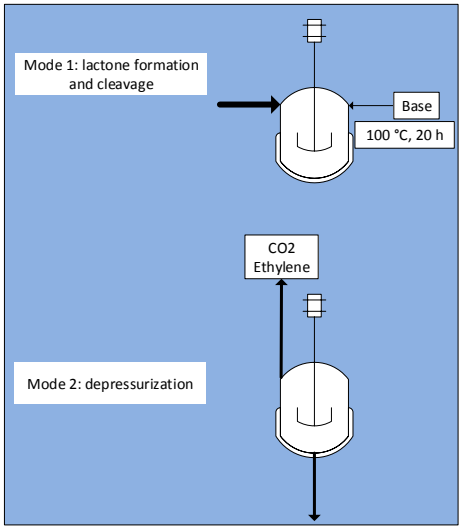

Figure 2-3: (cont.)

Due to the instability of the nickel complex, the process described above has also to be carried out strictly under oxygen-free conditions with low-temperature extraction and recycling steps. All solvents, including water and diethyl ether for product extraction, have to be degassed before use to remove oxygen.

2.1.2 Types of Bases

The effectivity of the bases during catalytic reaction was studied with the same process parameters for the sake of comparison using THF as solvent, 5 bar ethylene and 10 bar CO_2 at 80 °C (Figure 2-4 and Table 2.1). All bases with tertiary amine function investigated in this work displayed a very promising activity. During catalytic reaction, the tertiary amine function may facilitate sodium attacking the lactone forming the respective acrylate complex.

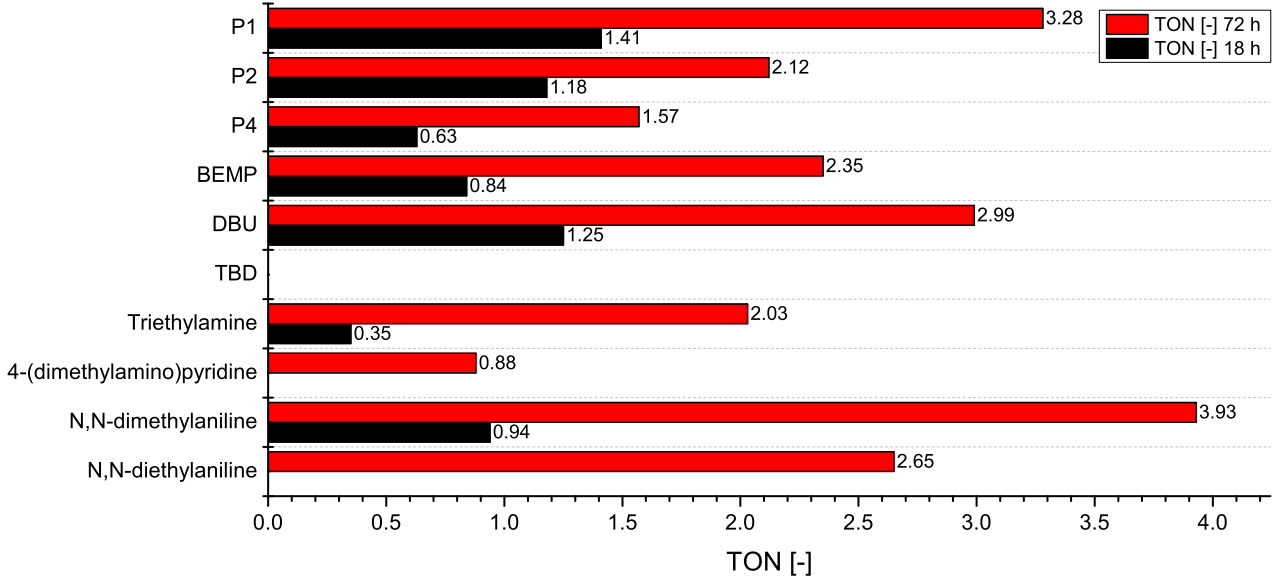

Figure 2-4: Effectivity of different liquid bases during catalytic reaction. Parameters: 0.2 mmol $Ni(COD)_2$, 0.22 mmol dcpe, 2.5 mmol base (except for P4: 1 mmol), 10 mmol NaH, 5 bar ethylene, 10 bar CO_2, 45 mL THF, T = 80 °C, t = 18 or 72 hours. See also Figure 2-6 for reactions with trioctylamine at optimized reaction parameters.

On the other hand, secondary or primary amines are supposed to be inactive due to their side reaction with CO_2 (Figure 2-5, forming insoluble, catalytic-inactive carbamate (for example 1,5,7-Triazabicyclo[4.4.0]dec-5-ene (TBD) yielded TON = 0).

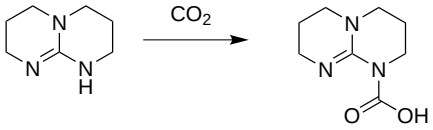

Figure 2-5: Side reaction of triazabicyclo[4.4.0]dec-5-ene (secondary amine) with CO_2 [211].

Of huge importance is the high activity of trioctylamine (Figure 2-6 Table 2.1 Entry 23) as well as *N,N*-dimethylaniline and *N,N*-diethylaniline (Table 2.1 Entry 24-25), which are hardly soluble in water (Solubility in water 0.0001 g/L, 1.2 g/L, and 0.13 g/L respectively) [212]. The application of such bases would not only improve the recyclability of the base itself, but also would simplify the process significantly. Conceptual process design utilizing such bases is further discussed in Subchapter 2.1.5.

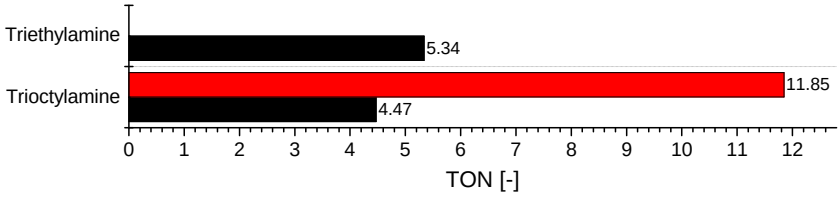

Figure 2-6: Effectivity of different liquid bases during catalytic reaction. Parameters: 0.2 mmol $Ni(COD)_2$, 0.22 mmol dcpe, 10 mmol base, 10 mmol NaH, 10 bar ethylene, 20 bar CO_2, 45 mL THF, T = 100 °C, t = 18 or 72 hours.

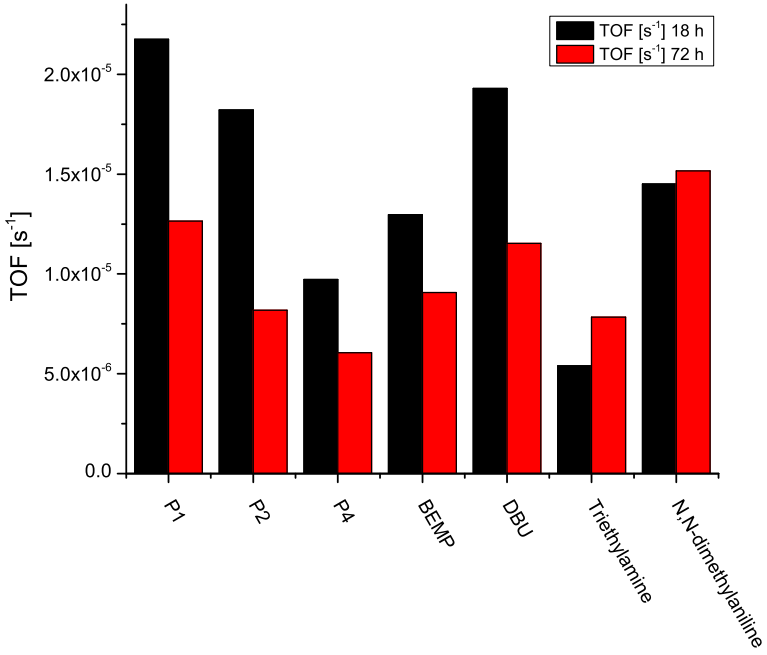

Figure 2-7: Effectivity of different liquid bases during catalytic reaction. Parameters: 0.2 mmol $Ni(COD)_2$, 0.22 mmol dcpe, 2.5 mmol base (except for P4: 1 mmol), 10 mmol NaH, 5 bar ethylene, 10 bar CO_2, 45 mL THF, T = 80 °C, t = 18 or 72 hours.

Despite the high TON values for all reactions mediated with the combination of NaH and P-N superbases or DBU for nickelalactone cleavage, a significant decrease in the average TOF values can be observed in reactions at long reaction time. Average TOF values for reactions carried out for 18 hours and 72 hours are illustrated in Figure 2-7. Compared to 48 hours reactions, average TOF values for reactions utilizing these bases were determined to be up to 55 % lower at 72 hours reaction. The P-N superbase or DBU may form a complex with nickel transition metal via exchange-substitution of the phosphine, which results in less active

nickel-amine complex formation. The resulting nickel-amine complex has the difficulty to undergo reaction with CO_2, which leads to lower amount of nickelalactone available for the catalytic reaction. In addition, less active base would be available for the nickelalactone cleavage. On the other hand, nickel transition metal with phosphine ligand is barely able to be substituted with triethylamine or dialkylaniline base, resulting in a constant average TOF observed for this system, even at long reaction time. The application of triethylamine or dialkylaniline can thus improve the catalyst lifetime compared to superbases investigated at the initial phase of this project. Further investigations with *in situ* NMR will allow to elucidate the side reactions postulated here.

Table 2.1: Effectivity of different liquid bases during catalytic reaction. Parameters: 0.2 mmol $Ni(COD)_2$, 0.22 mmol dcpe, 45 mL THF, cation source: NaH. Entries illustrated in Figure 2-4 and Figure 2-6 are marked in blue

Entry	Base	n_{Base} [mmol]	n_{Cation} [mmol]	T [°C]	$p_{C_2H_4}$ [bar]	p_{CO_2} [bar]	TON [-] t = 18h	t = 72h	t = 100h
1	P1	2.5	0	80	5	10	0	0	0
2	P1	0	10	80	5	10	0	0	0
3	P1	2.5	10	40	5	10	0	0	0
4	P1	2.5	10	60	5	10	0.3		
5	P1	2.5	10	70	5	10	0.41		
6	P1	2.5	10	80	5	10	1.41	3.28	3.11
7	P1	2.5	10	90	5	10	1.57		
8	P1	2.5	10	100	5	10	2.09	3.98	
9	P1	2.5	10	120	5	10	0.91		
10	P1	0.2	10	80	5	10	1		2.63
11	P1	1	10	80	5	10	0.66		2.8
12	P1	2.5	100	80	5	10	1.07		
13	P1	5	10	80	5	10	1.5		3.39
14	P2	2.5	10	80	5	10	1.18	2.12	

15	BEMP	2.5	10	80	5	10	0.84	2.35	
16	P4	1	10	80	5	10	0.63	1.57	
17	DBU	2.5	10	80	5	10	1.25	2.99	
18	triethylamine	2.5	10	80	5	10	0.35	2.03	
19	triethylamine	100	100	80	5	10	0.94	5.99	
20	triethylamine	2.5	10	100	5	10	3.56		
21	triethylamine	10	10	100	5	10	5.41	4.06	
22	triethylamine	10	10	100	10	20	5.34		
23	trioctylamine	10	10	100	10	20	4.47	11.85	
24	*N*,*N*-dimethylaniline	2.5	10	80	5	10	0.94	3.93	
25	*N*,*N*-diethylaniline	2.5	10	80	5	10		2.65	
26	4-(dimethylamino)pyridine	2.5	10	80	5	10		0.88	
27	TBD	2.5	10	80	5	10	0	0	0

The exact mechanism of the base catalyzed nickelactone cleavage is not yet clear. It is however evident that the nickelalactone cleavage with amine-NaH base system should occur catalytically (Figure 2-8, Table 2.1 Entry 6, 10, 11, 13).

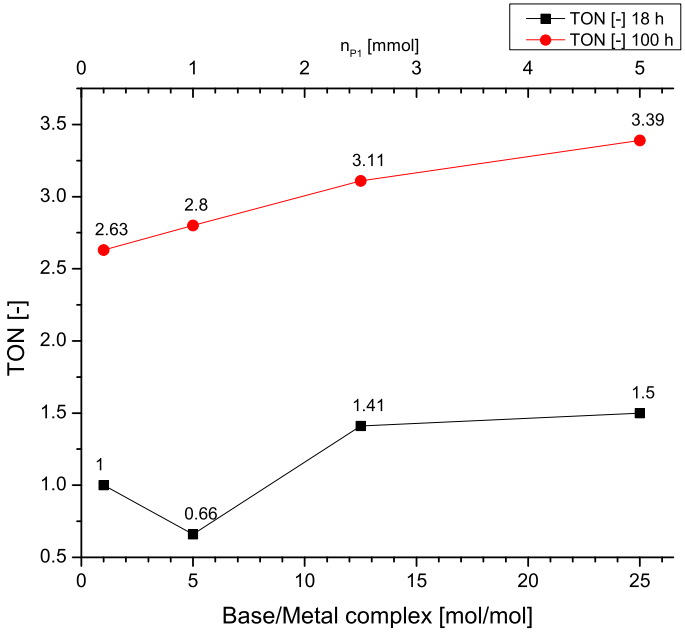

Figure 2-8: Dependency of base amount to catalytic activity. Parameters: 0.2 mmol $Ni(COD)_2$, 0.22 mmol dcpe, P1 base, 10 mmol NaH, 5 bar ethylene, 10 bar CO_2, 45 mL THF, T = 80 °C, t = 18 or 100 hours.

Catalytic amount of base (Base:metal complex ratio = 1) displayed TON of 1 and 2.63 for 18 hours and 100 hours reaction respectively. Increase of base amount did not increase the catalytic activity significantly. In the case of P1 base, the application of 25 eq. instead of 1eq. P1 resulted in an increase in sodium acrylate yield of only 50 % (TON 1 eq. P1 = 1, TON 25 eq. P1 = 1.5) and 28.9 % (TON 1 eq. P1 = 2.63, TON 25 eq.

P1 = 3.39) for 18 hours and 100 hours reaction time respectively (Table 2.1 Entry 10 and 13).

2.1.3 Effect of the Reaction Temperature

The nickelalactone formation is highly temperature dependent and favored at mild temperature of about 50 °C for the d*t*bpe ligand [203]. At lower temperature, the nickelalactone formation is thermodynamically limited, while at higher temperature the nickel complex decomposes forming the corresponding ligand dioxide or monooxide of biphosphines (Figure 2-9).

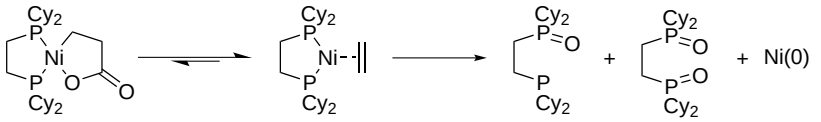

Figure 2-9: Decomposition of (dcpe)-nickelalactone yielding dcpe monooxide, dcpe dioxide, and Ni(0).

The catalytic acrylate formation can be considered as two separate reaction steps with nickel catalyzed lactone formation in the first step and base mediated lactone cleavage in the second step. As consequences, three different operating temperature regions can thus be derived (Figure 2-10):

- Reaction temperature below 60 °C: no sodium acrylate formation can be detected in reactions performed at 40 °C and below. At a slightly higher temperature, the yield of sodium acrylate begins to increase with the temperature.

- Reaction temperature between 60 and 100 °C: linear dependency between the sodium acrylate yield and the reaction temperature.

In this region, the rates of formation and cleavage of the nickelalactone increase with the temperature.

- Reaction temperature above 100 °C: nickelalactone begins to decompose (nickelalactone decomposition is faster than nickelalactone formation and cleavage). The decomposition is irreversible and lead to discontinuation of the catalytic cycle.

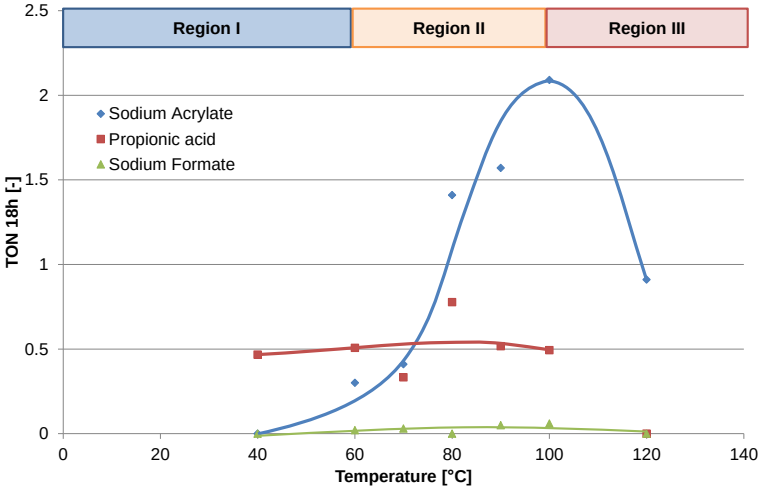

Figure 2-10: Temperature dependency of acrylate catalytic reaction. Parameters: 0.2 mmol $Ni(COD)_2$, 0.22 mmol dcpe, 2.5 mmol P1, 50 mmol NaH, 5 bar ethylene, 10 bar CO_2, 45 mL THF, t = 18 hours (Table 2.1 Entry 3-9).

The amounts of the byproducts, the propionic acid and sodium formate, are constant at around TON 0.5 and 0.03 respectively and are not influenced by reaction temperature. The detected propionic acid can be

formed via the hydrolysis of a fraction of (dcpe)-nickelalactone during the work-up (extraction with water) (Figure 2-11). These findings are consistent with the stability of the nickelalactone itself. The nickelalactone is formed already at low temperature of 40 °C and decomposes at high temperature. At reaction temperature of 120 °C, the amount of propionic acid in the reaction mixture was below the detection limit of the NMR measurement, which can be related to the scarce availability of the nickelalactone. The highest selectivity in sodium acrylate at 79 % can thus be achieved in catalytic reaction performed at 100 °C. A higher selectivity in sodium acrylate could be reached by preventing the hydrolysis of the nickelalactone. This can be realized for example by separating the molecular catalyst and the nickelalactone intermediate before contacting the reaction mixture with water. A representative process concept will be discussed in Chapter 4.

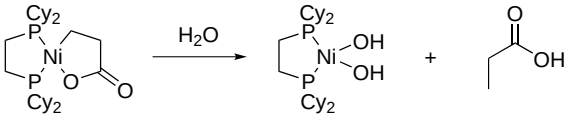

Figure 2-11: Hypothetical hydrolysis of (dcpe)-nickelalactone with water during extraction to give propionic acid.

2.1.4 Effect of the Cation Sources

In addition to the amine base, cation sources such as NaH are crucial for the catalytic cycle as they provide the Na cations and form an active species with amine basic system for the nickelalactone cleavage. Control experiments which only use base or only NaH did not yield any sodium acrylate (Table 2.1 Entry 2). The interaction between the amine base and the Na^+ cation (resulting in ammonium like compound)

may improve the availability of Na^+ cation, thus increasing the collision probability between nickelalactone intermediate and Na^+ during the nickelalactone cleavage. During the cleavage, Na^+ is stoichiometrically consumed while the amine base is not (Figure 2-12). Further in-situ study is necessary to confirm these findings. NaH was the most active

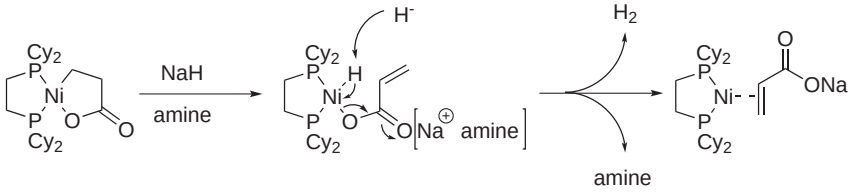

Figure 2-12: Hypothetical cleavage of (dcpe)-nickelalactone with amine-NaH base system to give sodium acrylate.

cation provider as substitution of NaH with LiH (Table 2.2 Entry 8: TON 1.13), KH (Table 2.2 Entry 10: TON 1.49), or NaHMDS (Table 2.2 Entry 6: TON 0.45) resulted in only 35%, 50%, and 14% of the maximum yield of acrylate derivatives observed for NaH (Table 2.2 Entry 1: TON 3.28 for 72 hours reaction time). Utilization of other cation sources, such as CaH_2 (Table 2.2 Entry 9), alkali carbonates (Table 2.2 Entry 3, 4, 12 - 14, and 16), alkali salts (Table 2.2 Entry 3 - 5, 11, and 16), or highly insoluble $NaNH_2$ (Table 2.2 Entry 15), combined with amine base did not deliver acrylate derivative product. Catalytic activity was achieved only with monovalent cations, Li^+, Na^+, and K^+. The effectivity of the cation source can be related to the Lewis acid strength and the size of the cation. Weak Lewis acid sodium cation is reported to be able to lower the energy barrier of β-hydride elimination from a nickelalactone [213]. Among alkali cations investigated in this work, Na^+ is the most effective cation for the nickelalactone cleavage. While K^+ is weaker Lewis acid than sodium, its bulky cationic radius (138 pm) may hinder coordination with lactone species during β-hydride

elimination, resulting in its lower activity. On the other hand, utilization of LiH instead of NaH yielded 50 % less acrylate product. This is due to the lattice energies of alkali hydrides which decreases progressively as the size of the metal cation increases, and as consequences, the stability of these hydrides decreases from LiH to KH [214]. The higher the stability of a cation source, the lower the amount of free cation available during the cleavage of the nickelalactone. Further investigation assisted with DFT calculations is required to elucidate the exact mechanism, in which the Lewis acid promotes β-hydride elimination. The addition of

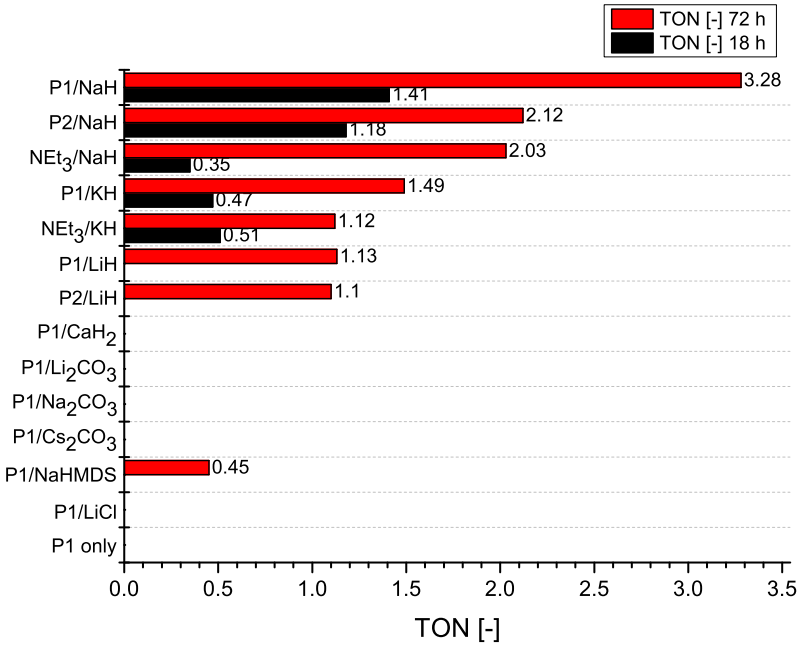

Figure 2-13: Effectivity of different liquid base - additive systems during catalytic reaction. Parameters: 0.2 mmol $Ni(COD)_2$, 0.22 mmol dcpe, 2.5 mmol base, 50 mmol additive, 5 bar ethylene, 10 bar CO_2, 45 mL THF, T = 80 °C, t = 18 or 72 hours.

500 eq. NaH instead of 50 eq. NaH did not increase the catalytic activity (Table 2.2 Entry 1 and 2). Excess base and NaH addition, each 500 eq instead of 50 eq, results in only a moderate increase in catalytic activity from 0.35 to 0.99 (180% increase) and 2.03 to 5.99 (195 % increase) for 18 hours and 72 hours reaction time respectively (Table 2.2 Entry 17 and 18). Due to low availability of nickelalactone species during catalytic cycle (reverse reaction to nickel ethylene complex) and β-hydride elimination step being the rate determining step, excess of base and NaH could not effectively increase the turn over number in a one-pot reaction. Instead, excess of base and NaH could undergo side reactions, reducing the efficiency of the base. Thus, step-wise addition of base and NaH combination may improve the base efficiency and catalytic activity.
The use of alkalihydride, especially NaH is very effective, generating no undesired byproducts. However, the instability and high cost associated with the NaH limits its industrial application. An insoluble heterogeneous base alternative, which is active in the presence of CO_2 under reaction conditions and can be eventually activated with alternative cation source may address this problem and is further discussed in Chapter 4.

Table 2.2: Effectivity of different cation sources during catalytic reaction. Parameters: 0.2 mmol $Ni(COD)_2$, 0.22 mmol dcpe, 45 mL THF, base: P1, P2, or triethylamine (NEt_3).

Entry	Base	n_{Base} [mmol]	Cation	n_{Cation} [mmol]	T [°C]	$p_{C_2H_4}$ [bar]	p_{CO_2} [bar]	TON [-]		
								t = 18h	t = 72h	t = 100h
1	P1	2.5	NaH	10	80	5	10	1.41	3.28	3.11
2	P1	2.5	NaH	100	80	5	10	1.07		
3	P1	5	$NaBAr_F$+Na_2CO_3	0.11+10	80	5	10	0	0	0
4	P1	2.5	$NaBAr_F$+Na_2CO_3	1+10	80	5	10	0	0	0
5	P1	2.5	$NaBAr_F$+NaH	0.2+10	80	5	10	0	0	1.16
6	P1	2.5	NaHMDS	10	80	5	10		0.45	
7	P1	2.5	NaHMDS+NaH	10+10	80	5	10			0.46
8	P1	2.5	LiH	10	80	5	10		1.13	
9	P1	2.5	CaH_2	10	80	5	10	0	0	0
10	P1	2.5	KH	10	80	5	10	0.47	1.49	0
11	P1	2.5	LiCl	10	80	5	10	0	0	0
12	P1	2.5	LiOH	5	80	5	10	0	0	0
13	P1	2.5	Li_2CO_3	5	80	5	10	0	0	0
14	P1	2.5	Cs_2CO_3	2	80	5	10	0	0	0

15	P1	2.5	$NaNH_2$	10	80	5	10	0	0	0
16	P2	2.5	$NaBAr_F$+Na_2CO_3	0.11+10	80	5	10	0	0	0
17	P2	2.5	LiH	10	80	5	10		1.1	
18	NEt_3	10	NaH	10	80	5	10	0.35	2.03	
19	NEt_3	100	NaH	100	80	5	10	0.94	5.99	
20	NEt_3	10	NaH	10	100	10	20		5.34	
21	NEt_3	10	KH	10	100	10	20	0.51	1.12	

2.1.5 Improvement in Process Design

Table 2.3: List of active bases and their solubility in water and THF.

Base	Solubility in water [M] [212]	Solubility in THF [M]
tert-butanol	miscible	3.53
Phenol	0.89	0
Triethylamine	1.31	2.35
DBU	$3.23 \cdot 10^{-2}$	0
N,N-dimethylaniline	$9.9 \cdot 10^{-3}$	1.79
N,N-diethylaniline	$8.71 \cdot 10^{-4}$	1.15
Trioctylamine	$2.83 \cdot 10^{-7}$	0

Base recyclability during the extraction process can be improved by utilizing hardly water-soluble amines: aliphatic amines with long chain or aromatic amines. After complete water removal, organic phase is separated during extraction containing nickel complex and base and can be directly used for the next catalytic cycle. Contrary to process 1.1 and process 1.2 described before, the process utilizing water-insoluble liquid base would only require a simple extraction process to separate the product and recycle the base from the reaction mixture, thus reducing the investment and operational costs.

Process 1.3: Similar to process 1.2, the process design is based on the experimental data with 0.2 mmol (dcpe)-nickelalactone catalyst precursor, 50 eq. trioctylamine as base, 50 eq. NaH as cation (Na^+) source, and 50 mL THF as solvent at 100 °C and 10 bar ethylene and 20 bar CO_2, yielding 155.54 mg sodium acrylate (TON = 8.27, Entry 10 Table 2.4).

Catalytic reaction

Dissolved nickel complex in organic solvent is preheated and mixed with gas (ethylene : CO_2 = 1:2), trioctylamine, and NaH base before entering the reactor. The autoclave reactor is further pressurized and heated to reach certain operating pressure (15 bar) and temperature (100 °C). In a one-pot reaction, the nickel complex forms a nickelalactone complex in the presence of ethylene and CO_2, which is subsequently cleaved with the trioctylamine-NaH combination. The catalytic cycle proceeds until the process is stopped. After the reactor is depressurized, the mixture is subsequently fed into an extraction module, where the acrylate is separated from the reaction mixture via water extraction. Similar to previous processes, the heat from the product stream can be recuperated and used to preheat the feed stream.

Product isolation and base recycling

The sodium acrylate product is extracted from water with diethyl ether to improve the miscibility gap. The liquid-liquid extraction process takes place at 25 °C. The organic phase containing diethyl ether, trioctylamine, and nickel complex solution is further vacuum distilled to separate the diethyl ether from the nickel complex solution, which can be recycled into the reactor. The diethyl ether is recovered and can be fed into the extraction column. The water phase containing sodium acrylate product is further reprocessed by solvent stripping to isolate the sodium acrylate as solid. The trioctylamine remains in the organic phase can be directly transferred, along with nickel complex, to the reactor.
Compared to the two processes 1.1 and 1.2 (Figure 1-23 and 2-3) described before, the process with trioctylamine-NaH system does not require a specific base recycling process. Multi-reactor systems operating alternately can be used to maximize the space time yield of the product.

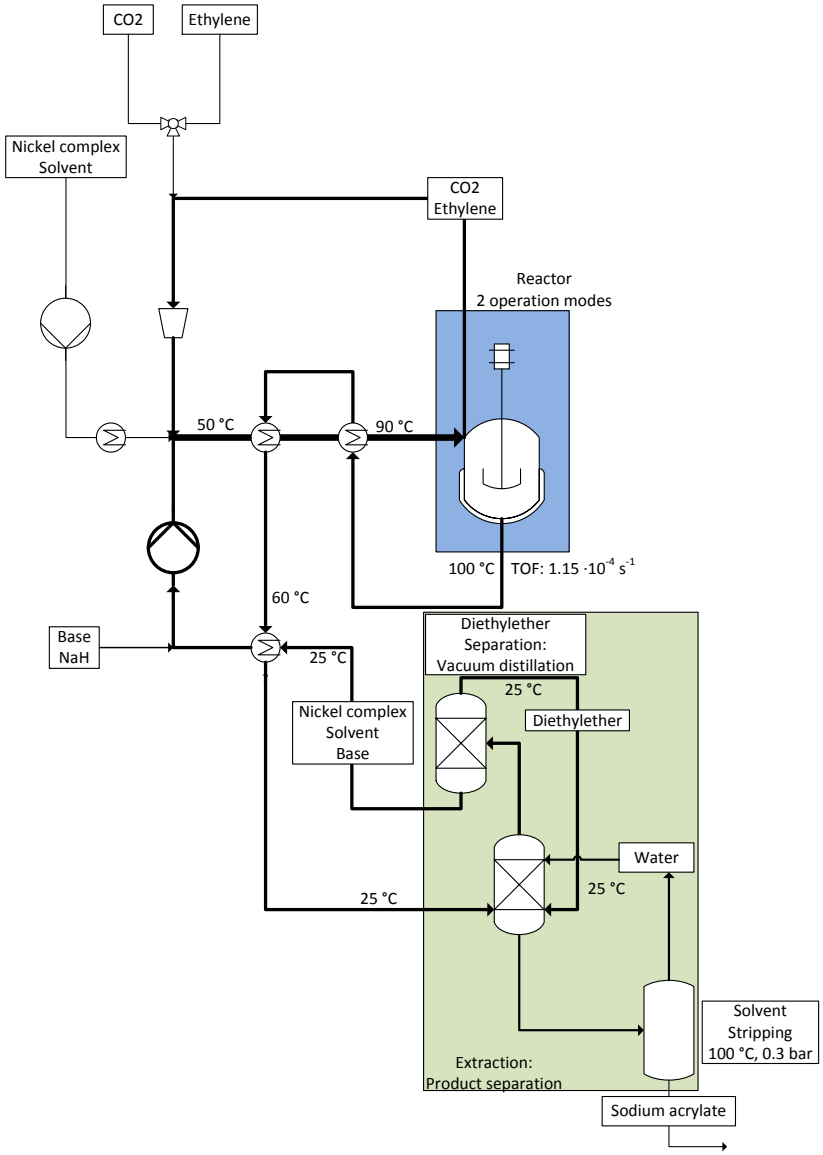

Figure 2-14: Process 1.3: Use of a molecular catalyst nickel complex and water-insoluble base in catalytic acrylate reaction.

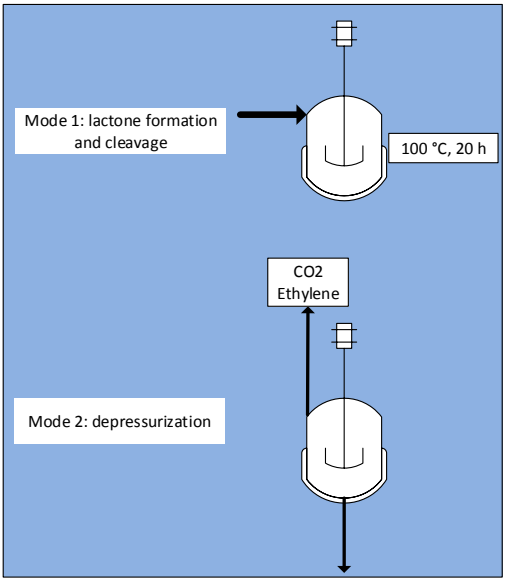

Figure 2-14: (cont.)

Due to the instability of the nickel complex, the process described has to be carried out strictly oxygen free with low-temperature extraction and recycling steps. All solvents, including water and diethyl ether for product extraction, have to be degassed before use to remove dissolved oxygen, which would complicate industrial application.

2.2 Nickelalactone as Starting Point in the Catalytic Cycle

The acrylate reaction comprises the formation of nickelalactone intermediate, which is catalyzed by a transition metal complex, and the cleavage of this intermediate, which is mediated by a base. In the case of one-pot reaction, such as Process 1.2 (Figure 2-3) and 1.3 (2-14) described before, the presence of both catalyst $Ni(COD)_2$, biphosphine ligand, amine base, and NaH at the beginning of the reaction could be problematic. Since $Ni(COD)_2$-ligand *in situ* complexation is a slow process, readily oxidizable phosphine ligand as well as unstable $Ni(COD)_2$ and its side reaction with other reactants are to be expected leading to a reduction of the amount of active species for the catalytic reaction. NaH may form NaOH with trace water, which coordinates to the transition metal nickel complex. This can be avoided by introducing an alternative nickel complex precursor, the nickelalactone complex, which is also an intermediate of the catalytic process. The nickelalactone can be separately prepared, for example via ligand exchange of (tmeda)-nickelalactone with biphosphine ligand (Figure 2-15) [200,215]. Ligand exchange with (tmeda)-nickelalactone is currently the most convenient route to obtain (dcpe)-nickelalactone in high yield (74.8 %, compared to preparation via oxidative coupling of CO_2 and ethylene, which is only

around 15 %). Since only catalytic amounts of (dcpe)-nickelalactone is needed, its preparation via more costly ligand exchange route (1 gram (dcpe)-nickelalactone = ca. 110 €, price calculated from the price of each chemicals needed Sigma Aldrich catalog in March 2014) instead of via oxidative coupling of CO_2 and ethylene (1 gram (dcpe)-nickelalactone = ca. 50 €) can be justified and will represent only a fraction of the final price of the sodium acrylate product in hypothetical industrial process with several thousands TON. The application of

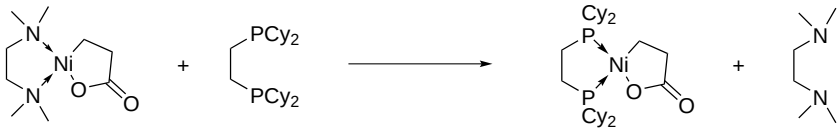

Figure 2-15: Preparation of (dcpe)-nickelalactone species via ligand exchange.

stable nickelalactone species as catalyst precursor improves the overall efficiency of the one-pot process. The use of nickelalactone as precursor significantly increased the TON of the catalytic cycle by approximately up to six times for triethylamine-NaH base systems (Figure 2-16). The improvement in catalytic activity is especially pronounced in 72 h reactions, underlining the amount of active nickel species in the long term. In case of catalytic reactions with triethylamine-NaH system, substitution of $Ni(COD)_2$-dcpe catalyst system with pre-formed (dcpe)-nickelalactone resulted in an increase of the catalytic activity from 0.94 to 5.53 (588 %) and from 4.06 to 18.84 (464 %) for 20 hours and 72 hours reaction time respectively. Constant TOF values for both reactions mediated with triethylamine-NaH with either 20 hours or 72 hours reaction time can be observed: in case of (dcpe)-nickelalactone at around $7.5{\cdot}10^{-5}$ s^{-1} and for $Ni(COD)_2$-dcpe precursors $1.5{\cdot}10^{-5} s^{-1}$ (Figure 2-17). This indicates that both the nickel complex catalyst and the

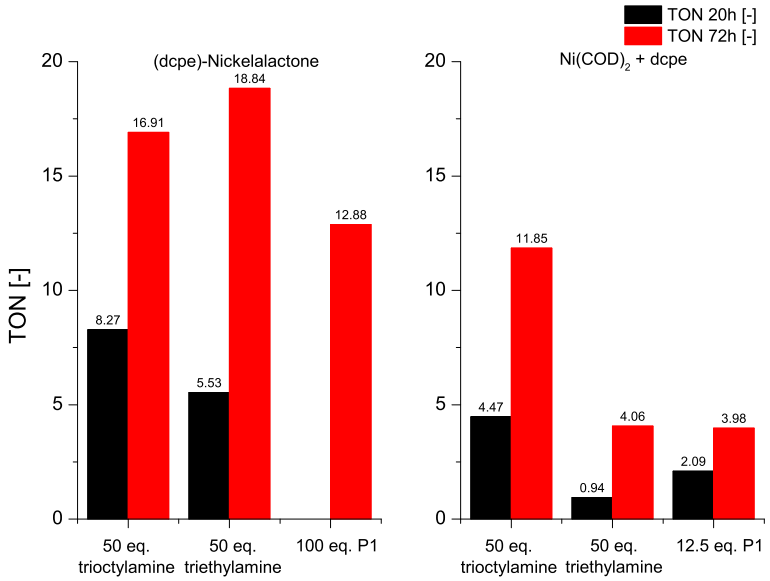

Figure 2-16: Nickelalactone as precursor for the catalytic cycle. Parameters: 0.2 mmol $Ni(COD)_2$ and 0.22 mmol dcpe or 0.2 mmol (dcpe)-nickelalactone, 100 eq. NaH, 10 bar ethylene, 20 bar CO_2, 45 mL THF, T = 100 °C, t = 20 or 72 hours.

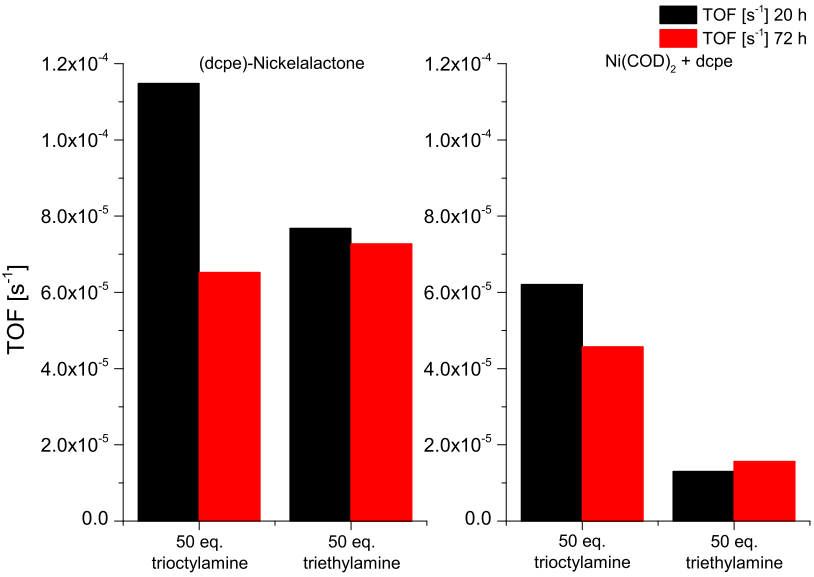

Figure 2-17: Nickelalactone as precursor for the catalytic cycle. Parameters: 0.2 mmol $Ni(COD)_2$ and 0.22 mmol dcpe or 0.2 mmol (dcpe)-nickelalactone, 100 eq. NaH, 10 bar ethylene, 20 bar CO_2, 45 mL THF, T = 100 °C, t = 20 or 72 hours.

triethylamine-NaH system retain their original activities, even at long reaction time. Both the formation and cleavage of the nickelalactone occured at similar constant rate. The TOF for (dcpe)-nickelalactone catalyzed reaction is six times higher than that for reaction with $Ni(COD)_2$-dcpe precursors.

On the other hand, in the reactions with trioctylamine, a decrease in TOF at long reaction time can be observed. In reactions with (dcpe)-nickelalactone as catalyst precursor, TOF value declines from $1.15 \cdot 10^{-4}$ s^{-1} for 20 hours catalytic reaction to about $6.52 \cdot 10^{-5}$ s^{-1} in 72 hours catalytic reaction. Possible explanation may be the high effectivity of the trioctylamine itself (TON for 20 hours reaction is 8.27 while TON for 72 hours reaction is 16.91, Table 2.4 Entry 10). Thus, the overall reaction is limited by the amount of nickelalactone during catalytic reaction. Trioctylamine-NaH system cleaves the nickelalactone intermediate as soon as it is formed. Since the catalytic reaction was started with nickelalactone intermediate, short reaction time would result in higher average TOF value. At long reaction time, however, the nickelalactone formation is the rate determining step, limiting the overall reaction, which leads to lower average TOF value. In reactions with $Ni(COD)_2$-dcpe as catalyst precursor, TOF value declines from $6.2 \cdot 10^{-5}$ s^{-1} for 20 hours catalytic reaction to about $4.6 \cdot 10^{-5}$ s^{-1} in 72 hours catalytic reaction. Further investigations with *in situ* NMR may confirm and elucidate the exact reaction limitation.

Similar to catalytic reactions utilizing a combination of $Ni(COD)_2$ and dcpe precursor, the base amount present during catalytic reaction did not significantly improve the catalytic activity (Figure 2-18 and Table 2.4 Entry 3 - 7). An increase in triethylamine amount from 0.5 eq. to 25 eq., 100 eq., or 200 eq. only yield TON of 5.38 (Entry 6), 5.53 (Entry 3), and 6.04 (Entry 7) respectively. It is also confirmed that

the nickelalactone cleavage with amine-NaH base system is catalytic in homogeneous base. Catalytic reaction with only 0.5 eq. of triethylamine base provided sodium acrylate with a TON of 4.7 (Table 2.4 Entry 5). On the other hand, in reactions with KH as cation (K^+) source, an increase in triethylamine amount results in a decrease in the yield of sodium acrylate (Entry 8 and 9). Catalytic reactions with 25 eq. and 50 eq. triethylamine-KH base system yielded sodium acrylate with TON of 2.2 and 0.73 respectively. The results also affirmed previous finding that weak Lewis acid NaH is the most suitable cation sources for nickelalactone cleavage (Subchapter 2.1.4).

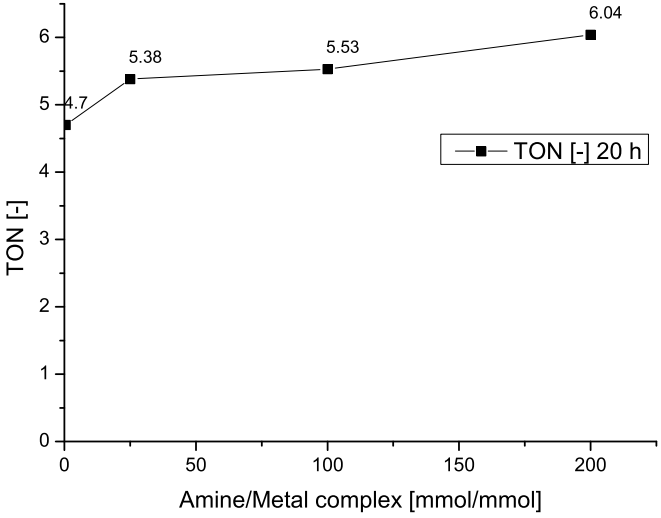

Figure 2-18: Dependency of base amount to catalytic activity. Parameters: (dcpe)-nickelalactone precursor, triethylamine base, NaH cation source, 45 mL THF, 10 bar ethylene, 20 bar CO_2, T = 100 °C, t = 20 hours.

Table 2.4: Use of (dcpe)-nickelalactone as catalyst precursor. Parameters: 10 bar ethylene, 20 bar CO_2, 45 mL THF, temperature = 100 °C, base: P1, triethylamine (NEt_3), or trioctylammine (TOA).

Entry	$n_{(dcpe)-nickelalactone}$ [mmol]	Base	n_{Base} [mmol]	Base/Metal complex [mmol/mmol]	Cation	n_{Cation} [mmol]	TON [-]	
							t = 20h	t = 72h
1	0.1	P1	10	100	NaH	10		15.06
2	0.1	P1	10	100	NaH	10		12.88
3	0.1	NEt_3	10	100	NaH	10	5.53	18.84
4	0.1	NEt_3	10	100	NaH	10	4.44	
5	0.2	NEt_3	0.1	0.5	NaH	10	4.7	
6	0.2	NEt_3	5	25	NaH	5	5.38	
7	0.1	NEt_3	20	200	NaH	20	6.04	
8	0.2	NEt_3	10	50	KH	10	0.73	
9	0.2	NEt_3	5	25	KH	5	2.2	
10	0.2	TOA	10	50	NaH	10	8.27	16.91

2.3 Conclusion

The application of amine-NaH base system is a major breakthrough in the catalytic formation of sodium acrylate, leading to an industrially applicable catalytic reaction. Since tertiary amine-hydride base system remains active under CO_2 atmosphere, both nickelalactone formation and cleavage can be carried out in one-pot process. This would simplify the process and reduce the operating cost significantly. Additionally, amine base mediates the nickelalactone cleavage and is not consumed during the process. The combination of amine base and NaH is crucial to shift the reaction to the product side. Neither of both components works separately for successful nickelalactone cleavage. The nickelalactone cleavage is only limited by the amount of nickelalactone intermediate and the amount of cation source NaH available during the process but not by the quantity of the amine base. TON of up to 18.84 (TOF $7.27{\cdot}10^{-5}$ s^{-1}) was observed in the catalytic reaction with a combination of nickel dcpe complex and triethylamine-NaH base system. Assuming a continuous semi batch reactor with 0.2 mmol nickel dcpe complex molecular catalyst, this would represents a space-time-yield (STY) of:

$$STY = \frac{TOF \cdot n_{Catalyst} \cdot M_{Sodium\ Acrylate}}{V_{reactor}}$$

$$STY = 8.21 \cdot 10^{-5}\ \frac{kg_{\ Sodium\ Acrylate}}{L \cdot h}$$

with $M_{Sodium\ Acrylate}$ = 94.04 g/mol and $V_{reactor}$ = 0.060 L.
The application of hydrophobic amine further underlines the advantage of this process against the homogeneous nickel complex and alkoxide base system reported by Limbach *et al* [203]. The nickel complex and hydrophobic amine-NaH combination would not only offers better base recycling and product separation, but also reduces the investment

costs greatly. TON of up to 16.91 (TOF $6.52 \cdot 10^{-5}$ s^{-1}) was observed in the catalytic reaction with a combination of nickel dcpe complex and trioctylamine-NaH base system. While the space-time-yield in the reaction utilizing hydrophobic amine is slighly lower than that with triethylamine-NaH base combination, the process profitability of that with hydrophobic amine is enhanced by the lower separation and recycle costs.

Chapter 3

Heterogeneous Process with Immobilized Complex

3.1 Theory

Over the past few decades, huge number of ligands and their transition metal complexes have been developed with far higher selectivity and activity compared to their heterogeneous counterparts. Despite this remarkable success, solid catalysts still dominate 90% of all chemical processes in the chemical and petrochemical industries [192]. Higher cost of metal-ligand system, cost- and energy-extensive separation, and the crucial catalyst recovery required in processes utilizing molecular catalysts are the main concern for their application in industrial large scale production. One prominent example is the hydroformylation of lower alkenes with cobalt catalyst. The separation of the cobalt metal from the low-boiling aldehydes can be achieved via simple distillation [216].

This sparks a growing interest in both academia and industry, to develop immobilized molecular catalysts, which combine the fast rates and high selectivity of molecular catalysts with the easy recovery of solid catalysts. There are several concepts to immobilized molecular catalysts [217–222]:

- Steric hindrance in porous systems ("ship in bottle" concept): Steric constraint can be introduced by assembling a catalytically active complex inside the cages of porous support or by building the framework surrounding the complex. The size of the metal complex relative to the dimension of the cages is the decisive factor in the stability of the catalyst and may also contribute to selectivity, activity and kinetics of the reaction. In addition, the dimension of the cages and the pore opening can also induce shape selectivity phenomenon in (micro-)porous catalyst.

- Non-covalent interactions due to physisorption (van der Waals interaction) and Ion Exchange (Electrostatic interactions): Non-covalent interactions offer a relatively easy preparation strategy, for example via a simple impregnation procedure. Due to weak interactions between ligand and support, the prepared catalysts often suffer from extensive leaching, especially during catalytic reactions, when solvents and/or substrates tend to be competitively adsorbed and replace the immobilized catalyst.

- Grafting: In grafting, one or more groups of the support surface are chemically bonded to a metal center. The covalent bond increases the stability of the catalyst, but also results in electron sharing between the metal center and the surface, which modifies

the whole metal complex properties (coordination number, oxidation state, or symmetry).

- Anchoring (tethering): Alternatively, metal complex can be covalently anchored by connecting to the support surface with a series of covalent bonds. Long linker between the metal complex and support ensures no electron sharing between the metal center and the surface group, thus the metal complex may retain its properties.

Both covalent immobilization concepts, grafting and anchoring, are the most synthetically demanding strategies, yet offering the strongest bond between the complex and support. For successful immobilization, they often require synthetic functionalization of the support. In case of anchoring, the immobilized molecular catalyst can retain its properties, thus similar high catalytic activity to the not-immobilized molecular catalyst.
In the development of such hybrid catalysts, disadvantages observed in both solid and molecular catalysis can not be neglected: limited contact between the reactants in the liquid phase and the active sites at the surface of the catalyst, generally observed in solid catalysis, and leaching of the metal component. Parallel adjustment of the catalytic process from the perspective of engineering as well as the process parameters themselves, is vital and should not be overlooked.
The study of ligand immobilization in this work will be strictly focused on anchoring metal complex with 1,2-bis(dicyclohexylphosphino)-ethane (dcpe) ligand, specifically at either the carbon atom position at the bridge or the cyclohexyl substituents (Figure 3-1). The commercially available bidentate dcpe ligand was reported to yield nickelalactone with a good solubility in common solvents [91]. In the experiments with amine-NaH base system, dcpe also showed a decent activity with TON

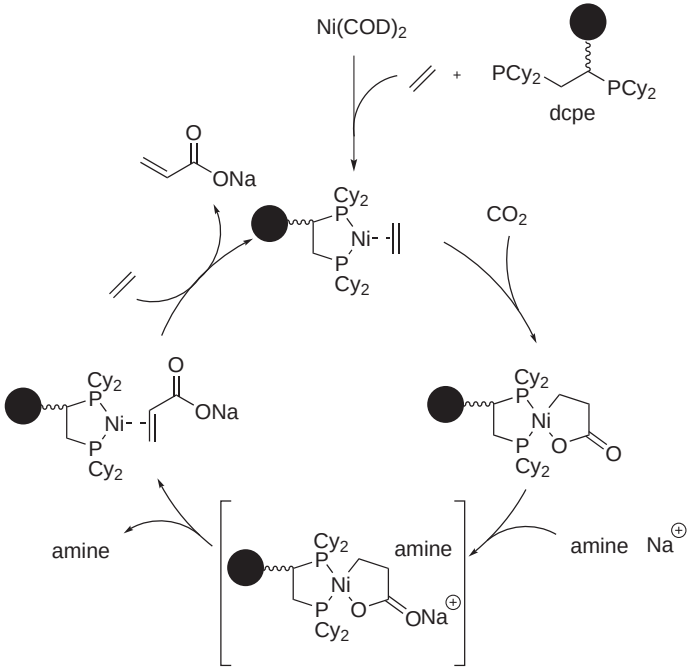

Figure 3-1: Hypothetical catalytic cycle leading to acrylates from CO_2 and ethylene with immobilized 1,2-bis(dicyclohexylphosphino)-ethane (dcpe) ligand and amine-NaH base system.

of up to 18.84 with triethylamine-NaH base combination and Ni as metal center (Table 2.4 Entry 3).

3.2 Process Design Options

From the process engineering point of view, homogeneously catalyzed process for acrylate production is very challenging. It requires a sophisticated and energy-intensive product separation step, during which the readily oxidizable catalyst may be deactivated upon contact with water used for extraction. In stark contrast, the heterogeneously catalyzed process offers several advantages. The application of solid catalyst allows continuous operation of the catalytic reaction. The process can be designed so that the catalyst remains catalytically active in the reactor while allowing the reaction solvent containing dissolved sodium acrylate product to be continuously isolated. This would avoid any unintentional oxidation of the air-sensitive nickel complex as well as increase the space time yield and reduce the operational cost.

Process 2 (immobilized catalyst): The process design is based on the experimental data discussed in the next section 3.4 (Table 3.10 Entry 8): an immobilized (dcpe)-nickel complex with polystyrene support (loading: 0.075 mmol dcpe for each gram immobilized catalyst), 260 eq. triethylamine or trioctylamine, 260 eq. NaH as cation (Na^+) source, and 50 mL THF as solvent with operating temperature of 100 °C and 10 bar ethylene and 20 bar CO_2. The preparation of immobilized ligand will be further discussed in the next section. The immobilized catalyst can be introduced into the reactor in two ways:

- introduction of immobilized ligand and $Ni(COD)_2$ into the reactor or

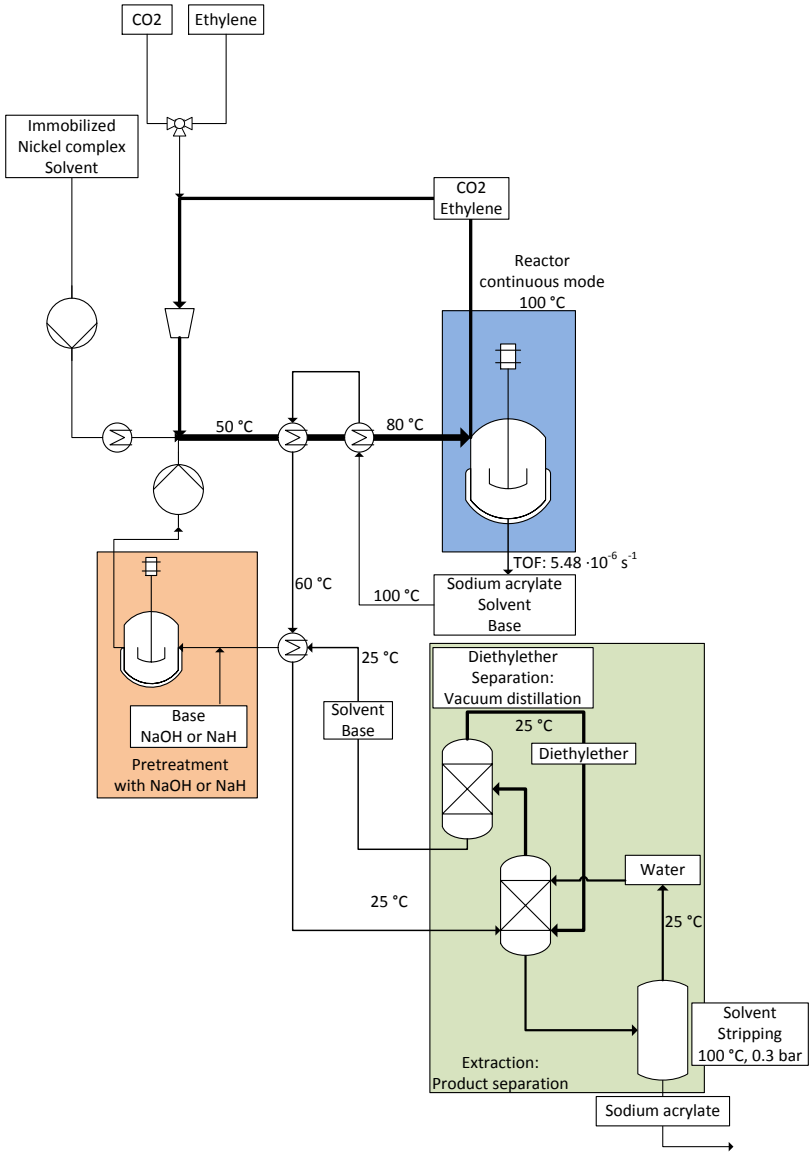

Figure 3-2: Process 2: Use of immobilized molecular catalyst and water-insoluble base in catalytic acrylate reaction.

- introduction as the stable key intermediate, the lactone species, analog to description in section 2.2.

In the latter approach, the lactone species can be prepared via ligand exchange with (tmeda)-nickelalactone either separately before the reaction or directly *in situ*. The exact approach will be discussed in the following section.

Catalytic reaction

The immobilized catalyst along with base is suspended in the reaction solvent THF, preheated, and mixed with amine and NaH before entering the reactor. Ethylene and CO_2 pressures are each 10 bar and 20 bar respectively. During the catalytic reaction, the operating pressure and temperature of the autoclave reactor are kept at 30 bar with ethylene to CO_2 ratio of 1:2 and temperature of 100 °C. Stirring with 2000 rpm is important to ensure sufficient contact probability between the reactants in the fluid phase and the catalytic active site on the solid material.

Product isolation and recycling of the reactants

A part of the liquid is continuously fed into an extraction module, where the acrylate product is isolated via water extraction. Similar to the previous processes described before, the sodium acrylate product is extracted from water with diethyl ether to improve the miscibility gap. The liquid-liquid extraction process is conducted at 25 °C. The organic phase containing diethyl ether, trioctylamine, and nickel complex solution is further vacuum distilled to separate the diethyl ether from the nickel complex solution, which can be recycled into the reactor. The diethyl ether is recovered and can be fed into the extraction column. The water

phase containing sodium acrylate product is further reprocessed by solvent stripping to isolate the sodium acrylate as solid. The trioctylamine remaining in the organic phase can be directly transferred, along with the nickel complex, to the reactor. Multi-reactors system operating in parallel can be used to further maximize the space time yield of the product.

3.3 Catalyst Design via Anchoring

Covalent immobilization of molecular catalysts to (in)organic materials via anchoring is one of the most popular concept for catalyst immobilization, especially in the fine chemical synthesis. Ideally, anchored catalysts should offer high stability and re-usability without leaching while at the same time display the same catalytic activities as their homogeneous counterparts. The character of immobilized catalyst depends on the linker, which connects the metal complex and the support. With increasing length of the linker, any unintentional interactions of the immobilized complex with the support can be minimized and the immobilized catalyst will become more mobile and more similar in activity to its homogeneous counterpart. This would affect the catalytic activity and product selectivity during the reaction. Use of a short linker may lower the catalytic activity or even lead to catalyst deactivation due to steric constraints of the support materials, leading to low accessibility of the active site. However, a very long flexible linker can lead to a higher risk of the metal complex interacting with solid matrix and being chemisorbed (Figure 3-3).
In addition, the support material and the linker should display sufficient

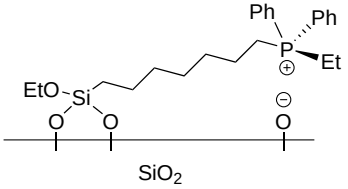

Figure 3-3: Long, flexible linker resulting in a strong interaction between metal complex and the solid matrix.

mechanical, thermal, and chemical stabilities during reaction. Poor stability of the immobilized complex or linker decomposition can result in leaching of the transition metal or ligand.
It is important that anchoring of the metal complex on the support surface occurs in such position that the metal complex retains its electronic and structural properties. Furthermore, synthetic approach for immobilization should omit any strong oxidizing or reducing reagents or other harsh conditions, which may lead to the decomposition of ligand of metal complex. Anchoring of the metal complex can be accomplished with two different strategies:

- Preassembly of metal complex with a linker functionality followed with immobilization of the whole structure on support.

- Modification of the support material with linker with active ligand functionality, followed with metal complexation in the final step.

While the first approach has the advantage that the metal complex can be well characterized before immobilization and obtained in high purity, it suffers from the decomposition of the metal complex and unintended side reactions with supports, especially when the support reacts more favorably with the catalytic species and not with the linker functionality.

In the second strategy, the step-wise functionalization, the linker-functionalized support can be prepared in large quantity, a part of which can be separately anchored with different metal complexes, easily resulting in a potentially large and diverse catalyst library. The step-wise functionalization also avoids decomposition of the unstable metal complex, commonly observed when preformed metal complex is directly anchored. Contrary to the first strategy, the step-wise functionalization may generate several side products on the surface of the support. This results in several structures on the surface, thus preventing the construction of a single-sited solid catalyst. Nevertheless, due to the added stability and versatility, the second approach, the step-wise functionalization, is widely employed to prepare immobilized catalyst and will be further discussed in this chapter.
Depending on how the active ligand component is formed, the second approach can be further differentiated into two synthetic strategies (Figure 3-4:

- Sequential assembly of active ligand.
  The support is incrementally functionalized with several building blocks to form a linker with ligand functionality at the other end, followed with metal complexation in the final step.

- Direct anchoring of pre-formed ligand on support.
  An active ligand is separately prepared and then directly reacted with reactive functional group of the support.

In both synthetic strategies, the linker is firstly anchored at the support, followed by immobilization of the ligand. The first synthetic strategy, while much more complicated and comprising several steps, offers the advantage that each synthetic steps during ligand immobilization can be controlled, thus minimizing the amount of side products and increasing

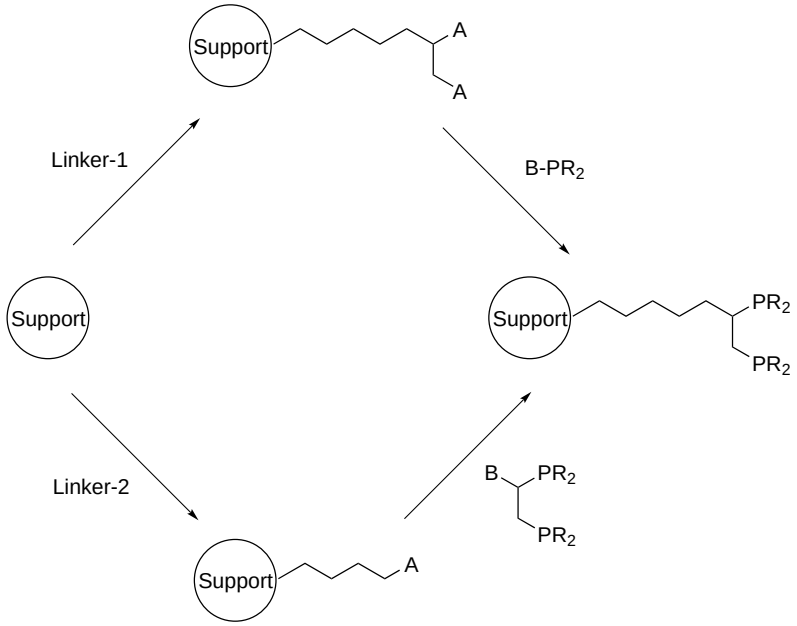

Figure 3-4: Simplified schema of two synthetic approaches for ligand immobilization. Top: Sequential assembly of active ligand, bottom: Direct anchoring of active ligand.

the ligand loading. On the other hand, the second strategy has the advantage that the ligand can be well characterized before immobilization. An additional advantage of the second synthetic strategy is the fact, that the catalytic activity of the metal complexes in homogeneous catalytic reaction can be directly compared with their activity in heterogeneous one after immobilization. However, contrary to the first strategy, the ligand can react with the reactive surface and not with the intended functional group, resulting in inactive or non-accessible ligand. It is therefore essential to protect the catalytic active site of the ligand with a certain protecting group to avoid any unintended reaction between support and the ligand.
In general, there are two types of support which are frequently used for immobilization purpose:

- Insoluble polymer supports
  Use of polymer support was introduced by Merrifield in the solid phase peptide synthesis [223]. The synthesis method is frequently used in combinatorial chemistry, which has the highest impact in the pharmaceutical industry and material science. The solid phase peptide synthesis utilizes a cross-linked polystyrene resin with reactive functionality, for example Cl or Br. The insoluble, yet in organic solvent swellable polymeric material is inert to common synthesis conditions during immobilization. Typically, it is prepared via radical suspension polymerization of styrene, functionalized styrene, and a cross-linker such as divinylbenzene. Polymeric supports are however not suitable for reaction with high temperature over 130 °C or when highly electrophilic reagents are used as it is no longer inert under those conditions.

- Oxide supports
  Oxides are cheap and abundantly available support materials. Oxides are one of the most frequently used types of supports in solid catalysis. Contrary to polymer supports, oxides are chemically and thermally more stable in organic solvents. Moreover, they display better thermal conductivity than polymer supports, so that local hot-spot effects during reaction can be avoided.

The anchoring of the ligand is accomplished via the functionality of the solid support. The choose of suitable support is therefore crucial to ensure facile substitution and high loading of the linker and/or ligand. In general, there are two different approaches, how the support can be functionalized with a meaningful linker:

- Simultaneous support synthesis and functionalization.
- Post-synthetic functionalization.

In the first approach, the linker with appropriate reactive moiety is added as the support synthesis takes place, whereas in the latter case the linker is added in a second step after the synthesis of the support is completed. The first approach can be achieved, for example via co-condensation [224–227] of various organosilanes in case of organosilica support or copolymerization of monomers with a certain functional group. This one-pot synthesis affords a material with homogeneous distribution of the linker. It also provides better control over the amount or loading of the linker in the support materials. This synthetic approach, however, is limited in that the linker, with their specific molecular sizes, hydrophobic/hydrophilic properties, and concentrations, may compromise the meso- or micro-structure of the resulting material [228]. Additional drawback is that a part of linker is sterically inaccessible for the reaction. The second synthetic approach can be accomplished, for example by

grafting a silica material with organosilanes [224, 227]. Post-synthetic modification of a support is advantageous in that the pore size is better defined and the exterior surface of support material can be selectively functionalized. The fraction of accessible linker is therefore much higher in material prepared with the second approach. The disadvantage of this method is, however, that the linker tend to be anchored in the opening of the pore, blocking the internal catalyst pore. In addition, due to mass transport phenomenon (film and pore diffusion), the reaction of a linker with the surface is limited, thus repeated grafting with longer reaction time is necessary to achieve high loading.

The immobilization effort discussed in this work will be based on two different support classes: commercial polymer support with linker functionality prepared via copolymerization of the respective monomer (Simultaneous support synthesis and functionalization) and silica materials, which was firstly grafted with organosilanes linker before further functionalization. The latter support material was prepared via post-synthetic modification via condensation of the organosilanes with the hydroxyl groups at the surface of the silica. The resulting Si-O-Si bond is strong such that it requires extreme conditions and strong acids or bases to detach the grafted linker [229]. Grafting is significantly affected by several factors: solvent used for the reaction [230–232], temperature [233–236], type of organosilanes precursor [233], reaction duration [234,236,237], and post-treatment [231,237–241]. In addition, silanization carried out in solution also greatly depends on the concentration of organosilane [233, 242, 243] precursor and the presence of trace water [237,242–244]. Generally, solvent with the presence of trace water is desirable to prepare a smooth grafted silane layer. However, excess water results in uncontrolled polymerization of the silane both on the surface of the support material as well as in solution, leading

to structural irregularities. Moreover, high silane concentration may accelerate the formation of oligomers and polymers in solution, which will reduce the amount of strongly grafted linker on the support material. It is also known that low reaction temperature promotes weakly bonded silane linker, which is readily displaced upon washing with toluene, ethanol, or water. Post-treatment drying ensures that covalent bond formation proceeds through condensation of hydrogen bonded silanol groups, and can be carried out either under vacuum [236] or under inert gas stream [245]. Among the organosilanes, ethoxysilanes are the most popular ones, yielding a well-defined functionalized surface without harmful acidic reaction byproducts and undesirable cross-linking [246]. While Chlorosilanes are more reactive than alkoxysilanes, the resulting HCl during the reaction with silanol surface groups may affect the stability of the anchored linker. Generally, grafting of organosilanes to the silica surface can be carried out in two ways:

- under anhydrous condition (Figure 3-5).
  Organosilane react with the silanol groups of the silica directly, resulting in grafted silane molecules. Anhydrous grafting was reported to afford equal and stable, monolayer functionalized surface [244, 247].

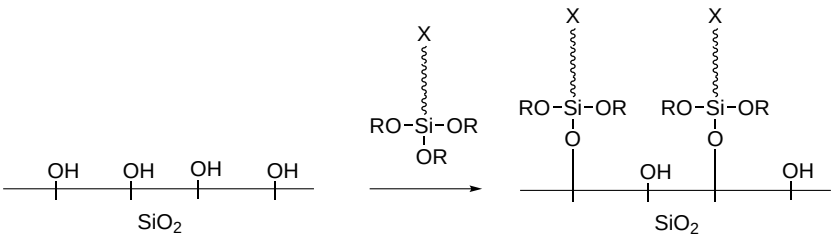

Figure 3-5: Functionalization of silica surface with silanes in anhydrous conditions [248].

- in acid-aqueous solution (Figure 3-6).
  Organosilane is firstly hydrolyzed through the presence of water. The organosilanes with three hydroxyl groups can either react with the silanol groups of the silica leading to grafting of the silane molecules or first react with each other leading to the formation of oligomers with subsequent grafting.

Further reaction of the linker on the catalyst surface to afford an active immobilized ligand can be achieved via several classical reactions, for example: nucleophilic substitution, metathesis, or click chemistry based on the azide-alkyne Huisgen cycloaddition. Depending on the complexity of the metal complex or ligand, the synthetic effort can be challenging and significantly determines the quality of the immobilized catalyst. In this work anchoring will be carried out via nucleophilic substitution. A support with reactive leaving group moiety is crucial for successful ligand anchoring. A list of possible leaving groups X for nucleophilic substitution is listed in Table 3.1.

Table 3.1: Leaving groups ordered approximately in decreasing ability to leave [249]

Substrate RX	**Leaving group**
$R-N_2^+$	dinitrogen
$R-OR_2^{'+}$	dialkyl ether
$R-OSO_2R^F$	perfluoroalkylsulfonates (e.g. triflate)
R−OTs, R−OMs, etc.	tosylates, mesylates, and similar
R−I	iodide
R−Br	bromide
$R-OH_2^+$	water, conjugate acid of alcohol
R−Cl	chloride, acyl halides
$R-ORH^+$	conjugate acid of ether

R–ONO_2, R–$OPO(OH)_2$, R–$OB(OH)_2$	nitrate, phosphate, and other inorganic esters
R–$SR_2^{'+}$	thiolate
R–$NR_3^{'+}$	amines
R–F	fluoride
R–OCOR	carboxylate, anhydrides
R–NH_3	ammonia
R–OAr	phenoxides, aryl esters
R–OH, R–OR	hydroxide, alkoxides
R–H	
R–NR_2	amides
R–Ar	aryl
R–R	alkyl

The greater the ability of the leaving groups to leave, the higher the probability of successful immobilization. However, the preparation of the support with very reactive leaving groups is challenging. In case of Br functionalized supports, the balance between efforts necessary for support preparation and the reactivity during immobilization purpose is optimal.

Before the ligand is anchored, it is sometimes necessary to protect other reactive nucleophilic moiety of the immobilized molecule before anchoring. This is especially relevant for strongly nucleophilic phosphine ligand. One elegant way to overcome this problem is to protect the nucleophilic phosphorous with BH_3. This approach has been used to synthesize various complex phosphine ligands, leading to significant progress in organophosphorous chemistry [250–253]. P-borane complexes can be prepared by reacting trivalent phosphorous compounds with BH_3-THF in ether as solvent or with BH_3-SMe_2 in benzene or

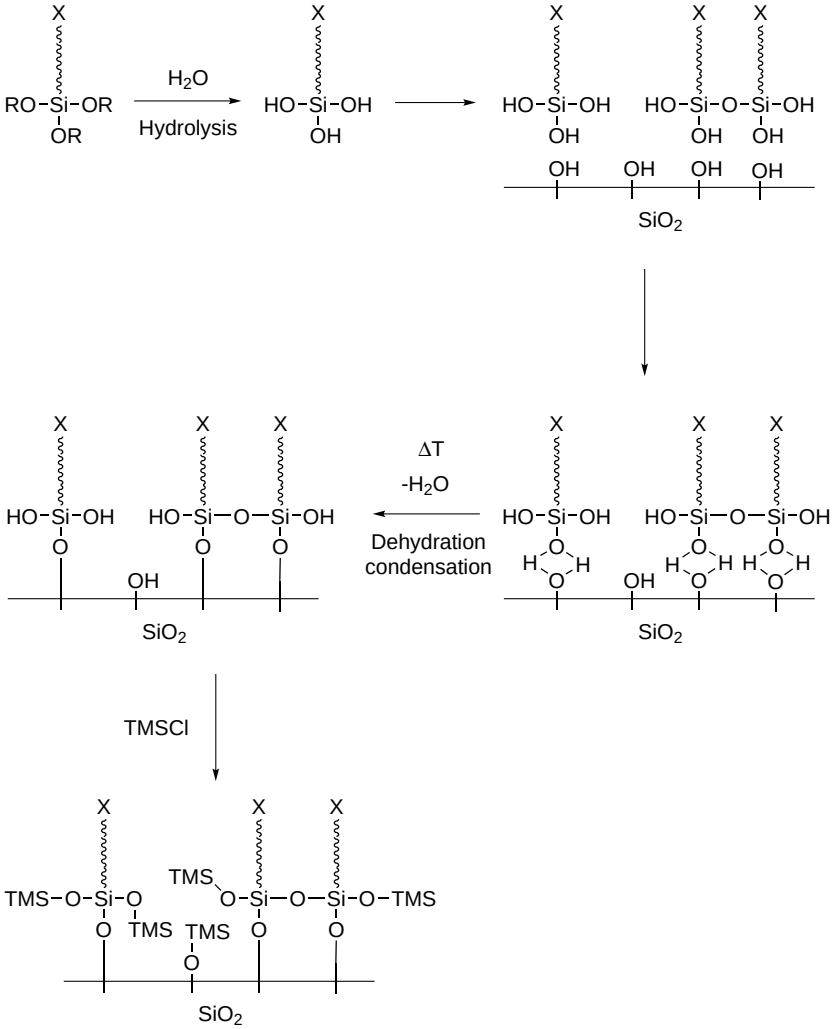

Figure 3-6: Functionalization of silica surface with silanes under aqueous conditions [248].

toluene. Since SMe_2 is less basic than THF, more BH_3 is available for the protection, thus the use of BH_3-SMe_2 results in more efficient reaction. The resulting P-borane complexes are generally inert and stable towards various reaction conditions [254]. P-B bond formation results in a change in the electronic properties of the phosphorous atom. The electron withdrawing effect of the P-B bond activates adjacent hydrogen and α-alkyl substituents (Figure 3-7). Treatment of the protected phosphine with organolithium reagent at low temperature further results in the formation of a highly nucleophilic carbanion which can react via nucleophilic substitution with the leaving group of the linker. After

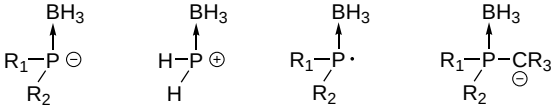

Figure 3-7: Activated position of a phosphorous compound upon complexation with BH_3 [250].

successful anchoring, the protecting group BH_3 has to be removed to allow the subsequent complexation with transition metal. Depending on the nucleophilicity of the phosphorous and thus the strength of the phosphorous-borane bond, borane decomplexation can be achieved using an amine [251, 255–257], a strong acid [258, 259], an alcohol [260–262], or an olefin [263]. The amine deprotection route is consistently more efficient and omits troublesome laborious workup, characteristic in other deprotection methods mentioned above, and therefore is more commonly used.

Due to the higher stability of the P-B bond than the N-B bond, an excess of amines, such as TMEDA, morpholine or diethylamine, is required for efficient deprotection. While deprotection of triphenylphosphine BH_3

complex into free phosphine can be reached in reaction with diethylamine for a few hours at 50 °C, the liberation of BH_3 from very basic phosphines may require more extreme conditions [257].
In this work, the strategy to immobilize bidentate dcpe ligand will be focused on anchoring at the bridge or on the cyclohexyl substituents of the ligand to minimize modification of the electronic and steric properties of the ligand. The dcpe ligand can be deprotonated with organolithium reagent, for example with *tert*-BuLi, generating the corresponding carbanion of the ligand. The carbanion reacts with brominated support material, resulting in a carbon-carbon bond formation, thus covalently anchoring the ligand (Figure 3-8).

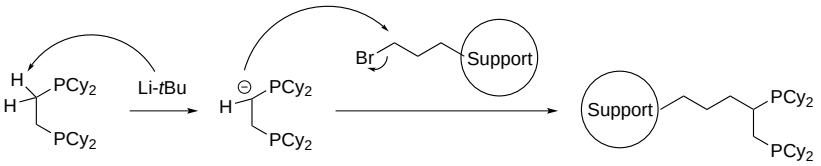

Figure 3-8: Simplified anchoring mechanism via S_N2 reaction between a linker-functionalized support and a ligand.

3.3.1 Route 1: *In situ* sequential assembly of active ligand

Anchored dcpe was prepared by firstly grafting a silica support with an appropriate linker followed with the generation of chelate phosphine functionality. The silica support used in this route is specified in Table 3.2. A linker with halogen functionality was prepared, so that its subsequent reaction with nucleophilic phosphine carbanion on the support surface may afford a dcpe ligand. Efficient synthesis and purification of each product at each step is the key factor to obtain highly uniform immobilized ligand. In this work, 1-allyloxy-2,3-epoxypropane was chosen as the linker backbone. Both the presence of oxygen atom and

Table 3.2: Silica support used for functionalization via Route 1: *In situ* sequential assembly of active ligand.

Properties	Cariact Q-20C
Average pore diameter [nm]	20
Specific surface area [m^2/g]	140
Pore volume [mL/g]	0.8

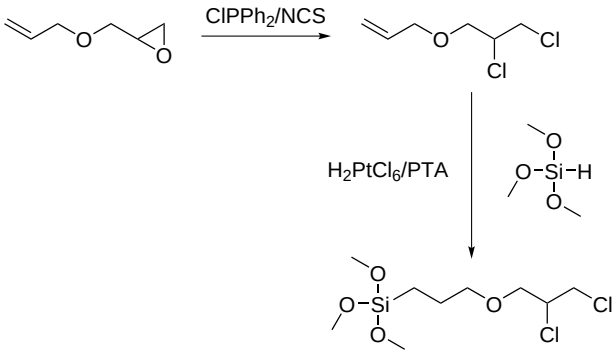

Figure 3-9: Preparation of 4-oxa-6,7-dichloro-1-heptyltrimethoxysilane linker.

the length of the linker ensure high flexibility and sufficient distance between metal complex and the support. 1-allyloxy-2,3-epoxypropane was first transformed into 4-oxa-6,7-dichloro-1-heptene with two reactive Cl moieties using chlorodiphenylphosphine ($ClPPh_2$) to regioselectively open the epoxide ring and N-chlorosuccinimide (NCS) as the electrophilic chlorine source [264, 265]. The product was then hydrosilylated to 4-oxa-6,7-dichloro-1-heptyltrimethoxysilane in the presence of H_2PtCl_6 catalyst and 1,3,5-triaza-7-phosphaadamantane (PTA) ligand

at 80 °C for 16 hours (Figure 3-9). The hydrosilylation conditions were optimized during preliminary experiments (Table 3.3).

Hydrosilylation preliminary experiments were carried out with two of the most popular industrial catalysts, the Speier's catalyst H_2PtCl_6 and Karstedt's (alkene-stabilized platinum(0): Platinum(0)-1,3-divinyl-1,1,3,3-tetramethyldisiloxane complex) catalyst. The hydrosilylation of the 4-oxa-6,7-dichloro-1-heptene is favored at temperature of 80 °C (Entry 6: yield = 45 %, Entry 7: yield = 54 %). H_2PtCl_6 catalyst display higher activity than the Karstedt's catalyst. In reactions without solvent, Karstedt's catalyst and H_2PtCl_6 provided product yield of 25 % (Entry 3) and 54 % (Entry 7) yield respectively. In reactions with deuterated toluene as solvent (Entry 4 and Entry 10 as well 11), Karstedt's catalyst afforded product in 15 % yield while H_2PtCl_6 yielded 85 - 92 % product. Although the application of isopropanol as solvent resulted in high conversion of the starting material (over 90 %), 4-oxa-6,7-dichloro-1-heptyltriisopropoxysilane was obtained as byproduct, presumably due to transesterification of the intended product with the solvent, isopropanol. H_2PtCl_6 catalyzed hydrosilylation can be improved with the addition of 1,3,5-triaza-7-phosphaadamantane (PTA) ligand to increase the stability and the solubility of the catalyst. This results in product formation with 62 % yield. Contrary to previous experiments with Karstedt's catalyst or previous H_2PtCl_6 catalyst, the reaction with H_2PtCl_6 and PTA ligand afforded 4-oxa-6,7-dichloro-1-heptyltrimethoxysilane with high selectivity (82 %).

In summary, hydrosilylation is a versatile tool to prepare a organosilicon compounds. The reaction mechanism and product distribution of the hydrosilylation reaction depend on the metal and the electronic and steric properties of the ligands. The hydrosilylation reaction by late transition

metal complexes involves an oxidative addition of silanes and coordination of alkene to a metal complex, followed by the subsequent migratory insertion of alkene into the M-H bond. Finally the resulting metal silyl alkyl complex undergoes reductive elimination, releasing an organosilane product with Si-C bond (Figure 3-10). Possible side reactions dur-

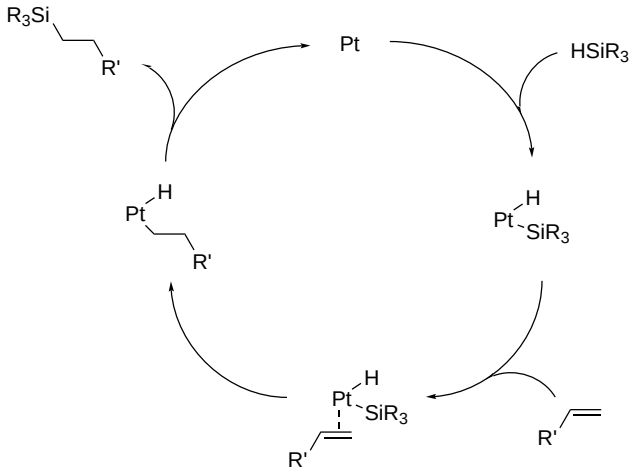

Figure 3-10: Chalk-Harrod mechanism for hydrosilylation of olefins by late transition metal complexes [266].

ing hydrosilylation may include isomerization, oligomerization, polymerization and hydrogenation of alkenes as well as redistribution and dehydrogenation of silicon hydrides. Moreover, the transition metal can also coordinate and form complex with the olefin or trimethoxysilane reactants, rendering the catalyst inactive. A coordinating ligand such as PTA would not only increase the stability of the catalyst but also improve the selectivity of the reaction [267].

Table 3.3: Hydrosilylation of 4-oxa-6,7-dichloro-1-heptene with 1.1 eq. trimethoxysilane to give 4-oxa-6,7-dichloro-1-heptyltrimethoxysilane. The conversion values are calculated from the ratio of hydrosilylated product to educt with double bond ^{1}H NMR spectra.
*byproduct: 4-oxa-6,7-dichloro-1-heptyltriisopropoxysilane.
Note that all reactions are carried out in a small vial with minimum amount of substances, thus inhomogenity is to be expected, which is caused primarily due to improper stirring.

Entry	Catalyst	Solvent	T [°C]	t [h]	Yield [%]	Remarks
1	1 mol % Karstedt's catalyst	no solvent	40	4	0	
2	1 mol % Karstedt's catalyst	THF	40	1	0	
3	5 mol % Karstedt's catalyst	no solvent	80	20	25	inhomogenity
4	5 mol % Karstedt's catalyst	toluene-d_8	80	20	15	several products
5	5 mol % H_2PtCl_6	no solvent	60	4	40	inhomogenity
6	5 mol % H_2PtCl_6	no solvent	60	20	45	inhomogenity
7	5 mol % H_2PtCl_6	no solvent	80	20	54	inhomogenity
8	5 mol % H_2PtCl_6	isopropanol	60	4	92*	*byproduct
9	5 mol % H_2PtCl_6	isopropanol	60	20	93*	*byproduct
10	5 mol % H_2PtCl_6	toluene-d_8	80	20	85	two products
11	5 mol % H_2PtCl_6	toluene-d_8	80	20	92	two products
12	5 mol % H_2PtCl_6 with 2eq. PTA ligand	toluene-d_8	80	20	43	

13	5 mol % H_2PtCl_6 with 1.2eq. PTA ligand	toluene-d_8	80	20	62

The grafting of the prepared vic-chlorides silane linker was carried out in anhydrous conditions with toluene as solvent at reflux temperature for 48 hours. Methoxysilanes can be successfully grafted at the surface without the need for any catalyst. To ensure complete silanes immobilization, trace amount of water was added to the reaction mixture and the reaction mixture was further stirred at reflux temperature for 24 hours. After washing and drying, the remaining hydroxyl groups of the silica was converted into silanes. Endcapping after silanization was necessary to eliminate all unreacted and accessible silanols on the silica surface. Endcapping was carried out with excess chlorotrimethylsilane (Me_3SiCl), starting at low temperature of about -40 °C with slow warming until reaching reflux temperature, at which the suspension is stirred for 15 hours. After slow cooling to 25 °C, the solid product was washed three times with each 50 mL toluene, ether, and THF. Finally, the grafted silica was dried in vacuum at 50 °C for 18 hours.

Each surface modification was accompanied with proper washing to prevent unintended side products in the following reaction. In addition, the drying temperature has to be carefully chosen to avoid the decomposition of the organic linker on the catalyst surface. The concentration of the vic-chlorides silane linker (4-oxa-6,7-dichloro-1-heptyltrimethoxysilane) on the surface was determined by elemental analysis at 0.045 mmol/g (0.09 mmol/g Cl). The low concentration of the grafting can be associated with limited collision probability of the silane in the liquid phase with the surface of the solid material. Multiple-steps grafting may be necessary to improve the loading of the linker on the catalyst support. After the silica support was successfully functionalized with 4-oxa-6,7-dichloro-1-heptene linker, $LiPCy_2$ was added to allow nucleophilic substitution with the chlorine moieties of the linker. Complete substitution generates anchored dcpe ligand. After

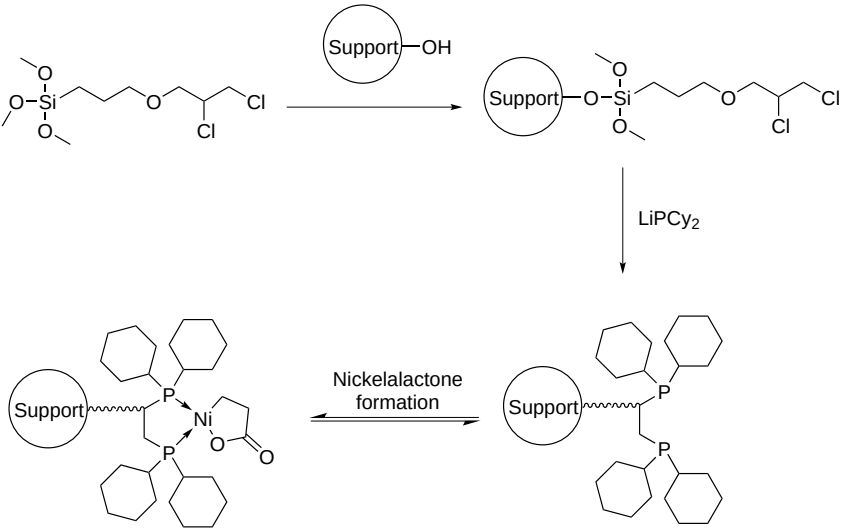

Figure 3-11: Assembling the building blocks of 1,2-bis(dicyclohexylphosphino)-ethane (dcpe) on support.

thorough washing and vacuum drying, the catalyst was subjected to ligand exchange reaction with (tmeda)-Nickelalactone, yielding anchored (dcpe)-nickelalactone. The concentration of phosphorous on the catalyst surface was determined with elemental analysis (0.056 mmol/g). However, the low concentration of the phosphorous on the catalyst surface prevents a thorough characterization by MAS-NMR. Therefore, the immobilized nickel complex catalyst prepared with this route was directly tested for its activity without previously confirming the presence of nickel complex on the surface of the material.

The catalyst was subjected to ligand exchange with (tmeda)-nickelalactone to give an immobilized (dcpe)-nickelalactone catalyst. The method already applied in Subchapter 2.2 was utilized for this purpose. The

immobilized catalyst and 2 eq. of (tmeda)-nickelalactone were suspended in THF and stirred at 25 °C for 18 hours. The reaction mixture is then filtrated, washed with *N,N*-dimethylformamide and THF to completely remove unreacted (tmeda)-nickelalactone, and dried in vacuum. Catalytic reaction was carried out in one pot process with 10 eq. triethylamine and 10 eq. NaH base system in the presence of 10 bar ethylene and 20 bar CO_2 at 100 °C for 72 hours with THF as reaction solvent. The sodium acrylate was extracted from the reaction mixture with D_2O and measured with ^{1}H NMR. The reaction yielded no detectable sodium acrylate product. This, however, is not a solid proof that the catalytic reaction with immobilized nickel complex did not work. The concentration of sodium acrylate generated from the catalytic reaction may be well below the detection limit of NMR. Further experiments with immobilized catalyst prepared with this route are necessary to confirm this hypothesis.

3.3.2 Route 2: Direct anchoring of active ligand

Alternatively, an active ligand can also be directly anchored onto support materials. For this purpose, a suitable support with appropriate reactive moiety to facilitate anchoring has to be prepared.

Support Materials

In this work, silica modified with 3-bromopropyltrimethoxysilane and commercially available halogenated crosslinked polystyrene were used as supports for ligand anchoring. The commercially available polystyrene support is typically prepared via copolymerization of the styrene monomer, divinylbenzene as crosslinker, and styrene with desired functionality [268,269]. Several polystyrene supports used in this work are illustrated in Figure 3-12. The brominated silica supports were prepared via con-

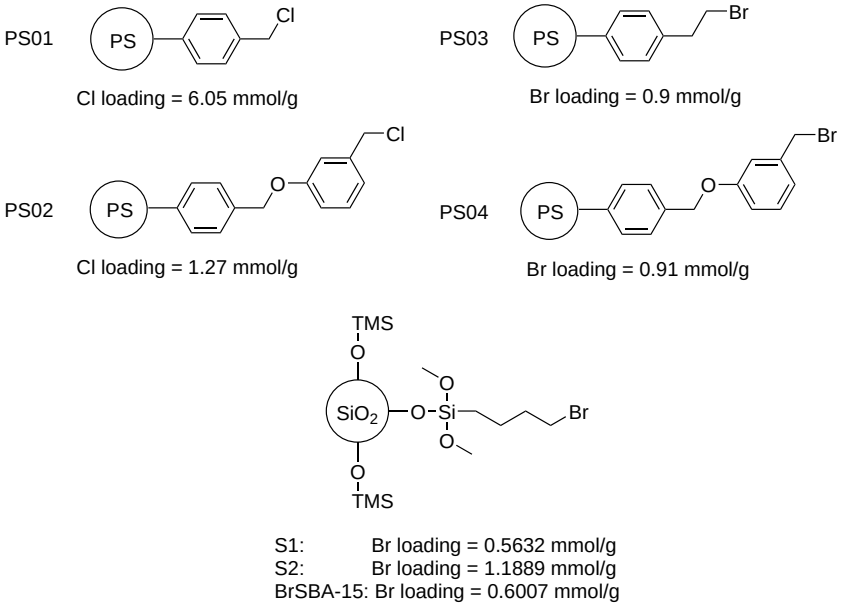

Figure 3-12: Supports used for dcpe immobilization via direct anchoring route. Loading of Cl and Br moiety was determined by elemental analysis department of BASF.

densation of 3-bromopropyltrimethoxysilane with the surface hydroxyl groups of Cariact Q-20C and SBA-15 (hydroxyl content: 2.8 mmol/g via quantitative ^{1}H MAS NMR, see also product specification in Table 3.4) [270] silica materials.

The grafting was carried out in the presence of a trace of water (0.3 mL water for each gram support) and HCl as catalyst at toluene reflux temperature.

High Br loading of the functionalized supports depends on the concentration of the surface hydroxyl group of the silica and the amount of 3-bromopropyltrimethoxysilane precursor added during the functionalization.

Table 3.4: Silica supports used for functionalization.

Properties	**Cariact Q-20C**	**SBA-15** [270]
Average pore diameter [nm]	20	6
Specific surface area [m^2/g]	140	1164
Pore volume [mL/g]	0.8	1.25
-OH content [mmol/g]	no data	2.8
Supplier	Fuji Silysia Chemical	University of Stuttgart

During grafting targeting the surface hydroxyl groups, the silane linker precursor may also react with each other. This would reduce the amount of the silane linker available for surface functionalization. From the amount of Br detected in the grafted silica, side reaction during functionalization was estimated to be about four times faster. Only about 20 % of starting material (3-bromopropyltrimethoxysilane) used could be detected in the modified silica after grafting (Table 3.5). Thus, multiple-steps functionalization reactions were carried out to increase the Br loading.

As comparison, two-steps functionalization yielded Br silica product with Br concentration as high as 1.1889 mmol/g (Entry 2: yield grafting 20.81 %) while one-step functionalization only yielded product with Br concentration of 0.5632 mmol/g (Entry 1: yield grafting 19.71 %). The percentage of starting material grafted at the support material, however, remains constant at around 20 %. This means that the grafting of the silane linker is strongly limited by the contact probability between the linker in the liquid phase and the silanol groups on the surface of the catalyst. After successful immobilization of the linker, the silica product was treated with excess chlorotrimethylsilane to eliminate all unreacted

and accessible silanols on the surface of the support material. Endcapping was carried out with excess chlorotrimethylsilane, starting at low temperature of about -40 °C with slow warming until reaching reflux temperature, at which the suspension is stirred for further 15 hours. The reaction mixture was slowly cooled down to 25 °C and the solid product was washed three times with toluene, ether, and THF. Finally, the grafted silica was dried in vacuum at 50 °C for 18 hours to remove traces of solvents. Each surface modification was accompanied with thorough washing to prevent unintended side products in the following reaction. In addition, the drying temperature has to be carefully considered to prevent the decomposition of the organic linker on the catalyst surface.

2

Table 3.5: Grafting of silica support with 3-bromopropyltrimethoxysilane (BrSi). Synthetic details can be found in Appendix A.3.2.

Sample name name	Support	BrSi educt [mmol/g Support]	Br loading [mmol/g]	Yield Grafting [%]	Remarks
S1	Cariact Q-20C	2.857	0.5632	19.71	one-step grafting
S2	Cariact Q-20C	2 x 2.857	1.1889	20.81	two-steps grafting
BrSBA-15	SBA-15	2.800	0.6007	21.45	one-step grafting

Ligand anchoring

The active ligand can be anchored onto support material by forming a covalent carbon-carbon bond via nucleophilic substitution of the nucleophilic carbanion ligand with the electrophilic linker on the surface of the support material. Before anchoring the ligand at the support material, it is necessary to ensure that the ligand does not display any active moiety which may disturb or react during the process. In case of dcpe ligand, one has to take care about the nucleophilic phosphorous, which may prone to side reactions, for example: oxidation, lithiation, or reaction with other reactive functional groups of the support. To prevent these unintended side reactions, the dcpe ligand was treated with BH_3-SMe_2 in THF as solvent. The reaction was carried out at 25 °C for 24 hours. After THF removal in vacuum, the dcpe·2 BH_3 complex was recrystallized from toluene. ^{31}P NMR confirmed a successful protection of the dcpe ligand, as indicated by a doublet at 28.37 ppm (solvent: $CDCl_3$, 202.55 MHz ^{31}P NMR, $^1J_{PB}$ = 64.4 Hz). Upon protection with BH_3, the electron withdrawing effect of the P-B bond activates adjacent α-carbon atom. Treatment with organolithium reagent at 0 °C for 2 hours further increases the nucleophilicity of the α-carbon, resulting in a highly nucleophilic dcpe carbanion which can attack the electrophilic carbon of the linker grafted on the catalyst support.
Support material bearing Br moiety, strong nucleophilic dcpe carbanion and polar aprotic solvent THF used during anchoring facilitate S_N2 type reaction. Successful anchoring of the ligand can be quantified by introducing the following equaton:

$$Degree\ of\ Anchoring = \frac{Amount\ of\ dcpe\ anchored\ at\ support}{Amount\ of\ dcpe\ educt\ at\ start} \tag{3.1}$$

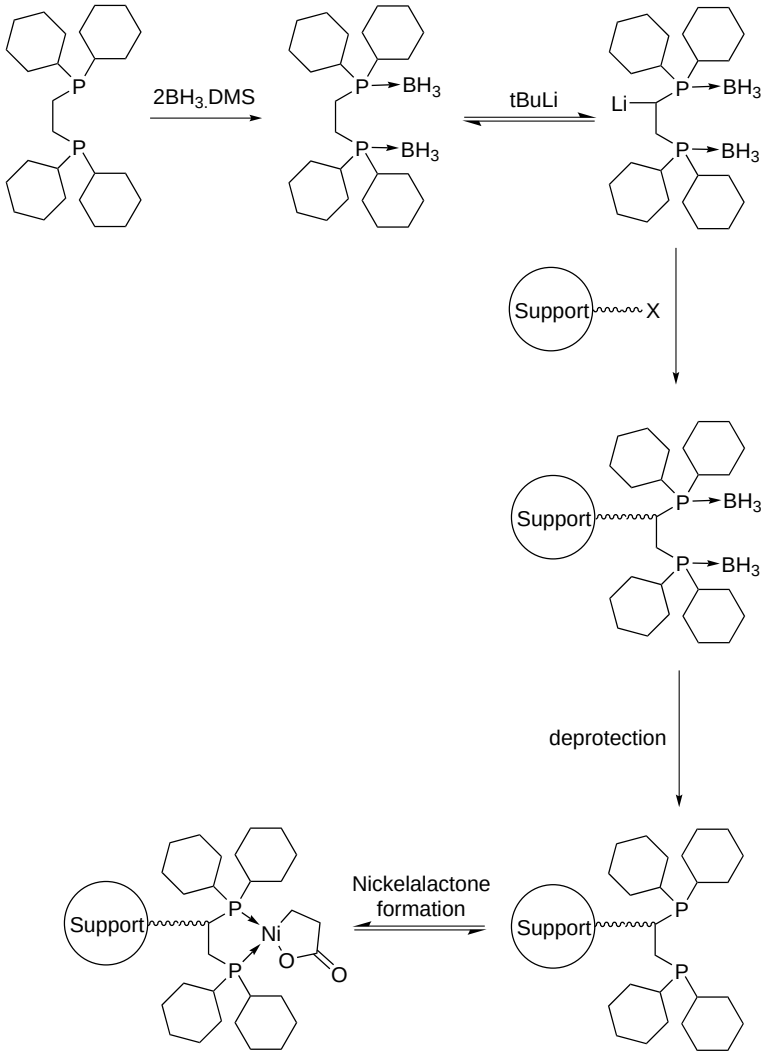

Figure 3-13: Direct anchoring of 1,2-bis(dicyclohexylphosphino)-ethane (dcpe).

The success of an anchoring of dcpe depends on several factor such as (Table 3.6):

- Solvent, which assists the coordination of organolithium reagent, thus increasing its reactivity and affect the amount of dcpe carbanion (Figure 3-14). It is important to keep the amount of solvent to minimum during lithiation as the solvent reduce the half time of the organolithium reagents. In this work, THF was chosen as lithiation solvent due to its relatively strong coordinating power and the high solubility of dcpe ligand in this solvent.

- Trace water and other impurities during the reaction, which may result in side reactions with the dcpe carbanion.
  The pre-treatment of the support determines the final dcpe loading greatly. This could be affected by the presence of trace water during the reaction. Polystyrene support PS03, which is pre-dried in vacuum at 25 °C overnight, yielded dcpe loading of 0.134 mmol/g (Table 3.6 Entry 8, degree of anchoring 29.13 %), while support, which is pre-dried in vacuum at 0 °C overnight yielded a constant dcpe loading of 0.065 mmol/g (degree of anchoring 14.44 %), 0.0775 mmol/g (degree of anchoring 16.85 %), and 0.0759 mmol/g (degree of anchoring 16.5 %). Support pre-dried at higher temperature should contain less trace water. This would prevent undesired hydrolysis of the dcpe carbanion. As a result, higher amount of dcpe carbanion would be available during the reaction, leading to a higher degree of anchoring. Support pre-dried at high temperature of 50 °C (Table 3.6 Entry 4) also displayed a moderate dcpe loading, 0.063 mmol/g (degree of anchoring 13.99 %). Although the anchoring conditions are not identical (-75 °C for 6 hours followed with 0 °C for 16 hours instead of

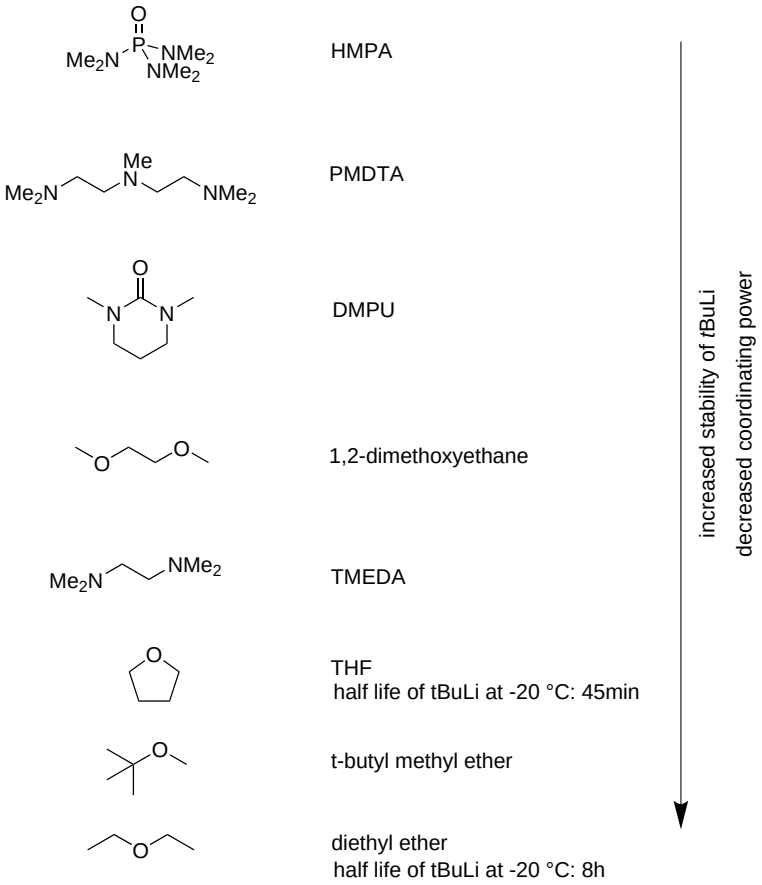

Figure 3-14: Common solvents for lithiation [271].

0 °C for 72 hours), this should serve as a proof that the primary brominated linker is also stable at high temperature and resistant to elimination reaction.

- The amount of dcpe carbanion starting material which is added into the reaction.

The amount of dcpe starting material reflects the final dcpe loading of the support, until a certain concentration, where the increase in dcpe starting material is no longer proportional to the dcpe loading of the support. This is demonstrated in Table 3.6 Entry 14 and 15. Reaction with dcpe starting material of 0.323 mmol/mmol Br moiety at the support yielded a material with dcpe loading of 0.0743 mmol/g (degree of anchoring 19.39 %). Four fold increase of the dcpe starting material to 1.2 mmol/mmol Br moiety at the support yielded material with dcpe loading of only 0.1566 mmol/g (degree of anchoring 11.08 %). After reaching a certain dcpe loading, the support becomes overcrowded and the resulting steric prevents any further anchoring of dcpe at the support.

- Temperature and duration of the anchoring.
  The best result for direct ligand anchoring was performed at 0 °C for 72 hours (Table 3.6 Entry 8 - 15). All anchoring reactions conducted under these conditions delivered high dcpe loading on the support with anchoring degree of over 10 %. Low temperature inhibits the decomposition of dcpe carbanion while long reaction duration favors the slow anchoring reaction of the ligand at the support.

Table 3.6: Direct anchoring of dcpe on the support material via nucleophilic substitution. Values of dcpe loading were derived from elemental analysis results. X = linker loading on the support material.
Degree of anchoring = ratio of anchored dcpe to dcpe starting material.
Conditions: ⋆A: 2h at -40 °C, 72h at 25 °C. ⋆B: 24h at 0 °C. ⋆C: 72h at 0 °C. ⋆D: 6h at -75 °C, 16h at 0 °C. ⋆E: 6h at -75 °C, 8h at 0 °C. ⋆F: 6h at -75 °C, 90h at 0 °C. ⋆G: 72h at 0 °C. Remarks: ⋆1: support pre-dried in vacuum at 50 °C overnight. ⋆2: support pre-dried in vacuum at 25 °C overnight, addition of 20 eq. LiH during anchoring. ⋆3: support pre-dried in vacuum at 25 °C overnight. ⋆4: support pre-dried in vacuum at 0 °C overnight.

Entry	Sample name	Support	Conditions	dcpe:X ratio [mmol/mmol]	dcpe loading on support [mmol/g]	Degree of anchoring [%]	Remarks
1	A5	PS01	⋆A	2.00	0.0200	0.16	⋆1
2	A6	PS02	⋆B	1.95	0.0180	0.72	⋆1
3	A7	PS04	⋆C	0.50	0.0280	6.14	⋆1
4	A8.1	PS03	⋆D	0.50	0.0630	13.99	⋆1
5	A8.2	PS03	⋆E	0.50	0.0095	2.12	⋆1
6	A8.3	PS03	⋆E	0.50	0.0274	6.10	⋆2
7	A8.4	PS03	⋆F	0.50	0.0194	4.31	⋆2
8	A8.5	PS03	⋆G	0.51	0.1340	29.13	⋆3
9	A8.6	PS03	⋆G	0.50	0.0650	14.44	⋆4
10	A8.7	PS03	⋆G	0.50	0.0775	16.85	⋆4

11	A8.8	PS03	⋆G	0.50	0.0759	16.50	⋆4
12	A4	S1	⋆G	0.68	0.0678	17.69	⋆1
12	A9.1	BrSBA-15	⋆G	1.48	0.1388	15.64	⋆1
13	A9.2	BrSBA-15	⋆G	1.48	0.1518	17.09	⋆1
14	A10.1	S2	⋆G	0.32	0.0743	19.39	⋆1
15	A10.2	S2	⋆G	1.20	0.1566	11.08	⋆1

The dcpe direct anchoring approach is readily reproducible. Anchoring on BrSBA-15 with the exact synthetic conditions yielded degree of anchoring of 15.64 % and 17.09 % (Entry 12 and 13). Another example are the immobilizations on PS03 support (Entry 9-11) with a degree of anchoring of each 14.44 %, 16.85 %, and 16.5 %.
The fraction of dcpe anchored on support materials may reach up to 29 % of the total dcpe starting material. This undermines the difficulty of surface solid-fluid reaction involving nucleophilic substitution. Higher availability of Br functional group did not result in an increased degree of anchoring. For example in Entry 12, S1 support with Br loading of 0.5632 mmol/g, which after treated with 0.68 eq. dcpe anion results in a catalyst with dcpe loading of 0.0678 mmol/g (degree of anchoring 17.69 %), while in Entry 15: S2 support with Br loading of 1.1889 mmol/g only yielded a catalyst with dcpe loading of 0.1566 mmol/g (degree of anchoring 11.08 %) after treated with 1.2 eq. dcpe anion. In addition, the dcpe loading on the support materials depends greatly on the physical properties of the support itself: the surface area, the pore size (see also Table 3.4), and the linker loading (see also Table 3.5 and Figure 3-12) of the support material. After reaching a certain dcpe loading, the support becomes overcrowded and the resulting steric barrier prevents any further anchoring of dcpe on the support.
Successful immobilization of dcpe·2 BH_3 on the silica surface was confirmed with ^{31}P MAS NMR (Figure 3-15) with characteristic chemical shift at around 24 ppm (as comparison: 202.55 MHz ^{31}P NMR δ = 28.37 ppm, solvent NMR: $CDCl_3$). The P-B coupling observed in solvent NMR at 64.4 Hz can hardly be distinguished in solid state NMR. The difference in chemical shift between solvent NMR and solid state NMR is solely due to the solvent effect. Similar ^{31}P MAS NMR pattern was

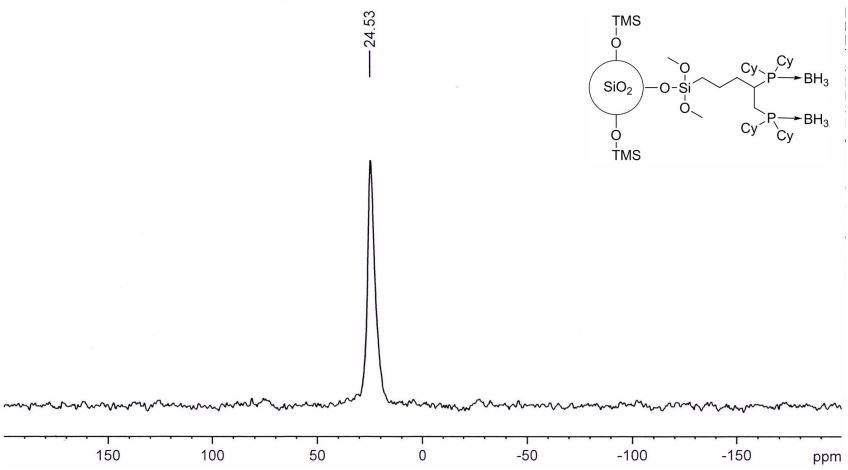

Figure 3-15: ^{31}P MAS NMR for immobilized dcpe·2 BH_3 on silica support S1 (A4, see also Table 3.6).

also observed for signals corresponding to the phosphorous atom of the dcpe·2 BH_3 immobilized at polystyrene surface (Figure 3-16).

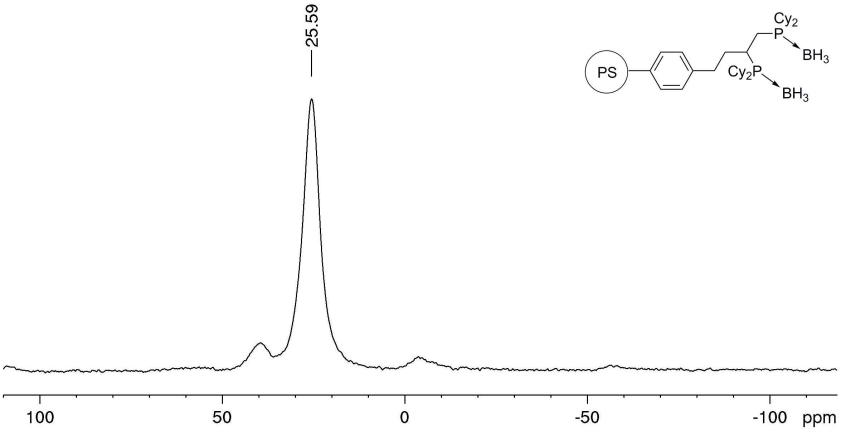

Figure 3-16: ^{31}P MAS NMR for immobilized dcpe·2 BH_3 on polystyrene support PS03 (A8.8, see also Table 3.6).

Activation: Deprotection of BH_3

After adequate filtration and washing to remove non-immobilized ligand, the catalyst was dried and subjected to treatment with nucleophilic amine base, such as dabco or morpholine, to deprotect the borane moiety. However, deprotection of BH_3 from the nucleophilic dcpe is not trivial. In preliminary deprotection experiments with non-immobilized dcpe (Table 3.7), several deprotection approaches were investigated: with amine base (Entry 1 - 3, and 5), with an alcohol (Entry 4), and with an acid (Entry 6). In deprotection experiments with excess diethylamine base, BH_3 removal is best achieved at long reaction time. While deprotection at 50 °C for 8 hours resulted in a conversion of just 64.5 % with dcpe selectivity of about 29 % (Entry 1), deprotection at 50 °C after 48 hours resulted in a conversion of 70.6 %, with higher dcpe selectivity of 49.5% (Entry 2). Temperature increase to 100 °C with shorter reaction time (24 hours), however, yielded less conversion of about 33 %, with dcpe selectivity of 34.2 % (Entry 3). Deprotection with methanol seems to be unsuitable for biphosphine with alkyl substituents: deprotection with this approach converted only about 11 % dcpe·2 BH_3, which transformed into an oxide of dcpe directly (Entry 4). On the other hand, deprotection with dabco (Entry 6) at 100 °C afforded a high conversion of 86.4 %, 32.2 % of which gave an active dcpe product. While deprotection with acidic HBF_4 (Entry 7) successfully converted 100 % of all dcpe·2 BH_3 with 94.8 % selectivity in dcpe, the subsequent work up associated with this approach is not well suited for immobilized ligand catalyst. The presence of acid may promote the decomposition of the linker connecting the active ligand with the support. Deprotection with morpholin at harsh condition, 110 °C for 3 hours, converted 89 % of all dcpe·2 BH_3 with 78.4 % selectivity in dcpe.

Table 3.7: Deprotection of non-immobilized dcpe·2 BH_3. NMR Selectivity and conversion were determined from the integral of each compound in ^{31}P NMR spectra.

Entry	Deprotection agent	Solvent	T [°C]	t [h]	NMR Selectivity dcpe [%]	NMR Conversion dcpe·2 BH_3 [%]
1	200 eq. diethylamine	-	50	8	28.99	64.5
2	200 eq. diethylamine	-	50	48	49.5	70.6
3	200 eq. diethylamine	-	100	24	34.2	33
4	molsieve - methanol	dioxane	115	100	0	11
5	12.5 eq. dabco	THF	100	96	32.2	86.4
6	20 eq. HBF_4	DCM	-10	12	94.8	100
7	1.5 eq. morpholin	-	110	3	78.4	89

The activity of some deprotected dcpe was tested in one-pot catalytic reaction with P1-NaH base system to validate the activity of the molecular catalyst after deprotection (Table 3.8). All deprotected ligands displayed catalytic activity similar to benchmark reaction with fresh dcpe. Both ligands deprotected with diethylamine (Entry 2) or dabco (Entry 3) yielded a normalized TON (hypothetical TON if 100 % ligand is active for the reaction) of 2.93 and 3.04 respectively for 72 hours reaction time. On the other hand, a catalytic reaction with dcpe ligand treated with HBF_4 yielded a TON of 0.62 for 18 hours reaction time. This may be caused by the presence of trace amount of acid, which can react with the base, reducing the amount of active base for the cleavage of the nickelalactone during the catalytic reaction. This phenomenon was not observed in ligand deprotected with amine base. Deprotection

Table 3.8: Catalytic activity of deprotected dcpe. Parameters: 0.2 mmol $Ni(COD)_2$, 0.22 mmol ligand, Base: 2.5 mmol P1, 10 mmol NaH, 5 bar ethylene, 10 bar CO_2, 45 mL THF, T = 80 °C. Values in parenthesis represent hypothetical TON for 0.2 mmol molecular catalyst (100 % ligand is active).

Entry	Ligand	Fraction of active ligand [%]	TON [-]	
			t = 18h	t = 72h
1	dcpe	100	1.41	3.28
2	Table 3.7 Entry 2	49.5	-	1.45 (2.93)
3	Table 3.7 Entry 5	32.2	-	0.98 (3.04)
4	Table 3.7 Entry 6	94.8	0.62 (0.65)	-

approaches with diethylamine and dabco were therefore directly applied

in immobilized catalysts. The immobilized catalyst was suspended in either neat diethylamine or THF with dissolved dabco and reacted at the same conditions as those in Table 3.7. However, ^{31}P MAS NMR investigation of the catalysts did not confirm any successful deprotection (Figure 3-17). Deprotection with morpholin at harsh conditions (110 °C

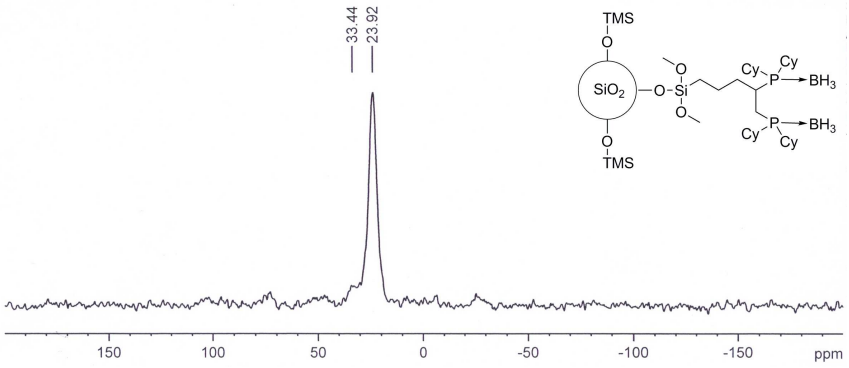

Figure 3-17: ^{31}P MAS NMR for dcpe·2 BH_3 immobilized on silica support S1 (A4, see also Table 3.6) after treatment with 20 eq. dabco with THF as solvent at 100 °C for 24 hours.

for 3 hours) successfully removed BH_3 from immobilized catalyst as monitored with ^{31}P MAS NMR (Figure 3-18 and Figure 3-19). The chemical shift at -7.45 ppm (silica support, Figure 3-18) or -4.99 ppm (polystyrene support, Figure 3-19) correspond to an active immobilized dcpe (as comparison, the corresponding non-immobilized dcpe ligand provided δ = 2.1 ppm in the ^{31}P NMR spectra with $CDCl_3$ as solvent), while that at 51.33 ppm corresponds to a dcpe oxide, which is formed when a dcpe ligand is exposed to oxidant. After a successful deprotection, the peak intensity at 23.75 ppm, which represents dcpe·2 BH_3, decreased significantly. The active catalyst can finally be used in catalytic reaction by introducing $Ni(COD)_2$ or (tmeda)-Nickelalactone, resulting in immobilized dcpe-Ni complex or immobilized (dcpe)-Nickelalactone

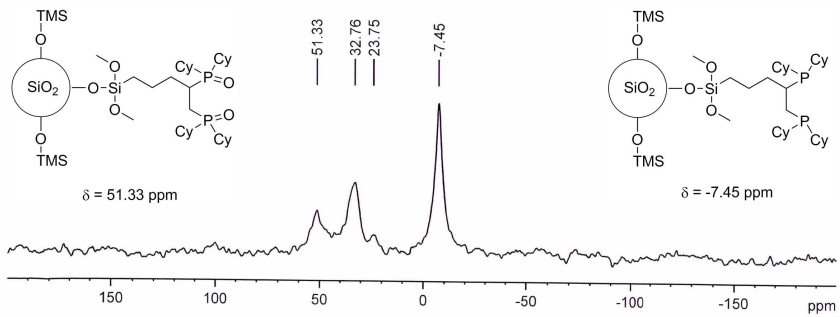

Figure 3-18: ^{31}P MAS NMR for dcpe immobilized on silica support S1 (A4, see also Table 3.6) after treatment with excess morpholin (10 mL for 1 g catalyst) at 110 °C for 3 hours.

Table 3.9: Reference data ^{31}P NMR.

Entry	Compounds	δ solvent NMR [ppm]	δ MAS NMR [ppm]
1	dcpe	2.1 ($CDCl_3$)	-7.45
2	dcpe·2 BH_3	28.7 ($CDCl_3$)	24.53
3	dcpe oxide	50 ($CDCl_3$)	51.3
4	(dcpe)-nickelalactone	61.98, 69.36 (CD_2Cl_2); 66.66, 72.89 (THF-d^8)	expected 60 - 80

complex as a catalytic species in the catalytic reaction respectively. In this work, three different pre-treatments were carried out to achieve these catalytic species:

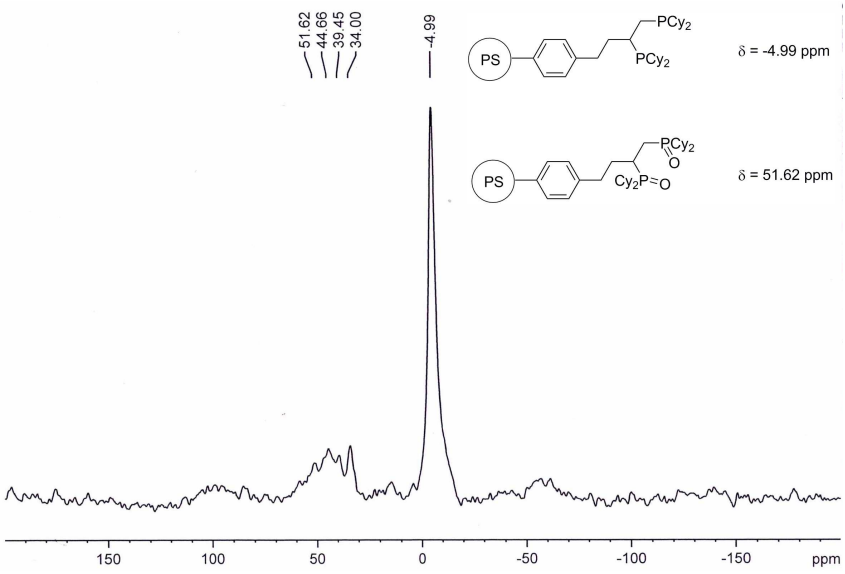

Figure 3-19: ^{31}P MAS NMR for dcpe immobilized on polystyrene support PS03 (A8.8, see also Table 3.6) after treatment with excess morpholin (10 mL for 1 g catalyst) at 110 °C for 3 hours.

- **Pre-treatment A:** introduction of $Ni(COD)_2$ and activated immobilized dcpe into the reactor. The immobilized nickel complex was formed *in situ*, which started the catalytic reaction in the presence of ethylene, CO_2, and amine-NaH base system.

- **Pre-treatment B:** *in situ* formation of immobilized (dcpe)-nickelalactone via ligand exchange with (tmeda)-nickelalactone. The ligand exchange was carried out at 25 °C for 3 hours, after which other reactants were added and the catalytic reaction was started.

- **Pre-treatment C:** separate formation of immobilized (dcpe)-nickelalactone via ligand exchange with (tmeda)-nickelalactone

under inert conditions. The ligand exchange was carried out in argon at 25 °C for 18 hours. The catalyst was subsequently washed to remove any byproducts and introduced into the reactor along with other reactants.

In the latter approach, the catalyst was also characterized with ^{31}P MAS NMR before catalytic reaction. The stability of immobilized (dcpe)-nickelalactone is however very limited and thus can hardly be confirmed via offline MAS NMR. As comparison, non-immobilized (dcpe)-nickelalactone decomposes readily in the presence of oxidant at 25 °C or at temperature above 60 °C in argon atmosphere to give dcpe oxide. In ^{31}P MAS NMR of immobilized catalyst on silica, strong dcpe oxide signal can be observed at around 52.19 ppm. The characteristic signal of free dcpe (at around -7 ppm) in catalyst after ligand exchange with (tmeda)-nickelalactone (Figure 3-20 and Figure 3-21) is not as pronounced as the signal in catalyst before ligand exchange (Figure 3-18). This indicates that the immobilized dcpe reacted with (tmeda)-nickelalactone, forming immobilized (dcpe)-nickelalactone complex, which decomposed to give immobilized dcpe oxide during or before the offline MAS NMR characterization took place. The chemical shift of immobilized (dcpe)-nickelalactone complex is expected at around 60 - 80 °C. The difference in chemical shift between solvent NMR and solid state NMR is solely due to the solvent effect. It is also interesting to observe a signal at 44 ppm in Figure 3-21, which may be related to dcpe interaction with silanol surface moiety. The signals at around 100 ppm are the spinning sidebands and should not be viewed as relevant.

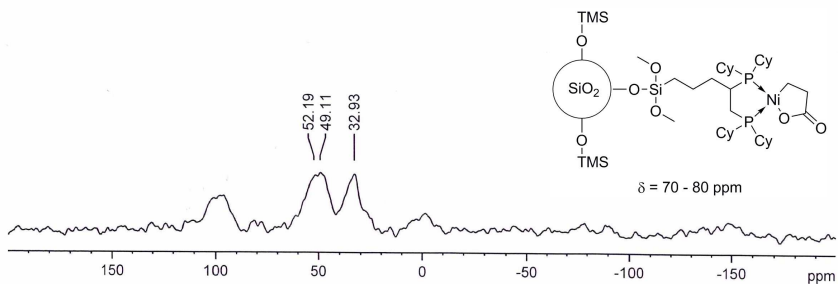

Figure 3-20: ^{31}P MAS NMR for immobilized dcpe anchored on SBA-15 after ligand exchange with (tmeda)-nickelalactone. Deprotection conditions: excess morpholin at 110 °C for 3 hours.

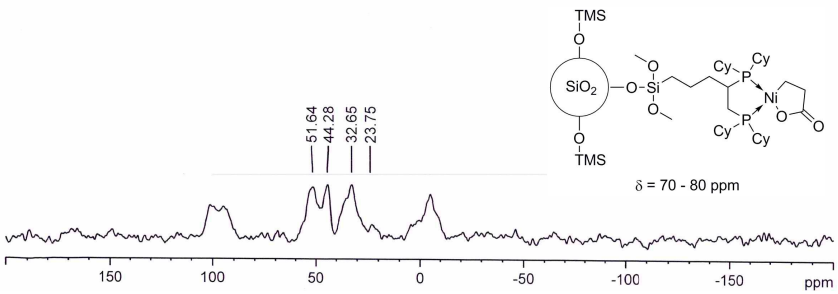

Figure 3-21: ^{31}P MAS NMR for immobilized dcpe anchored on silica gel Cariact Q-20C after ligand exchange with (tmeda)-nickelalactone. Deprotection conditions: excess morpholin at 110 °C for 3 hours.

3.4 Catalytic Performance Results

The prepared immobilized catalytic species was injected into autoclave via a charger system along with solvent, base, and sodium hydride. Liquid base was used to allow one-pot process and to improve the collision probability between the immobilized catalyst and the base.

All immobilized ligands tested in this work are depicted in Figure 3-22. Preliminary experiments with immobilized monophosphine with phenyl substituents (catalyst A1, A2, and A3) did not yield any catalytic activity. These results are in accordance to the preliminary experiments that most phosphines are inactive in the catalytic formation of sodium acrylate. Immobilized catalysts A4, A5, A6, A7, and A8.1 - A8.3 were prepared rather for proof-of-concept purposes and were not tested in catalytic reaction due to their low dcpe loading.

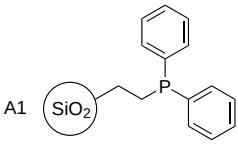

loading = 0.7 mmol/g

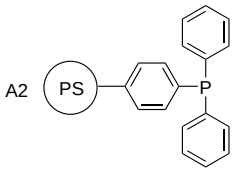

loading = 3.2 mmol/g

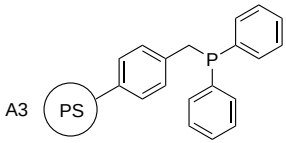

loading = 2.5 mmol/g

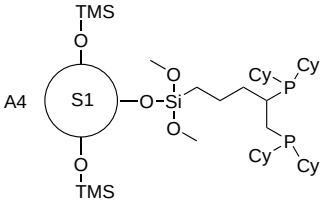

loading = 0.0678 mmol/g

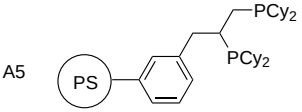

loading = 0.02 mmol/g

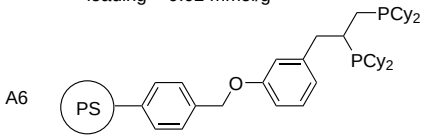

loading = 0.018 mmol/g

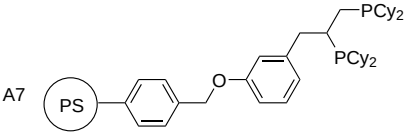

loading = 0.028 mmol/g

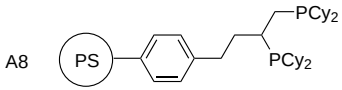

A8.1: loading = 0.063 mmol/g
A8.2: loading = 0.0095 mmol/g
A8.3: loading = 0.0274 mmol/g
A8.4: loading = 0.0194 mmol/g
A8.5: loading = 0.1340 mmol/g
A8.6: loading = 0.065 mmol/g
A8.7: loading = 0.0775 mmol/g
A8.8: loading = 0.0759 mmol/g

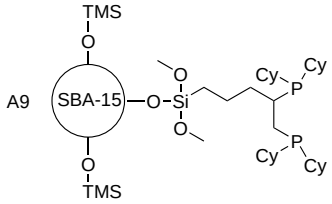

A9.1: loading = 0.1388 mmol/g
A9.2: loading = 0.1518 mmol/g

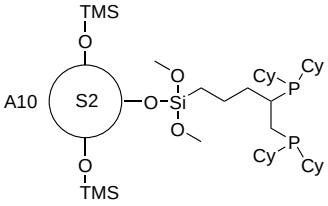

A10.1: loading = 0.0743 mmol/g
A10.2: loading = 0.1566 mmol/g

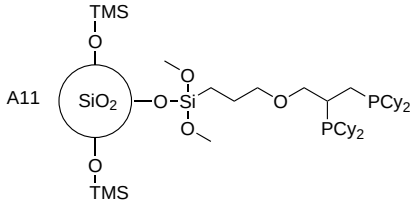

loading = 0.028 mmol/g

Figure 3-22: Overview of immobilized ligand investigated.

Table 3.10: Activity of immobilized ligand in the catalytic acrylate reaction. Solvent: 45 mL THF. Temperature = 100 °C, Cation source: NaH, Base: Triethylamine (NEt_3) or *N,N*-dimethylaniline (DMA). Assumption: all immobilized ligands are successfully complexated with Nickel and are active. TON is refered to the amount of immobilized ligand measured via elemental analysis.

Entry	Catalyst	Pre-treatment	$n_{catalyst}$ [mmol]	Base	n_{base} [mmol]	n_{cation} [mmol]	t [h]	$p_{C_2H_4}$ [bar]	p_{CO_2} [bar]	TON [-]
1	A8.4	A	0.0291	NEt_3	10	5	72	5	10	0.9622
2	A8.5	A	0.0938	NEt_3	5	10	72	5	10	0
3	A8.6	A	0.0130	NEt_3	5	5	72	5	10	0
4	A9.1	C	0.1388	NEt_3	10	5	48	5	10	0
5	A11	A	0.0297	NEt_3	10	5	48	5	10	0
6	A10.1	C	0.0371	NEt_3	10	5	92	5	10	0
7	A8.7	B	0.0886	NEt_3	10	5	92	5	10	0.6769
8	A8.8	C	0.0380	NEt_3	10	5	72	10	20	1.4198
9	A10.2	C	0.0371	DMA	5	5	72	10	20	0
10	A9.2	C	0.0371	DMA	5	5	72	10	20	0
11	A8.8 after 1 week	C	0.0380	NEt_3	10	5	72	10	20	0

In general, catalytic activity was only observed for catalysts prepared from ligands immobilized on polystyrene support (A8 class catalysts). For this immobilized ligand class, three different pre-treatments were carried out to prepare the relevant catalytic species. In Table 3.10 Entry 1 - 3 (Pre-treatment A), the catalyst was introduced as activated immobilized dcpe ligand along with $Ni(COD)_2$, triethylamine-NaH base system, and ethylene and CO_2. Catalyst A8.4 (Entry 1) displayed a sub-catalytic activity with TON of 0.9622, while the other catalyst A8.5 (Entry 2) and A8.6 (Entry 3) did not yield any sodium acrylate product. In case of catalyst A8.4 (Entry 1), two times as much triethylamine base was used, in order to increase the probability of immobilized nickel catalyst to come in contact with base, thus facilitating the cleavage of nickelalactone intermediate present at the catalyst surface. The exact reaction conditions were repeated with catalyst A8.7 (Table 3.10 Entry 7), which delivered sodium acrylate with TON of 0.6769. The catalytic species in Table 3.10 Entry 7 was prepared with pre-treatment B, where the activated immobilized dcpe was brought into contact with (tmeda)-nickelalactone in the autoclave at 25 °C. After 3 hours, other reactants were added and the catalytic reaction was started. Although catalyst A8.7 has higher dcpe loading, the *in situ* ligand exchange with (tmeda)-nickelalactone was estimated to deliver lower amount of active catalytic species. Table 3.10 Entry 7 highlights the possibility of convenient one-pot catalytic reaction where the unstable (dcpe)-nickelalactone species was prepared *in situ* just before reaction. The presence of (tmeda)-nickelalactone should not interfere with the catalytic reaction itself. The blank reaction with (tmeda)-nickelalactone and the combination of triethylamine-NaH base did not provide sodium

acrylate, which eliminates the possibility of (tmeda)-nickelalactone influencing the TON value. The catalytic reaction in Table 3.10 Entry 7 worked by firstly forming an immobilized (dcpe)-nickelalactone species, which was cleaved by triethylamine-NaH base to give sodium acrylate.

Catalyst A8.8, which is dcpe ligand immobilized at polystyrene as support material, also showed a high catalytic activity with TON of 1.4198 (Table 3.10 Entry 8). Contrary to previous catalytic reactions (Table 3.10 Entry 1 - 3 and 7), the reaction was carried out with higher ethylene (10 bar) and CO_2 pressure (20 bar). In addition, the catalytic species of A8.8 was prepared via a separate ligand exchange with (tmeda)-nickelalactone at 25 °C for 18 hours under argon atmosphere (Pre-treatment C). This probably allowed for the formation of high concentration of immobilized (dcpe)-nickelalactone at the surface of the support. After proper wash to remove unreacted (tmeda)-nickelalactone, the catalytic species was introduced into the autoclave along with triethylamine, NaH, THF solvent. Pressurization of the autoclave with 10 bar ethylene and 20 bar CO_2 started the catalytic reaction.

The immobilized (dcpe)-nickelalactone is unstable and should always be freshly prepared before reaction. Catalytic reaction with the same catalyst, after it had been stored under argon atmosphere at 25 °C for one week, did not display any detectable catalytic activity (Table 3.10 Entry 11). This can be attributed to the decomposition of the (dcpe)-nickelalactone itself.

On the other hand, all catalyst with silica support did not deliver any sodium acrylate product. Three different catalysts with silica as support were tested in catalytic reaction. Catalyst A9.1 and A9.2, which are dcpe anchored on SBA-15, were introduced into the reactor with pre-treatment method C. The catalyst was brought into contact with

(tmeda)-nickelalactone and stirred under argon atmosphere at 25 °C for 18 hours. The catalytic species was then introduced into the reactor with triethylamine for A9.1 (Table 3.10 Entry 4) or *N,N*-dimethylaniline for A9.2 (Table 3.10 Entry 10). In catalytic reaction with A9.1 catalyst, the ethylene and CO_2 pressure were 5 and 10 bar respectively. On the other hand, catalyst A9.2 used 10 bar ethylene and 20 bar CO_2. After 48 hours (Table 3.10 Entry 4: Catalyst A9.1) or 72 hours reaction (Table 3.10 Entry 10: Catalyst A9.2), no sodium acrylate product can be observed in ^{1}H NMR. Catalyst A10 with Cariact Q-20C as support were also tested under the same reaction conditions: After pre-treatment with method C, catalyst A10.1 (Table 3.10 Entry 6) and A10.2 (Table 3.10 Entry 9) were tested with triethylamine and *N,N*-dimethylaniline respectively. While catalyst A10.1 used 5 bar ethylene and 10 bar CO_2 during catalytic reaction, the reactor with catalyst A10.2 was pressurized with 10 bar ethylene and 20 bar CO_2. After 92 hours (Table 3.10 Entry 6: catalyst A10.1) or 72 hours (Table 3.10 Entry 9: catalyst A10.2), no sodium acrylate product can be observed in ^{1}H NMR. Finally, catalyst A11 (Table 3.10 Entry 5 Pre-treatment A) was introduced into the reactor along with $Ni(COD)_2$, triethylamine, NaH, 5 bar ethylene and 10 bar CO_2. After 48 hours reaction, no sodium acrylate could be observed.

The inability of silica supported immobilized catalysts to facilitate one-pot reaction can be related to the properties of the support used. Contrary to polystyrene support, silica support possesses a very reactive silanol moiety, which may disturb and influence the immobilized metal complex. It is also possible that the anchored metal complex is chemisorbed on the catalyst support (Figure 3-3). The ability of the polystyrene to swell in THF also plays a decisive role, resulting in a rapid, less restricted access of reactants to the catalytic sites on the support. The absence of any reactive moiety in polystyrene support, along

with shorter linker used (2 flexible carbon atoms for A8 class catalyst) and the ability of polystyrene support to swell allow the formation and cleavage of the nickelalactone with immobilized catalyst. The catalytic activity in immobilized metal complex with polystyrene support should represent a proof-of-concept requiring further optimization. Variation of the linker rigidity, length, and the degree of cross-linking of the support itself (thus swell-ability) are proposed for further investigation.

3.5 Conclusion

A process utilizing immobilized nickel complex combined with amine-NaH base system presents an alternative to its molecular catalyst counterpart. The process has the advantage that the immobilized nickel complex catalyst can be separated before liquid-liquid extraction, which can harm the molecular metal catalyst. This would increase the lifetime of the catalyst and reduce the number of components in the post-processing step. In addition, the application of hydrophobic amine base, such as *N,N*-dimethylaniline, *N,N*-diethylaniline, or trioctylamine, improves the base recycling and simplify the product isolation.

Immobilized dcpe on commercially available polystyrene and functionalized silica was achieved by modifying the support material with active ligand functionality, followed with metal complexation or ligand exchage with (tmeda)-nickelalactone to afford immobilized catalytic species. Two synthetic routes for the preparation of immobilized ligand were explored. Sequential assembly route offers a controlled functionalization of the support, which may result in higher loading of active immobilized catalytic species. On the other hand, direct anchoring route presents a simple and direct approach, yet demands ligand activation before complexation with metal and the subsequent catalytic reaction.

This will result in several unintended side products and the deactivation of the catalytic species. MAS NMR investigation clearly indicated the presence of ligand immobilized on the surface of the support material. Immobilized dcpe·2 BH_3 can be observed at around 24 ppm, while immobilized dcpe and dcpe oxide can be observed at around -7 ppm and 51 ppm respectively. Efforts to isolate and characterize immobilized (dcpe)-nickelalactone complex are hindered by the stability of the intermediate itself. Catalytic reaction with immobilized ligand and triethylamine-NaH base system provided sodium acrylate with TON of up to 1.42. Assuming a continuous semi batch reactor with 0.2 mmol nickel dcpe complex molecular catalyst, this would represents a space-time-yield (STY) of:

$$STY = \frac{TOF \cdot n_{Catalyst} \cdot M_{Sodium\ Acrylate}}{V_{reactor}}$$

$$STY = 6.19 \cdot 10^{-6}\ \frac{kg_{\ Sodium\ Acrylate}}{L \cdot h}$$

with $M_{Sodium\ Acrylate}$ = 94.04 g/mol and $V_{reactor}$ = 0.060 L.
The low activity of the immobilized catalyst can be related to the limited mobility of the catalyst itself, leading to decreased contact probability between the catalytic site on the surface of the solid and the reactants in the liquid phase. In addition, only metal complex anchored at polystyrene support displayed catalytic activity, while those anchored at silica support did not. This may be due to the presence of silanol group as well as the adsorbed oxygen impurities in the cavity of the silica support. These active impurities can affect and interact with the immobilized metal complex, resulting in catalyst decomposition and/or chemisorption, rendering the catalyst inactive. Since TON is referred to the amount of all immobilized ligand assuming they can be complexated and are active during reaction, the actual TON value may be higher.

Quantification of the actual active molecular catalyst during reaction is not trivial demanding sophisticated *in situ* measurements.
While the process utilizing immobilized molecular catalyst yielded less sodium acrylate product than the previous process utilizing molecular catalyst nickel complex and amine-NaH base combination, the former benefits from the long lifetime of the catalyst significantly. During the catalytic reaction, the immobilized molecular catalyst remains in the reactor and does not take part in the product separation step, thus minimizing any contact with harmful compounds.

Chapter 4

Heterogeneous Process with Immobilized Base

4.1 Theory: Cleavage of Ni-Lactone

Productive cleavage of metalalactone resulting in the formation of the corresponding metal acrylate complex is the most challenging step in the catalytic cycle of acrylate from ethylene and CO_2. DFT calculations suggest a high energy barrier associated with the metalalactone β-hydride elimination [200, 272]. Recently, Rieger *et al*. [197] and Kühn *et al*. [198, 201] reported a nickelalactone cleavage step with electrophilic agents, such as methyl iodide or methyl triflate, generating methylpropionate and methylacrylate in low yield. In addition, Bernskoetter *et al*. reported nickelalactone cleavage with a combination of Lewis acid and nitrogen-containing base [202]. Lewis acid promotes ring opening β-hydride elimination in the nickelalactone species, which readily forms an nickel acrylate complex upon contact with a base, such as *tert*-butylimino-tri(pyrrolidino)phosphorane (BTPP). The application

of the finding in catalytic reaction is, however, not yet realized. It can also be expected that a combination of both Lewis acid and Lewis base is limited to a specific class of sub reactions (Frustrated Lewis pair), making its application in industrial process very challenging. Limbach *et al*. [204] hinted that the nickelalactone cleaveage can be achieved by introducing non-nucleophilic base to give the respective nickel-π-sodium acrylate complex (Table 1.9) [203].
In this section, the application of immobilized base in the catalytic reaction will be explored (Figure 4-1).

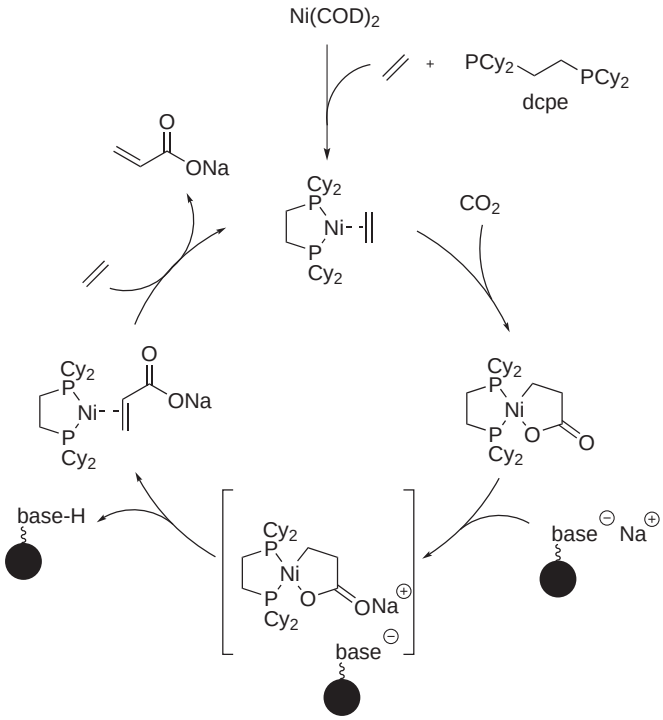

Figure 4-1: Hypothetical catalytic cycle leading to acrylates from CO_2 and ethylene with 1,2-bis(dicyclohexylphosphino)-ethane (dcpe) ligand and immobilized base system.

4.2 Process Design Options

Use of immobilized base would significantly simplify the process. The catalytic acrylate formation can be carried out continuously while at the same time the sodium acrylate product can be isolated and the immobilized base can be recycled or regenerated. Contrary to the previous processes (Process 1.1, 1.2, 1.3, and 2), the application of immobilized base results in a significant process simplification. Process 3 illustrated in Figure 4-2 is based on experimental data discussed in the next section 4.3 (Table 4.1 Entry 9): 0.1 mmol (dcpe)-nickelalactone complex to facilitate nickelalactone formation combined with immobilized sodium 2-fluorophenoxide, 100 eq. NaH as cation (Na^+) source, and 50 mL THF as solvent with operating temperature of 100 °C and 10 bar ethylene and 20 bar CO_2. The preparation of immobilized base will be further discussed in section 4.3.1. The process can be carried out in one-pot reaction: the catalytic species (dcpe)-nickelalactone is dissolved in THF and mixed with immobilized base and NaH. After the suspension is transferred into the reactor, the autoclave is stirred and pressurized with 10 bar ethylene and 20 bar CO_2 and heated to 100 °C. Two steps filtration is applied in the post-processing. In the first filtration step, a part of the suspension from the reactor is continuously filtrated to separate the filtrate containing active metal complex solution and the solid consisting of immobilized base and sodium acrylate product. The filtrate with the metal complex solution can be mixed with immobilized base and NaH and directly reintroduced into the reactor, without any contact with other harmful oxidizing agent. The solid mixture of immobilized base and sodium acrylate can be separated by firstly dissolving the sodium acrylate product in water followed with a second filtration to separate the immobilized base, which is insoluble in water. The sodium acrylate solution can be dried or directly polymerized. The immobilized

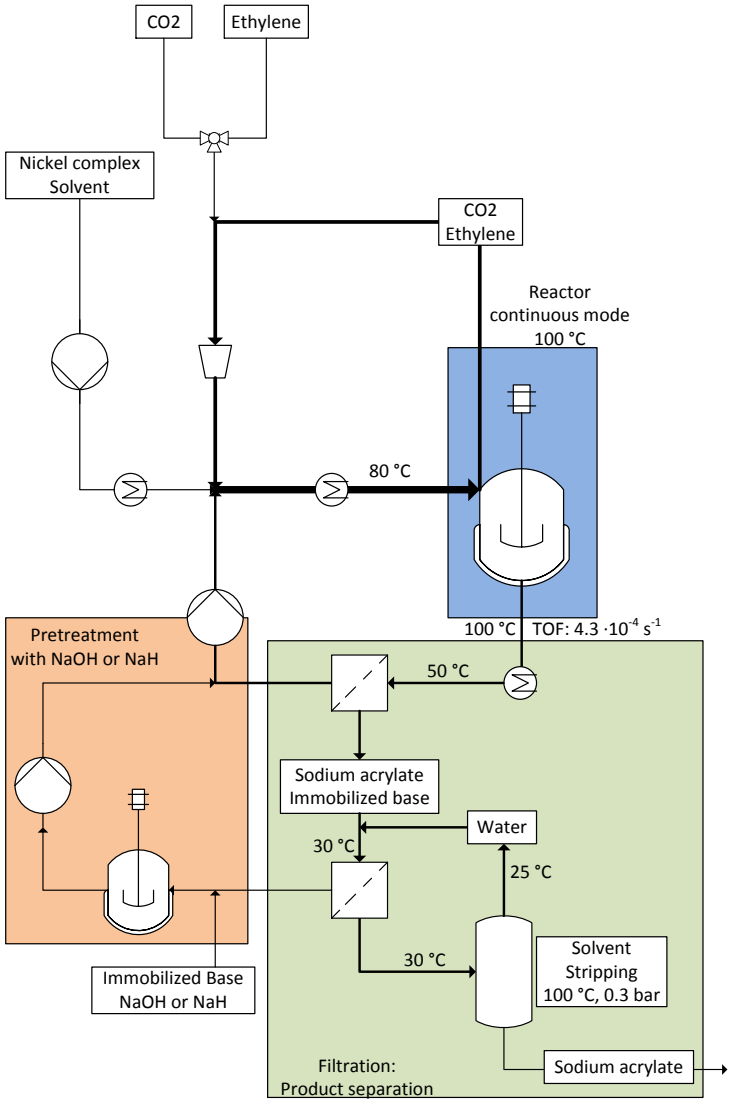

Figure 4-2: Process 3: Use of a molecular catalyst nickel complex and immobilized base in catalytic acrylate reaction.

base is reclaimed and dried to remove water. Due to the high stability of immobilized base, conventional drying in air or in vacuum at 100 °C can be carried out in this step. The immobilized base is reactivated with NaH-THF suspension or NaOH before reuse in catalytic reaction. In case of reactivation with NaOH aqueous solution, the immobilized base has to be completely dried from water.
Process 3 offers not only high activity of classical homogeneous metal complex, but also facile and efficient product isolation and base recycling. In addition, the contact between metal complex catalyst and harmful oxidizing agent can be minimized, thus improving the lifetime of the catalyst greatly. The use of filtration to separate the metal complex, immobilized base, and sodium acrylate product simplifies the process and reduces the operational and the overall investment cost. From the engineering point of view, process 3 is the most industrially relevant compared to process 1 and 2 discussed before. Improvement of the catalytic activity would make sodium acrylate production from ethylene and CO_2 industrially attractive. This can be achieved by increasing the activity of either the metal complex or the base used for the catalytic reaction.

4.3 Application of the Immobilized Bases

In this work, several immobilized bases based on the findings in Chapter 2.1 (tertiary amine base) and the publication of Limbach *et al* [203]. (alkoxide base) were investigated and are illustrated in Figure 4-3. Immobilized bases B1 - B4 are commercially available and were used in catalytic reaction in combination with NaH as a cation source. Immobilized bases B5 and B6 were prepared via anchoring and copolymerization respectively (Subchapter 4.3.1). Immobilized bases BR7 -

BR10 were regenerated from spent base B1.2 (Subchapter 4.3.2). The

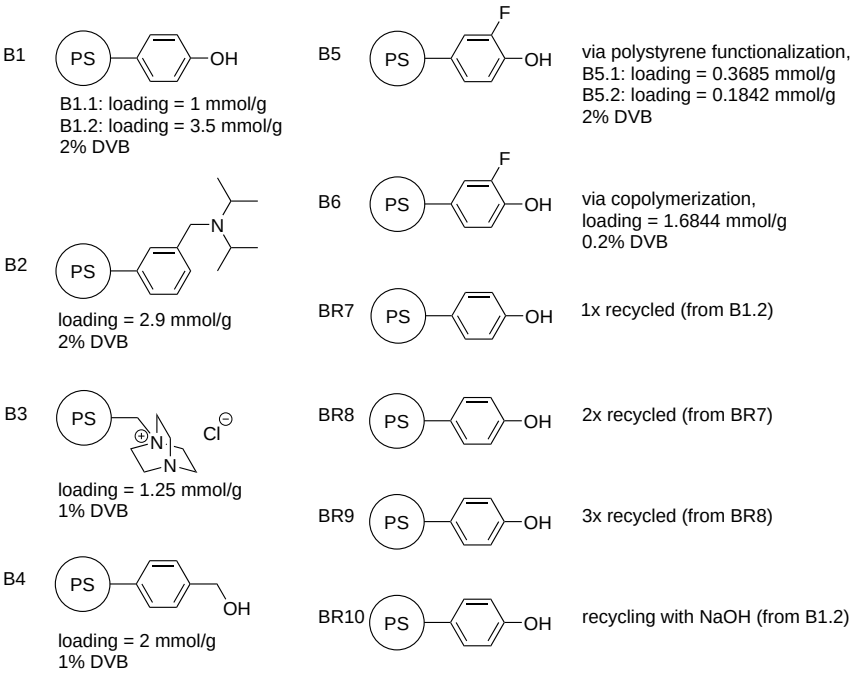

Figure 4-3: Overview of immobilized base investigated.

immobilized bases were utilized in catalytic reaction with either (dcpe)-nickelalactone or $Ni(COD)_2$-dcpe catalytic species and THF solvent. Excess NaH was added into the reaction to shift the equilibrium to the product side. All immobilized bases were active during catalytic transformation of ethylene and CO_2 into sodium acrylate (Table 4.1). Entry 1 represents a blank reaction with only nickel complex catalyst and NaH without any immobilized base, generating no sodium acrylate product, and should serve as a benchmark. Equation 4.1 and 4.2 are

introduced to better evaluate the effectivity of immobilized base during catalytic reaction:

$$TON_{Base} = \frac{TON}{n_{Base}} \tag{4.1}$$

$$TOF_{Base} = \frac{TOF}{n_{Base}} \tag{4.2}$$

Immobilized phenol on polystyrene B1 (Entry 2 - 4) afforded an average TOF of around 6 - 7·10^{-6} s^{-1}. The catalytic activity is not influenced by the loading or amount of the immobilized base. Entry 4 shows that immobilized base with higher loading yielded a similar TOF value at 6.17·10^{-6} s^{-1}. The reaction with immobilized base seems to be limited by the collisions probability of (dcpe)-nickelalactone and the surface of the immobilized base. This phenomenon should occur only with immobilized base anchored on polystyrene support with low degree of swelling. Immobilized base anchored on polystyrene support with high degree of swelling would behave more similar to homogeneous base, thus increasing the mobility of the base and providing an unhindered access of nickelalactone species to the base moiety.

Immobilized tertiary amine base B2 and B3 displayed slightly better activity. Higher average TOF of about 9·10^{-6} s^{-1} can be achieved. Normalized TOF_{Base} values shows a 85 % increase in base effectivity compared to immobilized phenol base B1. Immobilized benzyl alcohol B4 showed the highest TOF of all commercial bases investigated in this work (Entry 7). In term of base effectivity, TOF_{Base} of 4.22·10^{-6} $mmol^{-1}$ s^{-1} can be achieved, which is at least two times more effective than immobilized phenol base B1 (TOF_{Base} 2.18·10^{-6} $mmol^{-1}$ s^{-1}) and

17 % more active than tertiary amine immobilized at polystyrene support B2 and B3 (TOF_{Base} $3.72 \cdot 10^{-6}$ $mmol^{-1}$ s^{-1} and $3.61 \cdot 10^{-6}$ $mmol^{-1}$ s^{-1} respectively). Benzyl alcohol may offer less steric hindered hydroxyl moiety, thus increasing the probability of contacting the nickel-alactone species.

Table 4.1: Effectivity of immobilized base in the catalytic acrylate reaction. Parameters: 0.2 mmol $Ni(COD)_2$, 0.22 mmol dcpe, 45 mL THF, NaH as cation (Na^+) source. Exception: Entry 9 with 0.1 mmol (dcpe)-nickelalactone.

Entry	**Base**	$\mathbf{n}_{Base}$ **[mmol]**	$\mathbf{n}_{Cation}$ **[mmol]**	**T [°C]**	**t [h]**	$\mathbf{p}_{C_2H_4}$ **[bar]**	$\mathbf{p}_{CO_2}$ **[bar]**	**TON [-]**	**TOF** $[s^{-1}]$	$\mathbf{TON}_{Base}$ $[mmol^{-1}]$	$\mathbf{TOF}_{Base}$ $[mmol^{-1}\ s^{-1}]$
1	-	-	10	80	20	5	10	0	0	0	0
2	B1.1	3.3	6.6	80	20	5	10	0.5	$6.94{\cdot}10^{-6}$	0.152	$2.10{\cdot}10^{-6}$
3	B1.1	3.3	6.6	80	20	5	10	0.52	$7.22{\cdot}10^{-6}$	0.158	$2.18{\cdot}10^{-6}$
4	B1.2	5	10	80	72	5	10	1.6	$6.17{\cdot}10^{-6}$	0.32	$1.23{\cdot}10^{-6}$
5	B2	2.5	10	80	20	5	10	0.67	$9.30{\cdot}10^{-6}$	0.268	$3.72{\cdot}10^{-6}$
6	B3	2.5	10	80	20	5	10	0.65	$9.02{\cdot}10^{-6}$	0.26	$3.61{\cdot}10^{-6}$
7	B4	2.5	10	80	20	5	10	0.76	$1.05{\cdot}10^{-5}$	0.304	$4.22{\cdot}10^{-6}$
8	B5.1	0.368	10	80	72	5	10	0.28	$1.14{\cdot}10^{-6}$	0.761	$3.10{\cdot}10^{-6}$
9	B6	0.18	10	100	20	10	20	30.96	$4.30{\cdot}10^{-4}$	172	$2.39{\cdot}10^{-3}$

4.3.1 Design of the Immobilized Base

Developing an immobilized base, which is active in one-pot ethylene and CO_2 coupling to sodium acrylate, is of huge interest to further optimize the catalytic process. It is also important that the immobilized base can be cost-efficiently regenerated. From the results in the previous Subchapter 4.3, two different classes of active immobilized bases can be identified: immobilized alkoxides and immobilized tertiary amine bases. This chapter addresses the development of immobilized alkoxide base system, which can be utilized in one-pot catalytic acrylate reaction. There are two limitations, which make the application of commercially available immobilized bases difficult:

- Side reactions with CO_2.
- High divinylbenzene content in the polymer resulting in low swelling degree. The swelling degree affects the mobility of the immobilized base and accessibility of the base moiety and thus the effectivity of the base in catalytic reaction.

As already described in the previous Subchapter 4.3, it has been discovered that immobilized sodium phenoxide are active bases for the synthesis of sodium acrylate in a one-pot reaction. However, it is known that sodium phenoxide reacts with CO_2 in a Kolbe-Schmitt reaction (Figure 4-4) [50–53]. Reducing the base reactivity toward CO_2 can be achieved, for example by introducing an electron withdrawing group at the *ortho-* or *para-* position to improve the distribution of the electron density (Figure 4-5). Phenol is strongly activated at the *ortho-* and *para-* position, while 2-fluorophenol and 4-fluorophenol display an evenly distributed electron density. The fluorine atom is the most electronegative element with relatively small atom radius, resulting in a very close proximity to the carbon atom. Fluorine atom is therefore capable of removing

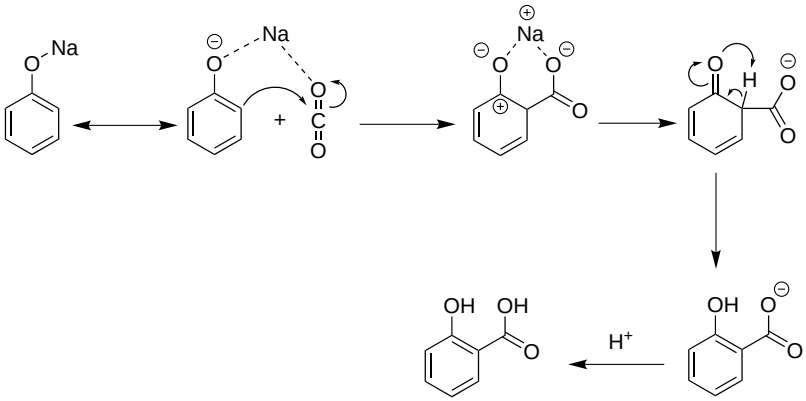

Figure 4-4: Kolbe-Schmitt reaction: aromatic electrophilic substitution of sodium phenoxide with CO_2 [50–53].

electron density from the benzene ring, thus preventing the electrophilic aromatic substitution at the phenol ring.

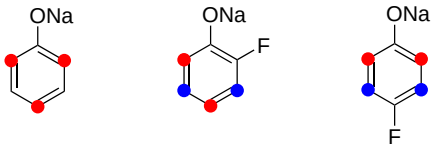

Figure 4-5: Activated position for aromatic electrophilic substitution. Red dot: activation due to ONa moiety. Blue dot: activation due to F moiety.

For immobilized bases, it is important to ensure high accessibility of the active moiety, which is in this case the -ONa group. The anchoring is therefore performed at the *para* position while F atom is attached at the *ortho* position. In this work, the immobilized 2-fluorophenol analogues were prepared using two different synthetic routes:

Direct anchoring of 2-fluorophenol onto polystyrene support with Br functionality

The anchoring was achieved via Grignard reaction to form C-C bond between the linker of polystyrene support PS05 and the 2-fluoro-4-bromo-phenol. To prevent side reaction, the hydroxyl moiety of 2-

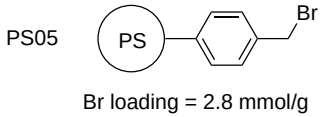

Figure 4-6: Support used for base immobilization via direct anchoring route.

fluoro-4-bromo-phenol was first protected with *tert*-butyldimethylsilyl (TBDMS) group. *tert*-butyldimethylsilyl ethers are stable toward basic reagents and can be removed with tetrabutylammonium flouride (TBAF). Introduction of silyl protecting group was carried out with *tert*-butyldimethylsilyl chloride and 2 eq. imidazole in *N,N*-dimethylformamide at 25 °C for 18 hours. After liquid-liquid extraction with hexane/water, drying ($MgSO_4$), and vacuum evaporation, pure *tert*-butyldimethylsilyl-2-fluoro-4-bromo-phenolate (yield = 85.4 %) was obtained. The protected phenol was then reacted with magnesium metal in THF at 50 °C to form the Grignard reagent. After cooling to 0 °C, the Grignard reagent was reacted with the electrophilic linker of polystyrene support for 24 hours. The solid product was filtrated, washed, and treated with 1 M TBAF in THF at 0 °C for 30 minutes to remove the silyl protecting group. Since the anchoring route involves a slow reaction between a solid and fluid, the long time stability of the Grignard reagent affects the final base loading on the support significantly. The stability of the Grignard reagents depends on the temperature, at which the anchoring takes place. While anchoring at 0 °C for 24 hours yielded 2-fluorophenol loading of 0.3685 mmol/g (Table 4.2 Entry 1), anchoring

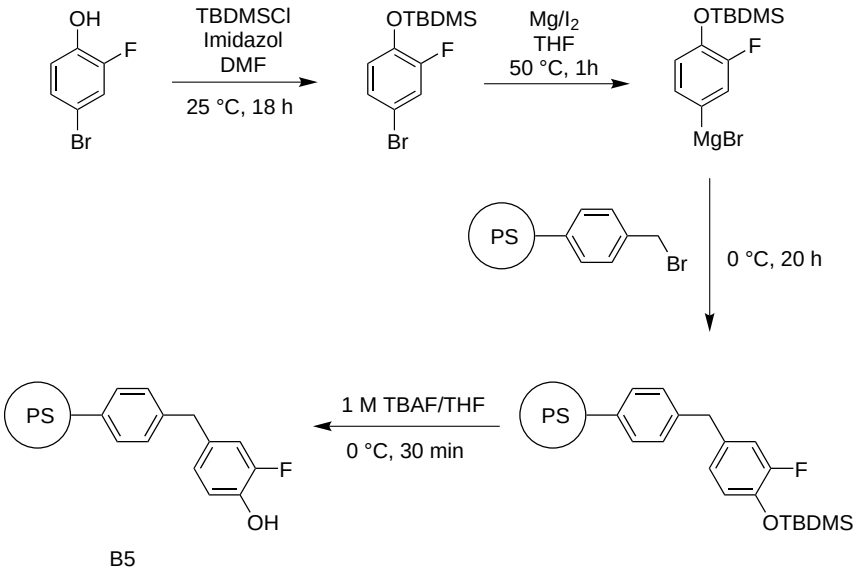

Figure 4-7: Anchoring of 2-fluorophenol onto polystyrene support.

at the same conditions but at 25 °C resulting in much lower base loading at 0.1842 mmol/g (Entry 2). Due to low contact probability between the

Table 4.2: Anchoring of 2-fluorophenol on the polystyrene support PS05. Base loading values were derived from elemental analysis results. X = Br moiety on the catalyst support. Base:X ratio = 0.5 mmol/mmol. Degree of anchoring = ratio of anchored base to base starting material.

Entry	Sample name	Conditions	Base loading on support [mmol/g]	Degree of anchoring [%]
1	B5.1	24h at 0 °C	0.3685	26.32
2	B5.2	24h at 25 °C	0.1842	13.16

elctrophile attached to the solid material and the nucleophilic phenolate in the liquid phase, the anchoring approach results in low loading of the base. Similar to the preparation of immobilized ligand discussed in Subchapter 3.3.2, the final base loading on the support material is greatly influenced by the physical properties of the support itself: the surface area, the pore size, and the linker loading. After reaching a certain dcpe loading, the support becomes overcrowded and the resulting steric prevents any further anchoring of the base at the support. Any unreacted base remaining in the solution was removed during washing. The direct anchoring strategy is thus ineffective; only a small fraction of the 2-fluorophenol educts could be anchored. In addition, since direct anchoring approach used a commercially available polystyrene support with 2 % divinylbenzene crosslinker (PS05, Figure 4-6), the second limitation associated with commercial immobilized base concerning the degree of swelling can not be addressed. Alternative preparation route to immobilized 2-fluorophenol via copolymerization is therefore explored in the next section.

Copolymerization of 2-fluoro-4-vinylphenol, styrene, and 1,4-divinylbenzene

The copolymerization approach allows a full control of the properties of the immobilized base. Materials with a high loading of the active moiety and a specific degree of swelling can be precisely tailored. Copolymerization can be performed by firstly preparing the necessary monomer. In this work, 2-fluoro-4-vinylphenol monomer was prepared by introducing a vinyl side chain to 2-fluoro-4-bromophenol. This was achieved via cross-coupling reaction of 2-fluoro-4-bromophenol with vinyl Grignard reagent, which took place in the presence of 1 mol%

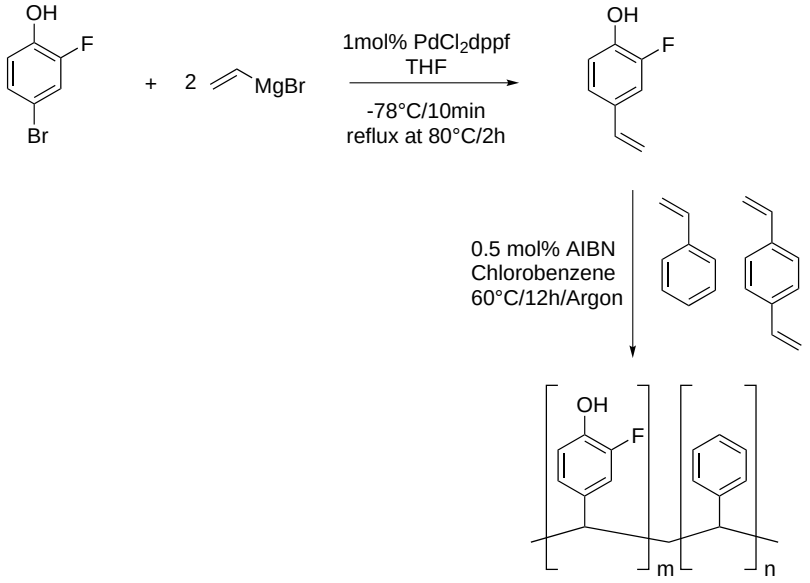

Figure 4-8: Immobilization of 2-fluorophenol via copolymerization.

[1,1-bis(diphenylphosphino)ferrocene]dichloropalladium ($PdCl_2$dppf) catalyst at 80 °C for 2 hours. Two eq. of Grignard reagent are required to protect the hydroxy groups, which can interfere during the reaction. After 2 hours, the reaction mixture was cooled, quenched with 1 M HCl solution and extracted with diethylether. The product was recrystallized to achieve pure 2-fluoro-4-vinylphenol monomer. The product was copolymerized with styrene and 1,4-divinylbenzene in the presence of 2,2-azobis(2-methylpropionitrile) (AIBN) as radical initiator at 60 °C for 12 hours. The ratio of 2-fluoro-4-vinylphenol:styrene:1,4-divinylbenzene was 3:7:0.2. After purification, the polymer product was characterized with elemental analysis to give an immobilized base with an active moiety loading of about 1.6844 mmol/g.

Both immobilized 2-fluorophenol prepared via anchoring (B5) and copolymerization (B6) routes displayed remarkable catalytic activities. Catalytic experiment with immobilized 2-fluorophenol base B5.1 afforded a TOF_{Base} value of about $4.22 \cdot 10^{-6}$ $mmol^{-1}$ s^{-1} (Table 4.1 Entry 8). The immobilized base B5.1 was prepared by anchoring 2-fluorophenol moiety onto a commercially available polystyrene support PS05, which is prepared via copolymerization with 2 % divinylbenzene as crosslinker. The high amount of crosslinker increases the polymer strength, hardness, and stability toward solvent and heat. When polymer chains are connected with each other or crosslinked, they lose some of their ability to expand or move as individual polymer strain. In polymers with low degree of crosslinking, organic solvent may separate the polymer chains which are not covalently linked. The polymer chains may expand, resulting in the swelling phenomenon of the polymer. As little as 0.5 % divinylbenzene in a styrene polymerization makes the polymer insoluble, yet still swellable. This may have an important consequence in the effectivity of the base: immobilized base B6, which was copolymerized with only 0.2 % divinylbenzene, thus low degree of crosslinking and high degree of swelling, yielded a significantly higher TOF, at $4.3 \cdot 10^{-4}$ s^{-1} (Table 4.1 Entry 9). In term of base effectivity, this would translate to a TOF_{Base} of $2.39 \cdot 10^{-3}$ $mmol^{-1}$ s^{-1}. Low degree of crosslinking of the immobilized base B6 allows the solvent to partially "dissolve" the polymer. Immobilized base would behave more similar to homogeneous base, thus increasing the mobility of the base and providing an unhindered access of nickelalactone species to the base moiety.

4.3.2 Recycling of the Immobilized Base System

Recyclability of immobilized base is one of the most important factors in the process 3. Highly recyclable material will contribute to efficient continuous process. The recyclability of immobilized base was investigated with commercial B1.2 as a representative model. The catalytic reaction was carried out with (dcpe)-nickelalactone catalyst and THF solvent with 10 bar ethylene and 20 bar CO_2 at 100 °C for 20 hours (Table 4.3). Reference reaction with fresh immobilized base B1.2 delivered a TON of 1.57 (Entry 1). After catalytic reaction, the spent base B1.2 was regenerated by five-times washing with:

- 1 M aqueous HCl solution to liberate all hydroxyl groups and
- ethanol to remove any chemisorbed nickel complex species.

The regenerated immobilized bases were dried at 50 °C in vacuum overnight to remove all volatile impurities to give immobilized phenol base. The base was suspended in THF and activated by the addition of NaH. BR7, BR8, and BR9 denote recycled immobilized base after one, two, and three catalytic reactions respectively.
Alternatively, the spent immobilized base from Entry 1 can also be regenerated with 1 M aqueous NaOH solution instead of HCl. Contrary to acidic regeneration with HCl, the base recycling with NaOH was ended with NaOH wash to afford immobilized sodium phenolate base. After regeneration, the immobilized base BR10 was dried at 50 °C in vacuum overnight to remove all volatile impurities.
The immobilized bases BR7 - BR10 were tested in the catalytic reaction under the same condition as Entry 1. The amount of recycled immobilized base in the catalytic reaction was not constant due to significant loss during recycling step. However, as already mentioned in the previous section 4.3, the catalytic activity is not influenced by the amount

of the immobilized base B1 present during the catalytic reaction but is limited by the collisions probability of (dcpe)-nickelalactone and the surface of the solid immobilized base B1. The immobilized base can thus be assumed to be available in excess during the reaction and is not rate limiting. The effectivity of base recycling can be quantified by introducing a dimensionless quantity, which normalizes the TON of the recycled base with the value in the previous catalytic reaction:

$$Activity\ recovery = \frac{TON\ after\ recycling}{TON\ before\ recycling} \tag{4.3}$$

In general, all recycled immobilized bases displayed the ability to facilitate the nickelalactone cleavage (Figure 4-9). Reaction with immobilized base after one time recycling (Table 4.3 Entry 2: TON 1.18) produced 25 % less sodium acrylate compared to the reaction with fresh immobilized phenol B1.2 (Entry 1: TON 1.57). On the other hand, immobilized base after two times recycling regained its full effectivity (Entry 3: TON 1.29), which is 109 % TON value of immobilized base after one time recycling. Similarly, the effectivity of immobilized base after three times recycling (Entry 4: TON 1.16) is comparable to that after two times recycling. Further investigations are necessary to elucidate the limitation of recycled base.

On the other hand, the application of BR10 base, which is regenerated with NaOH, resulted in significantly lower activity (Entry 5). Catalytic reaction with BR10 yielded sodium acrylate with TON of 0.54, which represents only 47 % activity of fresh immobilized base. The limited activity of BR10 base can be related with trace water in the recovered material. While acidic regeneration with HCl was completed with washing with ethanol to remove traces water followed with vacuum drying, water removal in NaOH regenerated immobilized base was limited to vacuum

drying, which may result in higher water content in the recovered BR10 base.

Table 4.3: Recyclability of immobilized sodium phenoxide in the catalytic acrylate reaction. Parameters: 0.2 mmol (dcpe)-nickelalactone, Base loading = 3.5 mmol/g, 45 mL THF, 10 bar ethylene, 20 bar CO_2, 100 °C, and 20 hours reaction. Cation source: 10 mmol NaH.

Entry	Base	n_{Base} [mmol]	TON [-]	Activity recovery [%]
1	B1.2	5	1.57	100
2	BR7	5	1.18	75
3	BR8	4.255	1.29	109
4	BR9	2.882	1.16	90
5	BR10	5	0.54	47

4.4 Conclusion

A process utilizing homogeneous nickel complex combined with immobilized base system can be considered as the most industrially feasible one from all four process concepts previously discussed. In addition to more superior catalytic activity comparable to its molecular catalyst - alkoxide and amine-NaH base system (Process 1.1, 1.2, and 1.3), the process with immobilized base offers excellent product separation and base recycling. The post reaction process requires a simple two steps filtration to separate the sodium acrylate product and to recover the immobilized base. Immobilized base can be regenerated with either NaH or cost-efficient NaOH as alternative. This would significantly reduce the energy consumption and the investment cost for a complex extraction process required in other concepts described before. In addition,

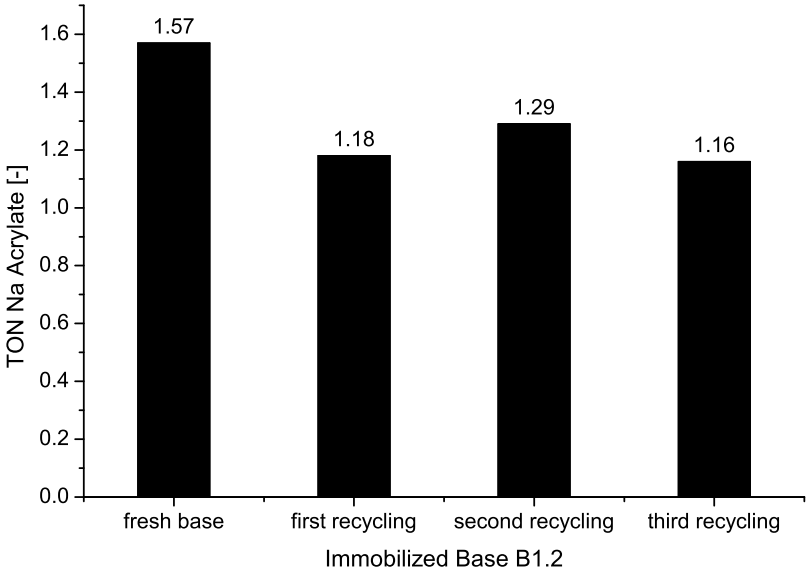

Figure 4-9: Recyclability of immobilized sodium phenoxide in the catalytic acrylate reaction.

the process can also be carried out continuously, which would reduce the labor cost and increase the overall efficiency. The catalytic nickel complex species remains during the whole process in the reactor under inert atmosphere and thus retains its catalytic activity during the whole process.

The improvement in the catalytic activity of the metal complex as well as the effectivity of the immobilized base would translate to a highly efficient chemical process. Effectiveness of the immobilized base can be achieved by decreasing the reactivity of the base towards CO_2 and increasing the swell-ability of the material. The latter factor would increase the mobility of the active base moiety during catalytic reaction. These two factors are key points in designing a highly effective immobilized base. Immobilized 2-fluorophenol base prepared via copolymerization of the monomer with 0.2 % divinylbenzene provided a promising candidate, enabling a TON of 30.94 in catalytic reaction with (dcpe)-nickelactone (TOF $4.30 \cdot 10^{-4}$ s^{-1}). Assuming a continuous semi batch reactor (process concept 3) with 0.2 mmol nickel dcpe complex molecular catalyst, the highest TOF achievable in this work of about $4.30 \cdot 10^{-4}$ s^{-1} represents a space-time-yield (STY) of:

$$STY = \frac{TOF \cdot n_{Catalyst} \cdot M_{Sodium\ Acrylate}}{V_{reactor}}$$

$$STY = 4.86 \cdot 10^{-4}\ \frac{kg_{\ Sodium\ Acrylate}}{L \cdot h}$$

with $M_{Sodium\ Acrylate}$ = 94.04 g/mol and $V_{reactor}$ = 0.060 L.

The recyclability of the catalyst is another important aspect required in this process. It is noteworthy that successful recycling of the base was demonstrated. Base regeneration could be achieved either with acidic HCl solution or basic NaOH solution. Acidic HCl regeneration resulted in high base activity, comparable to that of the fresh immobilized base.

Basic regeneration with NaOH resulted in a material which activity (TON 0.54) was much lower than that of the fresh immobilized base (TON 1.57).

In addition to the high catalytic activity of the reaction utilizing molecular catalyst and immobilized base, this process concept also benefits from the significantly lower separation and recycle costs. Moreover, the separation of the molecular catalyst from the product - immobilized base mixture can be achieved with a filtration step, which minimizes the contact of the active molecular catalyst with any harmful compounds.

Chapter 5

Conclusions

The molecular nickel complex in combination with alkoxide base was reported as the only working catalytic reaction of ethylene and CO_2 leading to sodium acrylate [203]. The system is constrained to two-pot process with nickelalactone formation in the first step and nickelalactone cleavage in the second step. The two-pot process prevents the unintended side reaction of the alkoxide base with CO_2 forming an inactive semi-carbonate. Unfortunately, the formation of a conjugate acid of the alkoxide base during reaction is unavoidable. The resulting conjugate acid reacts with and deactivates the nickel complex catalyst. Moreover, liquid-liquid extraction is required to separate the water soluble sodium acrylate product from the nickel complex solution. In this step, traces of oxygen or other impurities may oxidize and deactivate the nickel complex catalyst, which complicates the recyclability of the catalyst. Limbach *et al* [203]. reported a catalytic reaction with TON of up to 10 with a combination of (d*t*bpe)-nickel complex and NaO*t*Bu base. Limitations of the state-of-the-art process reported by Limbach *et al* [203]. are successfully addressed in this work. Three different system concepts are proposed:

- Homogeneous process with a molecular nickel complex catalyst and amine-NaH base systems (Chapter 2).

- Heterogeneous process with an immobilized nickel complex catalyst and amine-NaH base systems (Chapter 3).

- Heterogeneous process with a molecular nickel complex catalyst and an immobilized base (Chapter 4).

The application of CO_2-stable amine-NaH base system allows one-pot process, which reduces the complexity of the process greatly. Several tertiary amine alkali hydride combinations have been successfully identified as an effective system for the nickelalactone cleavage. A combinaton of (dcpe)-nickelalactone catalyst with triethylamine-NaH delivered a TON of 18.84 (TOF $7.27 \cdot 10^{-5}$ s^{-1}). In addition, the application of hydrophobic amines further improves the recyclability of the base and simplifies the post-treatment greatly. Liquid-liquid extraction separates the organic base containing hydrophobic base and nickel complex catalyst from the sodium acrylate in the aqueous phase. After simple pre-treatment of the organic phase to remove remaining water, the base along with the nickel complex catalyst can be directly reused. The combination of nickel dcpe complex with *N,N*-dimethylaniline, *N,N*-diethylaniline, trioctylamine and NaH yielded sodium acrylate with TON of up to 3.93, 2.65, and 16.91 respectively.
Heterogenization of the nickel complex catalyst or base allows the process to be run continuously. The sensitive nickel complex remains in the reactor without contact with other impurities, thus increasing the lifetime of the catalyst during the catalytic reaction.
Heterogenization of the nickel complex was achieved via anchoring on silica and polystyrene support materials. Metal complex loading of up to 0.1566 mmol/g and 0.134 mmol/g can be achieve with silica gel and

polystyrene support respectively. MAS NMR investigations confirmed the presence of active dcpe immobilized on the surface of the support materials. Immobilized (dcpe)-nickelalactone intermediate species is instable and decomposes readily. The immobilized nickel complex on polystyrene support delivered catalytic activity with TON of up to 1.42 with triethylamine-NaH base combination. On the other hand, immobilized nickel complex on silica support did not display observable sodium acrylate product. This might be due to strong interaction of the active nickel complex with either the silanol moiety or the chemisorbed oxygen, which may preset on the inner and outer surface of the support. A combination of homogeneous nickel complex and immobilized base showed high activity, especially in case of immobilized sodium 2-fluorophenolate. Immobilized sodium 2-fluorophenolate was prepared either via direct anchoring on linker-functionalized polystyrene support or via copolymerization of the 2-fluoro-4-vinylphenol monomer with styrene and 1,4-divinylbenzene in the presence of radical initiator. A combination of (dcpe)-nickelalactone catalyst with immobilized sodium 2-fluorophenolate delivered a TON of up to 30.94 (TOF $4.30 \cdot 10^{-4}$ s^{-1}). The immobilized sodium 2-fluorophenolate was prepared via copolymerization with 0.2 % divinylbenzene, resulting in highly swellable material with exceptional accessibility of the base moiety.

Recycling of the immobilized base was successfully represented with commercially available immobilized phenol on polystyrene. The recyclability of the immobilized base is crucial and can be applied in a highly efficient continuous process. The solid immobilized base and sodium acrylate can be continuously separated from the reactor with simple filtration step. The molecular nickel complex catalyst dissolved in organic solvent can be directly mixed with regenerated immobilized base and reintroduced into the reactor. The immobilized base can be

separated from the sodium acrylate by first dissolving the latter one and then by filtrating of the insoluble base. The immobilized base can be regenerated either with aqueous HCl or NaH solution. The process using a combination of molecular nickel complex catalyst and immobilized base is currently the most industrially applicable process. It offers not only high activity of the molecular catalyst, but also continuous recycling of the base and isolation of the sodium acrylate product. Utilization of energy-efficient filtration process during the post-treatment would omit complex liquid-liquid extraction approach, thus reduce the investment and operational cost significantly.

The characteristics of four different metal catalyst - base combinations for sodium acrylate reaction from ethylene and CO_2 are summarized in Figure 5-1 and Table 5.1. From all processes investigated here, the combination of homogeneous nickel complex with immobilized base delivered the most industrially relevant process. It allows for the combination of both high activities of the homogeneous nickel complex with the easy recycling of the catalyst and base. Further optimizations of the active metal complex and of the structure of the immobilized base will improve the overall effectivity of the system.

The direct synthesis of sodium acrylate from ethylene and CO_2 still requires a major improvement in the catalytic activity to achieve an industrial-scale. Assuming a continuous semi batch reactor (process concept 3) with 0.2 mmol nickel dcpe complex molecular catalyst, the highest TOF achievable in this work of about $4.30 \cdot 10^{-4}$ s^{-1} represents a space-time-yield (STY) of:

$$STY = \frac{TOF \cdot n_{Catalyst} \cdot M_{Sodium\ Acrylate}}{V_{reactor}}$$

$$STY = 4.86 \cdot 10^{-4}\ \frac{kg_{\ Sodium\ Acrylate}}{L \cdot h}$$

with $M_{Sodium\ Acrylate}$ = 94.04 g/mol and $V_{reactor}$ = 0.060 L. An ideal STY value [273] between 0.01 - 1 $\frac{kg}{L \cdot h}$ for an industrial process would require a TOF of about $8.86 \cdot 10^{-3}$ - 0.886 s^{-1}, which is achievable with a more active nickel complex and an improved base system.

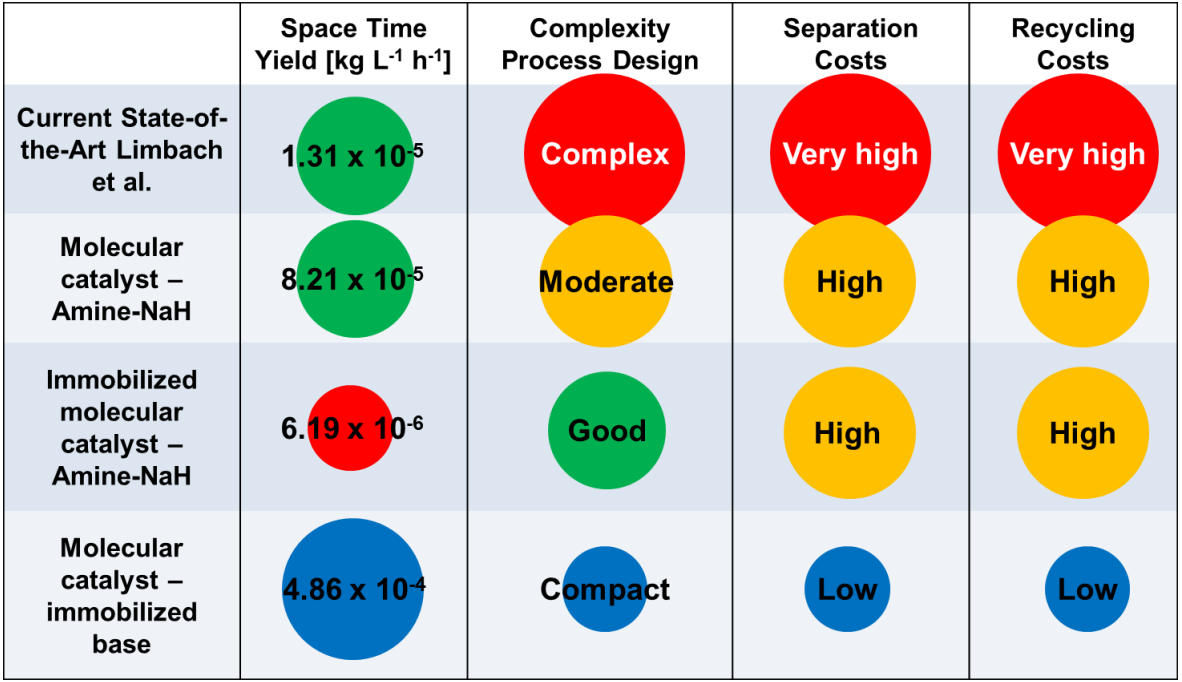

Figure 5-1: Process profitability of different metal catalyst - base combinations for sodium acrylate reaction from ethylene and CO_2. Values were calculated from the experiments with the highest yield in sodium acrylate.

Table 5.1: Comparison of different metal catalyst - base combinations for sodium acrylate reaction from ethylene and CO_2.

	Molecular nickel complex catalyst - alkoxide [203]	**Molecular nickel complex catalyst - amine-NaH**
Catalytic activity	High, however catalyst deactivates due to reaction with the conjugate acid of the base	High
Catalyst lifetime	Low, may be oxidized during product separation (liquid - liquid extraction) and side reaction with conjugate acid of the base	Low, may be oxidized during product separation
Product separation	Difficult, liquid-liquid extraction from reaction mixture	Moderate
Base recycling	Difficult, conjugate acid of the base forms azeotrope with water	Good, especially for hydrophobic amine
Process (Product separation and base recycling)	Energy intensive	Moderate (hydrophilic amine) - Good (hydrophobic amine)

Table 5.1: (cont.)

	Immobilized nickel complex catalyst - amine-NaH	**Molecular nickel complex catalyst - immobilized base**
Catalytic activity	Low, due to low mobility of the immobilized catalyst, thus lower contact probability between nickelalactone species on the catalyst surface and base in the liquid phase	High, especially when highly swellable polymer support is used to immobilize base
Catalyst lifetime	Good, catalyst can be separated before liquid - liquid extraction	Good, catalyst can be separated and directly used for the catalytic reaction before contact with other compounds
Product separation	Easy	Excellent (energy efficient filtration)
Base recycling	Good, especially for hydrophobic amine	Excellent, only requires simple filtration
Process (Product separation and base recycling)	Moderate (hydrophilic amine) - Good (hydrophobic amine)	Excellent (energy efficient filtration)

Appendix A

Experimental Section

Unless otherwise stated in this section, all commercially available chemicals were directly used. For reactions where oxygen and water contents are crucial, the solvents were degassed (e.g. Freeze-Pump-Thaw) and/or dried with activated molecular sieves or elementary sodium.
^{1}H, ^{13}C, and ^{31}P NMR spectra were recorded on Bruker Avance 50, 125, 200 or 500 MHz spectrometers and were referenced to the residual proton (^{1}H) or carbon (^{13}C) resonance peaks of the solvent. Chemical shifts (δ) are reported in ppm. Elemental analysis were recorded by the analytical service of BASF. MAS NMR spectra were recorded on a Bruker MSL-400 spectrometer by apl. Prof. Dr. Michael Hunger at the University of Stuttgart.

A.1 High Throughput Experimentation

The close connection between the catalyst and the reaction conditions has always led to a multidimensional effort with extensive resources.

The introduction of high throughput experimentation with the emphasis on miniaturization, parallelization, and automation of experiments allows for increased experimental load without additional time and personal resources, thus accelerating the research and development process. Over the past years, high throughput experimentation has facilitated significant advances in the discovery and optimization of chemical processes. High throughput experimentation can be applied in the synthesis of new or optimized catalyst as well as the subsequent catalyst screening.

In this work, high throughput experimentation was carried out for the testing of the catalysts and the base systems in a 4-fold 160 mL titanium autoclave system and 6-fold 60 mL steel autoclave system. The reaction conditions in each autoclave can be individually adjusted, offering a broad possibility of performing several experiments in parallel. A simplified schematic drawing of a single autoclave unit is illustrated in Figure A-2 below. Each autoclave is equipped with a charger port, allowing the introduction of chemicals under inert condition. Argon was used to pressurize and facilitate inert transfer of the chemicals into the autoclave. Ethylene, CO_2, and optionally nitrogen as well as argon can be introduced into the reactor via gas inlet 1 and 2. A fourth port line was used as a gas release mechanism. Each autoclave was also equipped with a rupture disk to protect the vessel from any unintended overpressurization. The temperature and pressure inside each autoclave were individually controlled and recorded. Two autoclave types were used for the screening purpose (Table A.1).

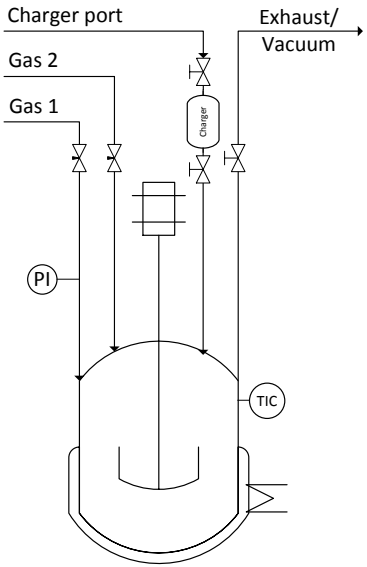

Figure A-1: Schematic drawing of a single autoclave unit.

Table A.1: Types of autoclave used for the screening purpose.

	Titanium autoclave	**Steel autoclave**
Max volume [mL]	160	60
Max operating pressure [bar]	80	180
Max operating temperature [°C]	120	200
Chemical resistance	Very good	No corrosive chemicals

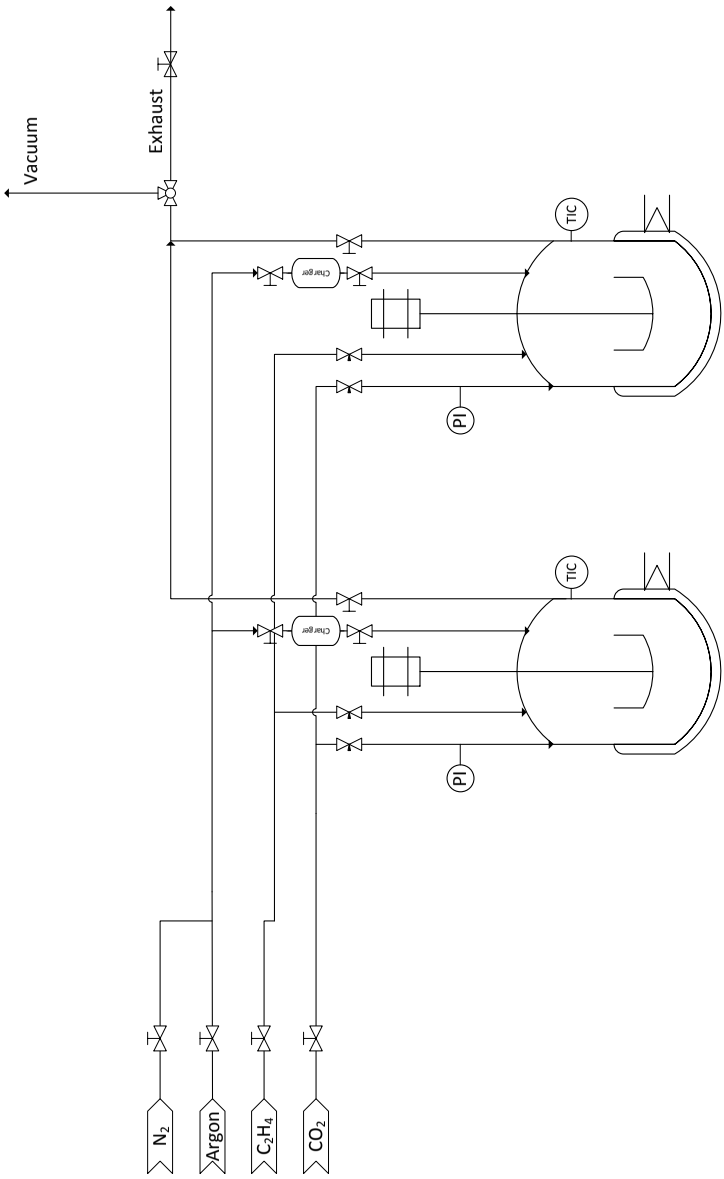

Figure A-2: Schematic representation of a multi-fold autoclave system (only two autoclaves are shown).

The high throughput experimentation is particularly useful in the early research of a chemical process, where several reaction parameters have to be identified. The iterative improvement in the catalysis research as well as in the reaction and process engineering parts will effectively lead to shorter time-to-market.

A.2 Catalytic reaction

One-pot catalytic reaction was performed in a 4-fold 160 mL titanium autoclave system and 6-fold 60 mL steel autoclave system. All reactants were prepared under inert conditions in a glovebox and transferred into the autoclave via a charger. After all required components were successfully introduced, the autoclave was mechanically stirred (2000 rpm) and pressurized with ethylene until the solvent was saturated (15 minutes). The autoclave was then further pressurized with CO_2 until saturation (15 minutes). After reaching a constant pressure, the autoclave was heated up to a certain temperature within five minutes. After the indicated reaction duration, the autoclave was cooled to room temperature and depressurized. Unless otherwise stated, the autoclave was opened in air and standard work up procedure was carried out to isolate the sodium acrylate product.

Work up: Product isolation

A mixture of 10 mL D_2O and 10 mL THF was added dropwise into the reaction mixture. Additional 15 mL D_2O was added and the mixture

was extracted twice with 2 times 20 mL diethylether. Tetramethylammonium iodide (NMe_4I 0.125 mmol, 25.1 mg) and 2,2,3,3-d_4-3-(trimethylsilyl)propionic acid (0.167 mmol, 28.7 mg) were added to the aqueous phase as internal standard.

NMR Quantification

The amount of sodium acrylate product was determined by ^1H NMR spectroscopy with two internal standards for quantification. The internal standards were chosen with the following requirements:

- chemically inert.
- low volatile.
- highly soluble in aqueous phase (D_2O).
- simple NMR spectra, with chemical shift in ^1H NMR preferably in the range 0 - 1 ppm or 3 - 3.5 ppm.

The integrated intensity of a resonance due to the analyte nuclei is directly proportional to its molar concentration and to the number of nuclei that gives rise to that resonance:

$$Concentration \sim \frac{Integral\ Area}{Number\ of\ nuclei} \tag{A.1}$$

thus the amount of dissolved sodium acrylate product can be calculated by comparing the integral of sodium acrylate to that of a standard compound of known concentration:

$$c_{Sodium\ Acrylate} = \frac{NA_{Sodium\ Acrylate} \cdot c_{Standard}}{NA_{Standard}} \tag{A.2}$$

or

$$n_{Total\ Sodium\ Acrylate\ produced} = \frac{NA_{Sodium\ Acrylate} \cdot n_{Standard}}{NA_{Standard}} \quad (A.3)$$

with

$$NA = \frac{Integral\ Area}{Number\ of\ nuclei} \quad (A.4)$$

Table A.2: Relevant chemical shift of sodium acrylate and internal standards in ^{1}H NMR for quantification. Solvent: D_2O.

Compound	δ **[ppm]**	**Number of proton**
Sodium Acrylate	5.65 (dd)	1
2,2,3,3-d_4-3-(trimethylsilyl)propionic acid	0 (s)	9
Tetramethylammonium iodide	3.19 (s)	12

Finally TON can be calculated from the amount of sodium acrylate relative to the amount of (immobilized) catalyst:

$$TON = \frac{n_{Sodium\ Acrylate}}{n_{Catalyst}} \quad (A.5)$$

$$TOF = \frac{TON}{t} \quad (A.6)$$

Preparation of catalytic species

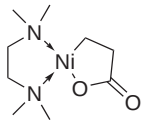

Synthesis of **(tmeda)-Nickelalactone** [199]: Bis(1,5-cyclooctadiene)nickel(0) (10 g, 36.356 mmol), succinic anhydride (3.032 g, 30.296 mmol) were suspended in tmeda (32 mL). The mixture was stirred under Argon at room temperature for 9 h. The light green complex was filtered, washed three times with 20 mL diethyl ether and dried in vacuum to give 5.48 g light green (tmeda)-Nickelalactone (Yield = 73.24%). 200.15-MHz ^{1}H NMR (DMF-d_7): δ 0.17 (2H, triplet), 1.58 (2H, triplet), 2.19 (6H, singlet), 2.23 (4H, singlet), 2.35 (6H, singlet). 50.3-MHz ^{13}C NMR (DMF-d_7): δ -1.71, 46.32, 48.42, 56.03, 60.87.

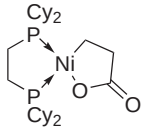

Synthesis of **(dcpe)-Nickelalactone** method 1: tmeda-Nickelalactone (4.5 g, 18.22 mmol) and 1.1 eq dcpe (8.470 g, 20.042 mol) were suspended in 100 mL THF. The mixture was stirred under Argon for 16 h at room temperature. The yellow product was filtered, washed with three times 30 mL hexane to remove tmeda and unreacted dcpe. The yellow solid was recrystallized from hexane/THF and dried in vacuum to give 7.65 g yellow-orange (dcpe)-Nickelalactone powder (Yield = 75.7%). 500.36-MHz ^{1}H NMR (CD_2Cl_2): δ 0.77 (2H, multiplet), 1.2 - 1.5 (22H, multiplet), 1.65 - 1.95 (22H, multiplet), 2.13 (4H, multiplet), 2.21 (2H, multiplet). 125.82-MHz ^{13}C NMR (CD_2Cl_2): δ 0.14, 12.37, 17.85, 24.91, 26.71, 27.64, 29.4, 29.87, 30.24, 34.14, 35.92, 37.66. 202.55-MHz ^{31}P NMR (CD_2Cl_2): δ 61.98, 69.36.

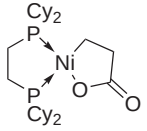

Synthesis of **(dcpe)-Nickelalactone** method 2: Bis(1,5-cyclooctadiene)nickel(0) (110 mg, 0.4 mmol) and 1.1 eq dcpe (185.9 mg, 0.44 mmol) were dissolved in 50 mL THF. The solution was charged into titan autoclave and

stirred. The autoclave was pressurized with 5 bars ethylene and the mixture was stirred further at 25 °C for 15 min. After the pressure in autoclave reach equilibrium at 5 bars, the autoclave was pressurized with 20 bars CO_2 and stirred for further 15 min until reach equilibrium. The reaction took place at 50 °C for 3 days. The autoclave was depressurized and the yellow product solution was taken with syringe. THF was removed in vacuum and the solid was redissolved in THF and precipitated with hexane to give 44 mg yellow-orange (dcpe)-Nickelalactone powder (Yield = 20 %). 500.36-MHz ^{1}H NMR (CD_2Cl_2): δ 0.77 (2H, multiplet), 1.2 - 1.5 (22H, multiplet), 1.65 - 1.95 (22H, multiplet), 2.13 (4H, multiplet), 2.21 (2H, multiplet). 125.82-MHz ^{13}C NMR (CD_2Cl_2): δ 0.14, 12.37, 17.85, 24.91, 26.71, 27.64, 29.4, 29.87, 30.24, 34.14, 35.92, 37.66. 202.55-MHz ^{31}P NMR (CD_2Cl_2): δ 61.98, 69.36.

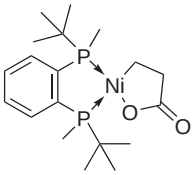

Synthesis of **(BenzP)-Nickelalactone**: tmeda-Nickelalactone (87.4 mg, 0.354 mmol) and 1 eq (*S,S*)-(-)-1,2-bis(*t*-butylmethylphosphino)benzene (BenzP) (100 mg, 0.354 mmol) were suspended in 2.5 mL THF. The mixture was stirred under Argon for 16 hours at room temperature. The reaction mixture was filtered, washed with three times 5 mL THF. The filtrate was dried in vacuum and recrystallized from hexane/THF and dried in vacuum to give 17.5 mg orange (BenzP)-Nickelalactone powder (Yield = 12%). 500.36-MHz ^{1}H NMR (CD_2Cl_2): δ 0.99 (1H, multiplet), 1.05 - 1.4 (18H, multiplet), 1.57 (6H, multiplet), 2.05 - 2.45 (3H, multiplet), 7.55 - 7.75 (4H, multiplet). 125.82-MHz ^{13}C NMR (CD_2Cl_2): δ 0.09, 4.83, 16.65, 27.37, 27.8, 33.1, 34.56, 37.32, 131.03, 132.1, 140.04, 142.33.

202.55-MHz ^{31}P NMR (CD_2Cl_2): δ 45.03, 59.74.

A.3 Ligand immobilization

A.3.1 Route 1: In situ sequential assembly of active ligand

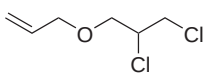

Synthesis of **4-oxa-6,7-dichloro-1-heptene** [265]: 1-allyloxy-2,3-epoxypropane (2.283 g, 20 mmol) was thoroughly mixed with Chlorodiphenylphosphine ($ClPPh_2$) (4.412 g, 20 mmol) and stirred at 25 °C for 40 min. After TLC confirmed complete disappearance of epoxide, 1.2 eq. *N*-chlorosuccinimide (3.204 g, 24 mmol) was slowly added at 10 °C. After complete addition, the reaction mixture was slowly heated to 25 °C and stirred for further 18 hours. Column chromatography (ethyl acetate:hexane = 1:1) of the crude product gave symmetrical *vic*-dihalide 4-oxa-6,7-dichloro-1-heptene (orange oil). 200.15-MHz ^{1}H NMR ($CDCl_3$): δ 3.62 - 3.65 (2H, doublet), 3.72 - 3.74 (2H, doublet), 3.85 - 3.88 (2H, doublet of triplets), 4.62 (1H, multiplet), 5.04 - 5.21 (2H, multiplet), 5.65 - 5.85 (1H, multiplet).

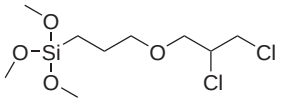

Synthesis of **4-oxa-6,7-dichloro-1-heptyltrimethoxysilane**: 4-oxa-6,7-dichloro-1-heptene (4.05 g, 24.1 mmol), 1.1 eq. trimethoxysilane (3.085g, 26.51 mmol), and 5 mol% Pt catalyst (H_2PtCl_6 (609.2 mg, 1.205 mmol) and 1.2 eq. 1,3,5-triaza-7-phosphaadamantane (PTA) (234.3 mg, 1.446 mmol)) were dissolved in 10 mL toluene. The mixture was stirred under Argon at 80 °C for 18 hours. The reaction mixture was filtered and the product was extracted with hexane. The hexane phase was dried in

vacuum and distilled (125 °C, 67 Pa) to give 5 g colorless 4-oxa-6,7-dichloro-1-heptyltrimethoxysilane oil (Yield = 71.4%). 500.36-MHz ^{1}H NMR (toluene−d_8): δ 0.87 (2H, multiplet), 1.47 (2H, multiplet), 3.51 (9H, singlet), 3.45 (2H, multiplet), 3.5 - 3.7 (4H, multiplet).

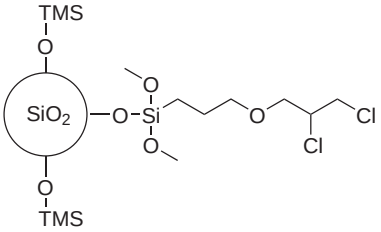

Preparation of **vic-chlorides functionalized silica** [274–276]: Silica Cariact Q-20 was dried in vacuum at 100 °C for 24 hours. 7 g of pretreated silica was suspended in 100 mL toluene. 3.4 g 4-oxa-6,7-dichloro-1-heptyltrimethoxysilane oil was added and the suspension was stirred under reflux for 72 hours. 10 mL distilled water was added and the condensation was further continued for 48 hours. The mixture was cooled to room temperature, filtered, washed three times with 50 mL distilled water and dried at 200 °C in vacuum for 4 hours. The white powder was washed three times with 50 mL dry acetone and dried in vacuum at 50 °C to give g linker functionalized silica. Protection of remaining surface hydroxyl group: at -40 °C, an excess of trimethylchlorosilane (TMSCl) was added to the silica product. The mixture was slowly warmed up to 25 °C and refluxed for 16 hours. The solid is filtered off, washed three times with each 50 mL toluene, ether and THF and dried in vacuum at 50 °C for 24 hours to give 7.425 g silica product. Elemental analysis: 3.9 wt% C 0.9 wt% H 0.32 wt% Cl.

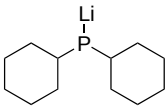

Synthesis of **Lithium dicyclohexyl phosphide**: 3.26 mL tert-Butyllithium solution(1.7 M in pentane, 5.55

mmol)was slowly added into a solution of dicyclohexylphosphine (1g, 5.05 mmol) in 20 mL diethyl ether at 25 °C. The mixture was stirred under Argon for 1 hour at 25 °C. The solid yellow precipitate was filtered off, washed two times with 2 mL diethyl ether, and dried. Lithium dicyclohexyl phosphide emits a strong yellow-green chemo luminescence upon contact with air.

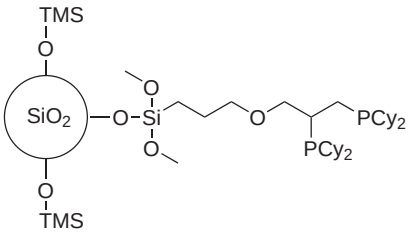

Preparation of **dcpe functionalized silica** Route 1: A solution of $LiPCy_2$ (204.22 mg, 1 mmol) in 30 mL THF was slowly added into g of the vic-chlorides functionalized silica product at -20 °C. The mixture was slowly warmed up to 25 °C and stirred for 72 hours. The mixture was filtered, washed three times with THF and dried in vacuum to give g dcpe functionalized silica.

A.3.2 Route 2: Direct anchoring of active ligand

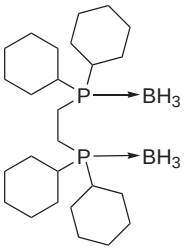

Synthesis of **dcpe·2 BH_3 complex**: Borane dimethylsulfide complex (26 mL, 2 M solution in THF, 1.1 eq.) was added dropwise under argon to a solution of 1,2-bis(dicyclohexylphosphino)ethane (10 g, 23.66 mmol) in 150 mL anhydrous THF at 25 °C. The solution was stirred at 25 °C overnight. Excess of borane dimethylsulfide complex was removed by bubbling argon. The solvent was removed in vacuum and the white solid was recrystallized from toluene and dried in vacuum to give 9.24 g dcpe·2 BH_3 complex (Yield = 86.7%). 500.36-MHz ^{1}H NMR ($CDCl_3$): δ 0 - 0.5 (6H, multiplet), 1.1 - 1.4 (22H, multiplet), 1.6 - 1.9 (26H, multiplet). 125.82-MHz ^{13}C NMR ($CDCl_3$): δ 13.17 - 13.41 (2C, doublet), 25.88 (4C, singlet), 26.59 (4C, singlet), 26.7 - 26.8 (8C, triplet), 26.92 (4C, singlet), 31.5 - 31.76 (4C, doublet). 202.55-MHz ^{31}P NMR ($CDCl_3$): δ 28.42 ($J_{P,B}$ = 64.4 Hz)

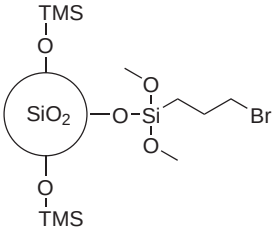

Preparation of **Bromopropyl functionalized silica** [117]: A suspension of 6 g silica (predried at 120 °C in vacuum for 24 hours) and 3.09 mL (3-Bromopropyl)trimethoxysilane (16 mmol) in 100 mL toluene was stirred at 25 °C for 1 hour. A solution of 4.3 mL ethanol, 2 mL H_2O, and 80 μL HCl was added and the mixture was refluxed for 5 hours. After further stirring for 18 hours at 25 °C, the solid was filtered off, washed three times with each 50 mL methanol, pentane, and THF. The solid was dried in vacuum overnight at 50 °C. The Bromopropyl functionalization can be repeated to achieve high Br loading. Elemental

analysis after 1 functionalization step: 3.8 wt% C 1 wt% H 4.8 wt% Br. Elemental analysis after 2 functionalization steps: 8.8 wt% C 2 wt% H 9.5 wt% Br. See also Table 3.5.

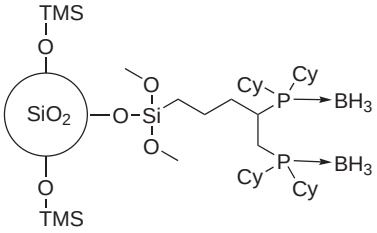

Preparation of **dcpe functionalized silica** Route 2: A solution of dcpe·2 BH_3 (1.667 g, 3.83 mmol) in 14 mL THF was cooled to 0 °C. tBuLi solution (1.7 M in n-pentane, 5.6 mL) was slowly added and the reaction was stirred at 0 °C for 2 hours. The solution was then added into a suspension of bromopropyl functionalized silica prepared before (10 g in 40 mL n-pentane, Br loading = 1.189 mmol Br/g silica). The reaction mixture was further stirred at 0 °C for 72 hours. The light yellow product was filtered off, washed three times with 50 mL THF, and dried in vacuum at 40 °C for 24 hours. Loading of dcpe see also Table 3.6.

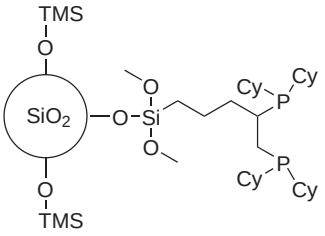

Deprotection of **dcpe functionalized silica** with morpholine: One gram of dcpe functionalized silica prepared in the previous step was suspended in 40 mL morpholin and stirred at 110 °C for 3 hours. The product was filtered off in argon, washed four times with 20 mL THF, and dried in vacuum for 16 hours.

Deprotection of **dcpe functionalized silica** with dabco/toluene: One gram of dcpe functionalized silica (dcpe loading = 0.1388 mmol/g support) prepared in the previous step was suspended in 20 mL toluene. 40 eq. dabco (622.7 mg, 5.552 mmol) and stirred at 100 °C for 96 hours. The product was filtered off in argon, washed four times with 20 mL THF, and dried in vacuum for 16 hours.

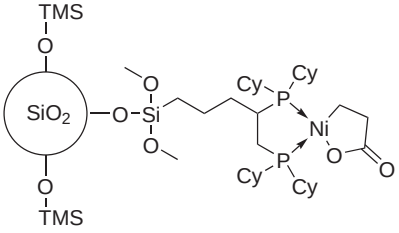

Synthesis of **(dcpe)-Nickelalactone functionalized silica**: One gram of deprotected dcpe functionalized silica prepared in the previous step was suspended in 5 mL THF. 1 eq. (tmeda)-nickelalactone (0.1388 mmol, 34.3 mg) was added into the suspension and the mixture was stirred at 25 °C for 24 hours. The light yellow product was filtered off in argon, washed three times with 10 mL THF, and dried in vacuum for 16 hours.

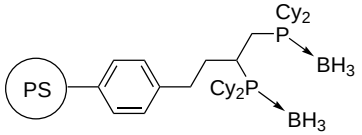

Preparation of **dcpe functionalized polystyrene** Route 2: A solution of

dcpe·2 BH_3 (0.5 g, 1.15 mmol) in 4 mL THF was cooled to 0 °C. tBuLi solution (1.7 M in n-pentane, 1.7 mL) was slowly added and the reaction was stirred at 0 °C for 2 hours. The solution was then added into a suspension of PS03 support (2.5 g in 5 mL n-pentane, Br loading = 0.9 mmol Br/g support, support pre-dried in vacuum at 0 °C overnight). The reaction mixture was further stirred at 0 °C for 72 hours. The light yellow product was filtered off, wash three times with 50 mL THF, and dried in vacuum at 40 °C for 24 hours. Loading of dcpe see also Table 3.6.

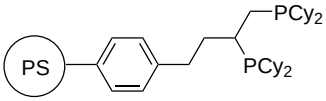

Deprotection of **dcpe functionalized polystyrene** with morpholine: One gram of dcpe functionalized polystyrene prepared in the previous step was suspended in 40 mL morpholin and stirred at 110 °C for 3 hours. The product was filtered off in argon, washed four times with 20 mL THF, and dried in vacuum for 16 hours.

Deprotection of **dcpe functionalized polystyrene** with dabco/toluene: One gram of dcpe functionalized silica (dcpe loading = 0.0759 mmol/g support) prepared in the previous step was suspended in 20 mL toluene. 40 eq. dabco (340.55 mg, 3.036 mmol) and stirred at 100 °C for 96 hours. The product was filtered off in argon, washed four times with 20 mL THF, and dried in vacuum for 16 hours.

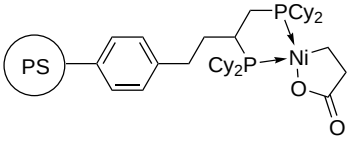

Synthesis of **(dcpe)-Nickelalactone functionalized polystyrene**: One gram of deprotected dcpe functionalized polystyrene prepared in the previous

step was suspended in 5 mL THF. 1 eq. (tmeda)-nickelalactone (0.0759 mmol, 18.7 mg) was added into the suspension and the mixture was stirred at 25 °C for 24 hours. The light yellow product was filtered off in argon, washed three times with 10 mL THF, and dried in vacuum for 2 hours.

A.4 Base

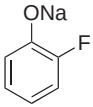

Synthesis of **Sodium 2-fluorophenoxide**: 10 g 2-fluorophenol (89.21 mmol) was mixed with 50 mL THF and stirred in argon at 25 °C. 1.05 eq. NaH (2.248 g, 93.67 mmol) was added in portion so that the temperature during the reaction did not exceed 40 °C. Additional THF can be added to maintain a certain volume of solution. After all NaH was added, the mixture was further stirred at 25 °C for 2 hours and in vacuum dried.

A.4.1 Synthesis of immobilized base via direct anchoring

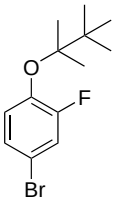

Synthesis of ***tert*-butyldimethylsilyl-2-fluoro-4-bromo-phenolate**: 5.73 g 2-fluoro-4-bromo-phenol (0.03 mol) and 4.22 g Imidazol (0.062 mol) were dissolved in 15 mL *N,N*-dimethylformamide and cooled to 0 °C. A solution of 5.1 g *tert*-butyldimethylsilyl chloride in 5 mL *N,N*-dimethylformamide was added. The reaction mixture was slowly heated up to 25 °C and stirred for further 18 hours. The product was extracted with 40 mL hexane. The organic phase was washed two times with 15 mL brine and dried ($MgSO_4$). After vacuum drying at 40 °C, 7.823 g colorless oil (0.0256 mol, Yield = 85.4 %) can

be isolated.

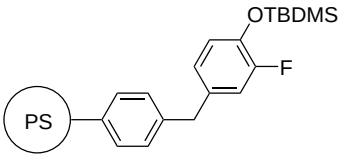

Preparation of **polystyrene immobilized *tert*-butyldimethylsilyl-2-floro-phenolate** via direct anchoring: 87.6 mg Magnesium turnings was suspended in 5 mL THF. A small piece of iodine was added at 0 °C and the suspension was stirred for 10 minutes. A solution of 1 g *tert*-butyldimethylsilyl-2-fluoro-4-bromo-phenolate (3.276 mmol) in 5 mL THF was added and the reaction mixture was stirred at 50 °C for 60 minutes. The Grignard reagent was cooled to 0 °C. 2.34 g PS05 (Br loading: 2.8 mmol/g) was added to the Grignard reagent and the reaction mixture was further stirred at 0 °C for 20 hours. The solid was filtered off, washed three times with 30 mL THF, and dried in vacuum.

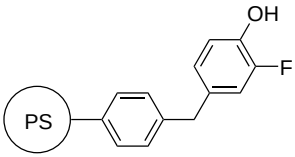

Deprotection of **polystyrene immobilized *tert*-butyldimethylsilyl-2-florophenolate B5** with TBAF: 1 g of immobilized *tert*-butyldimethylsilyl-2-florophenolate was suspended 5 mL THF. A solution of 1 M TBAF in THF (403 mg in 1.5 mL THF) was added and the reaction mixture was stirred at 0 °C for 30 minutes. The reaction mixture was slowly heated up to 25 °C and diluted with 10 mL ethyl acetate. 10 mL 1 M aqueous HCl solution was added and the reaction mixture was stirred for 30 minutes. The solid was filtered off, washed four times with 10 mL ethyl acetate, and dried in vacuum. Elemental analysis B5.1: 61.7 wt% C, 5.9 wt% H, 0.7 wt% F. Elemental analysis

B5.2: 63.9 wt% C, 6.0 wt% H, 0.35 wt% F.

A.4.2 Synthesis of immobilized base via copolymerization

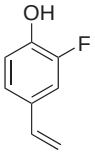

Synthesis of **2-fluoro-4-vinyl-phenol** [277]: 3.82 g 4-bromo-2-fluorophenol (20 mmol) was mixed with 20 mL THF. 1 mol% [1,1-bis(diphenylphosphino)ferrocene]-dichloropalladium(II) ($PdCl_2$dppf) (146.2 mg, 0.2 mmol) was added into the solution and the mixture was stirred at -78 °C for 10 min. 2 eq. of vinylmagnesiumbromide solution (0.7 M in THF, 57.1 mL) was slowly added and the reaction mixture was further stirred at -78 °C for 10 min. The mixture was slowly warmed to 25 °C and refluxed for two hours. After cooling to room temperature, the reaction was slowly quenched with 40 mL 1 M HCl solution. The mixture was further stirred at 25 °C for 30 min. The product was extracted from diethylether and dried followed with recrystallization from hexane/diethylether to give 1.86 g yellow oil (13.45 mmol, yield = 67%). 200.15-MHz ^{1}H NMR ($CDCl_3$): δ 5.0 - 5.05 (1H, doublet), 5.43 - 5.52 (1H, doublet), 6.4 - 6.55 (1H, doublet of doublets), 6.6 - 7.2 (3H, multiplet), 8.12 (1H, singlet).

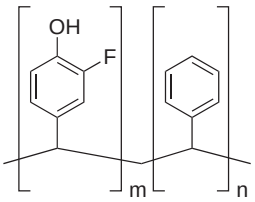

Copolymerization of 2-fluoro-4-vinyl-phenol and styrene B6: 729.05 mg styrene (7 mmol), 414.42 mg 2-fluoro-4-vinyl-phenol (3 mmol), 2.6 mg 1,4-divinylbenzene (0.02 mmol), and 0.05 mmol 2,2-Azobis(2-methylpropionitrile) solution in toluene (0.25 mL, 0.2 M) were mixed with 1 mL chlorobenzene. The mixture was heated up to 60 °C and stirred for 12 hours in Argon. The mixture

was cooled to 25 °C and the polymer was precipitated into methanol. The precipitated methanol was dissolved in THF and reprecipitated into methanol. The purification procedure was repeated twice and the solid polymer product was dried in vacuum to give 300 mg light yellow polymer. Elemental analysis: 85.7 wt% C, 7.2 wt% H, 3.2 wt% F.

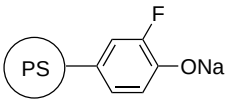

Preparation of **immobilized sodium 2-fluoro-phenolate**: 1g of immobilized 2-fluorophenol prepared in the previous step (OH loading: 1.6844 mmol/g) was suspended in 10 mL THF in argon at 25 °C. 40.42 mg NaH (1.684 mmol) was slowly added into the suspension mixture and stirred for further 15 minutes. The resulting immobilized sodium 2-fluoro-phenolate can be directly used in the catalytic reaction.

Recycling of **immobilized phenol** with aqueous HCl solution: spent base after the acrylate catalytic reaction was suspended in 1 M aqueous HCl solution and stirred for 30 minutes at 25 °C to liberate all hydroxyl groups. The solid was filtrated and washed with ethanol to remove any physisorbed and chemisorbed nickel complex species. The regeneration procedure was repeated five times until the color of spent base is similar to fresh immobilized base (pale yellow beads). The regenerated immobilized base was dried at 50 °C in vacuum overnight to remove all volatile impurities to give immobilized phenol base. The recycled base can finally be reactivated with the same procedure as immobilized sodium 2-fluoro-phenolate described above.

Recycling of **immobilized phenol** with aqueous NaOH solution: spent base after the acrylate catalytic reaction was suspended in 1 M aqueous NaOH solution and stirred for 30 minutes at 25 °C to liberate all hydroxyl groups. The solid was filtrated and washed with ethanol to remove any physisorbed and chemisorbed nickel complex species. The regeneration procedure was repeated five times until the color of spent base is similar to fresh immobilized base (pale yellow beads). At the final step, the immobilized base was suspended again in 1 M aqueous NaOH solution and subsequently dried at 50 °C in vacuum overnight to remove all volatile impurities to give immobilized sodium phenolate base.

Appendix B

List of Chemicals

Table B.1: List of Solvents.

Name	Specification	Supplier
1,4-Dioxane	99.8 %, H_2O < 0.003 %	Sigma Aldrich
Chlorobenzene	99.8 %, H_2O < 0.005 %	Sigma Aldrich
D_2O	99.8 atom % D	Sigma Aldrich
Dichloromethane	99.8 %, H_2O < 0.001 % with 50-150 ppm amylene as stabilizer	Sigma Aldrich
Diethyl ether	99.9 %, H_2O < 0.03 %	Sigma Aldrich
Ethanol	99.8 %, absolute	Sigma Aldrich
Ethyl Acetate	99.8 %	Sigma Aldrich
Hexane	95 %, H_2O < 0.001 %	Sigma Aldrich
Methanol	99.8 %, H_2O < 0.002 %	Sigma Aldrich
N,N-dimethylformamide	99.8 %, H_2O < 0.005 %	Sigma Aldrich
Pentane	99 %, H_2O < 0.002 %	Sigma Aldrich
Tetrahydrofuran	99.5 %, absolute over molecular sieve with 0.025 % 2,6-di-*tert*-butyl-4-methylphenol as stabilizer, H_2O < 0.005 %	Sigma Aldrich
Toluene	99.8 %, H_2O < 0.001 %	Sigma Aldrich

Table B.2: Silica supports used for functionalization.

Properties	**Cariact Q-20C**	**SBA-15** [270]
Average pore diameter [nm]	20	6
Specific surface area [m^2/g]	140	1164
Pore volume [mL/g]	0.8	1.25
-OH content [mmol/g]	no data	2.8
Supplier	Fuji Silysia Chemical	University of Stuttgart

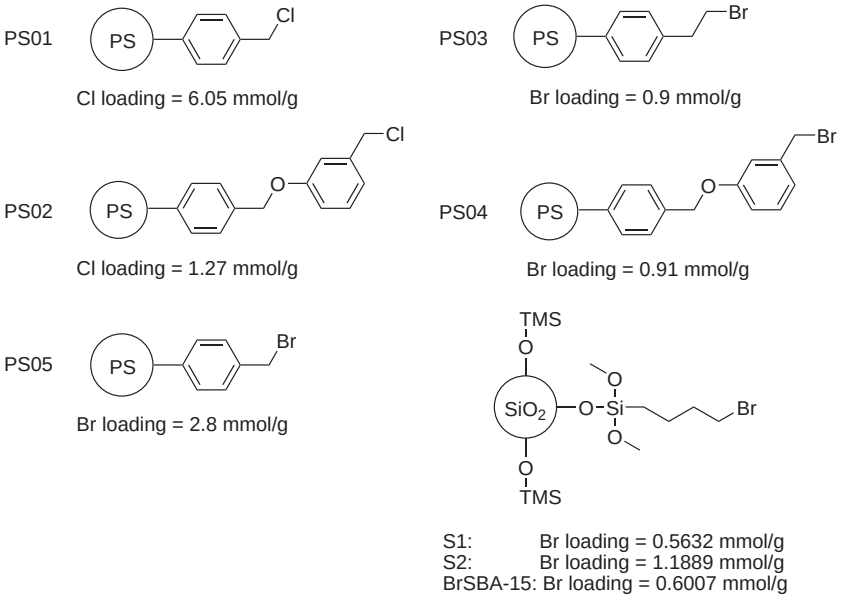

Figure B-1: PS01 - PS05 were purchased from Sigma Aldrich. S1 and S2 supports were prepared from Cariact Q-20C. BrSBA-15 was prepared from SBA-15. For preparation method see also Appendix A.3.2.

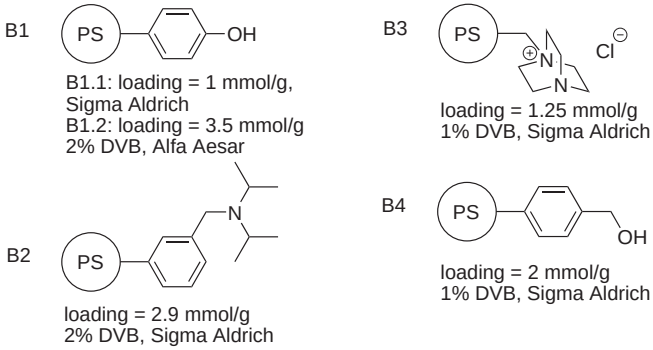

Figure B-2: Commercial immobilized base.

Table B.3: List of Chemicals.

Name	Specification	Supplier
1,1-Bis(diphenylphosphino)ferrocene]dichloropalladium		Sigma Aldrich
1,2-Bis(dicyclohexylphosphino)ethane	99.9 %	Sigma Aldrich
1,3,5-triaza-7-phosphaadamantane	97 %	Sigma Aldrich
1,4-Diazabicyclo[2.2.2]octane	99 %	Sigma Aldrich
1,4-Divinylbenzene	85 %	Sigma Aldrich
1,5,7-Triazabicyclo[4.4.0]dec-5-ene	98 %	Sigma Aldrich
1,8-Diazabicyclo[5.4.0]undec-7-ene	98 %	Sigma Aldrich
1-allyloxy-2,3-epoxypropane	99 %	Sigma Aldrich
1-*tert*-butyl-2,2,4,4,4-pentakis(dimethylamino)-$2\lambda^5,4\lambda^5-catenadi(phosphazene)$	2 M solution in THF	Sigma Aldrich
1-*tert*-butyl-4,4,4-tris(dimethylamino)-2,2-bis[tris(dimethylamino)-phosphoranylidenamino]-$2\lambda^5,4\lambda^5-catenadi(phosphazene)$	0.8 M solution in hexane	Sigma Aldrich
2,2,3,3-d_4-3-(trimethylsilyl)propionic acid	98 atom % D	Sigma Aldrich
2,2-Azobis(2-methylpropionitrile)	0.2 M solution in toluene	Sigma Aldrich

2-fluorophenol	98 %	Sigma Aldrich
2-*tert*-Butylimino-2-diethylamino-1,3-dimethylperhydro-1,3,2-diazaphosphorine	98 %	Sigma Aldrich
(3-Bromopropyl)trimethoxysilane	97 %	Sigma Aldrich
4-(Dimethylamino)pyridine	99 %	Sigma Aldrich
Bis(1,5-cyclooctadiene)nickel(0)	99.9 %	Acros
Borane dimethylsulfide complex	2 M solution in THF	Sigma Aldrich
Calcium hydride	99 %	Sigma Aldrich
Cesium carbonate	99.9 %	Sigma Aldrich
Chlorodiphenylphosphine	96 %	Sigma Aldrich
Chloroplatinic acid hydrate	99.9 %	Sigma Aldrich
Dicyclohexylphosphine	97 %	Sigma Aldrich
Diethylamine	99.5 %	Sigma Aldrich
Hydrochloric acid, 37 %, Sigma Aldrich		
Imidazole	99 %	Sigma Aldrich
Iodine	99.9 %	Sigma Aldrich
Lithium carbonate	99 %	Sigma Aldrich
Lithium chloride	99 %	Sigma Aldrich

Lithium hydride	95 %	Sigma Aldrich
Magnesium	99.95 %, turnings	Sigma Aldrich
Magnesium sulfate	99.5 %, anhydrous	Sigma Aldrich
Morpholin	99.5 %	Sigma Aldrich
N-chlorosuccinimide	98 %	Sigma Aldrich
N,N-diethylaniline	99.5 %	Sigma Aldrich
N,N-dimethylaniline	99.5 %	Sigma Aldrich
N,N,N,N-Tetramethylethylenediamine	99.5 %	Sigma Aldrich
Potassium hydride	30 wt% in mineral oil	Sigma Aldrich
Platinum(0)-1,3-divinyl-1,1,3,3-tetramethyldisiloxane	0.1 M in poly(dimethylsiloxane)	Sigma Aldrich
(*S,S*)-(-)-1,2-Bis(*t*-butylmethylphosphino)benzene	99.9 %	ABCR
Sodium acrylate	97 %	Sigma Aldrich
Sodium bis(trimethylsilyl)amide	1 M solution in THF	Sigma Aldrich
Sodium carbonate	99 %	Sigma Aldrich
Sodium hydride	95 %	Sigma Aldrich
Sodium hydroxide	98 %	Sigma Aldrich
Sodium tetrakis[3,5-bis(trifluoromethyl)phenyl]borate		Sigma Aldrich
Succinic anhydride	99 %	Sigma Aldrich

tert-Butyldimethylsilyl chloride	97 %	Sigma Aldrich
tert-Butyllithium	1.7 M solution in pentane	Sigma Aldrich
tert-butyl-tris(dimethylamino)phosphorane	97 %	Sigma Aldrich
Tetrabutylammonium fluoride hydrate	98 %	Sigma Aldrich
Tetrafluoroboric acid	50 %	Sigma Aldrich
Tetramethylammonium iodide	99 %	Alfa Aesar
Triethylamine	99 %	Sigma Aldrich
Triocthylamine	98 %	Sigma Aldrich
Trimethylchlorosilane	99 %	Sigma Aldrich
Trimethoxysilane	95 %	Sigma Aldrich
Vinylmagnesium bromide	0.7 M solution in THF	Acros

Bibliography

[1] M. Aresta, A. Dibenedetto, *Key Issues in Carbon Dioxide Utilization as a Building Block for Molecular Organic Compounds in the Chemical Industry*, chapter 5, pp. 54–70.

[2] T. Ohara, T. Sato, N. Shimizu, G. Prescher, H. Schwind, O. Weiberg, K. Marten, H. Greim, *Acrylic Acid and Derivatives* in *Ullmann's Encyclopedia of Industrial Chemistry*, Wiley-VCH Verlag GmbH & Co. KGaA, **2000**.

[3] J. Glauser, M. Blagoev, T. Kumamoto, *Acrylic Acid, Acrylate Esters and Superabsorbent Polymers*, SRI Consulting, **2011**.

[4] M. Frank, *Superabsorbents* in *Ullmann's Encyclopedia of Industrial Chemistry*, Wiley-VCH Verlag GmbH & Co. KGaA, **2000**.

[5] F. L. Buchholz, *Superabsorbent Polymers* in *Encyclopedia of Polymer Science and Technology*, John Wiley & Sons, Inc., **2002**.

[6] K. Weissermel, H.-J. Arpe, *Propene Conversion Products* in *Industrial Organic Chemistry*, Wiley-VCH Verlag GmbH, **2007**, pp. 265–310.

[7] W. Reppe, *Neue Entwicklungen auf dem Gebiet der Chemie des Acetylen und Kohlenoxyds*, Springer, **1949**.

[8] W. Bertleff, M. Roeper, X. Sava, *Carbonylation*, Wiley-VCH Verlag GmbH & Co. KGaA, **2000**.

[9] S. Masato, S. Takeshi, K. Chiyoji, *Production of carbonate compound*, **1999**.

[10] M. Tanimoto, N. Hakozaki, *Process for producing acrolein and/or acrylic acid*, **2013**, US Patent 8,415,498. https://www.google.com/patents/US8415498.

[11] N. Fukumoto, T. Nishiguchi, *Catalyst for producing of acrylic acid, method for producing acrylic acid using the catalyst and method for producing water-absorbent resin using the acrylic acid*, **2013**, US Patent 8,507,626. https://www.google.com/patents/US8507626.

[12] J. Macht, A. Karpov, C. Dobner, F. Rosowski, U. Hammon, K. Mueller-Engel, *Mo-, bi- and fe-comprising multimetal oxide compositions*, **2013**, US Patent App. 13/546,546. https://www.google.com/patents/US20130023699.

[13] K. Gehrmann, A. Hauser, W. Lork, K. Sennewald, K. Steil, *Process for isolating acrylic acid from the reaction gases obtained by the oxidation of propylene or a acrolein*, **1973**, US Patent 3,717,675. https://www.google.com/patents/US3717675.

[14] G. Fisher, T. Horlenko, *Acrylic acid purification*, **1979**, US Patent 4,156,633. https://www.google.com/patents/US4156633.

[15] C. Boswell. Acrylate prices drive new manufacturing routes. *ICIS Chemical Business* **2011**.

[16] A. Lundgren, T. Hjertberg, *Ethylene from Renewable Resources* in *Surfactants from Renewable Resources*, M. Kjellin, I. Johansson (Eds.), John Wiley & Sons, Ltd, **2010**, pp. 109–126.

[17] M. Aresta, *Carbon Dioxide: Utilization Options to Reduce its Accumulation in the Atmosphere*, Wiley-VCH Verlag GmbH & Co. KGaA, **2010**, pp. 1–13.

[18] M. R. Kember, A. Buchard, C. K. Williams. Catalysts for CO2/epoxide copolymerisation. *Chem. Commun.* **2011**, *47*, 141–163.

[19] P. Tans, R. Keeling, *Trends in Atmospheric Carbon Dioxide*, **2014**. http://www.esrl.noaa.gov/gmd/ccgg/trends/.

[20] M. T. Ho, G. W. Allinson, D. E. Wiley. Reducing the Cost of CO2 Capture from Flue Gases Using Membrane Technology. *Industrial & Engineering Chemistry Research* **2008**, *47*, 1562–1568.

[21] M. T. Ho, G. W. Allinson, D. E. Wiley. Reducing the Cost of CO2 Capture from Flue Gases Using Pressure Swing Adsorption. *Industrial & Engineering Chemistry Research* **2008**, *47*, 4883–4890.

[22] M. Tuinier, M. van Sint Annaland, G. Kramer, J. Kuipers. Cryogenic capture using dynamically operated packed beds. *Chemical Engineering Science* **2010**, *65*, 114 – 119, 20th International Symposium in Chemical Reaction Engineeringâ€"Green Chemical Reaction Engineering for a Sustainable Future.

[23] D. Singh, E. Croiset, P. Douglas, M. Douglas. Techno-economic study of {CO2} capture from an existing coal-fired power plant: {MEA} scrubbing vs. O2/CO2 recycle combustion. *Energy Conversion and Management* **2003**, *44*, 3073 – 3091.

[24] Z. Liu, C. A. Grande, P. Li, J. Yu, A. E. Rodrigues. Multi-bed Vacuum Pressure Swing Adsorption for carbon dioxide capture from flue gas. *Separation and Purification Technology* **2011**, *81*, 307 – 317.

[25] E. S. Kikkinides, R. T. Yang, S. H. Cho. Concentration and recovery of carbon dioxide from flue gas by pressure swing adsorption. *Industrial & Engineering Chemistry Research* **1993**, *32*, 2714–2720.

[26] B.-K. Na, H. Lee, K.-K. Koo, H. K. Song. Effect of Rinse and Recycle Methods on the Pressure Swing Adsorption Process To Recover CO2 from Power Plant Flue Gas Using Activated Carbon. *Industrial & Engineering Chemistry Research* **2002**, *41*, 5498–5503.

[27] K. T. Chue, J. N. Kim, Y. J. Yoo, S. H. Cho, R. T. Yang. Comparison of Activated Carbon and Zeolite 13X for CO2 Recovery from Flue Gas by Pressure Swing Adsorption. *Industrial & Engineering Chemistry Research* **1995**, *34*, 591–598.

[28] J.-H. Park, H.-T. Beum, J.-N. Kim, S.-H. Cho. Numerical Analysis on the Power Consumption of the PSA Process for Recovering CO2 from Flue Gas. *Industrial & Engineering Chemistry Research* **2002**, *41*, 4122–4131.

[29] A. D. Ebner, J. A. Ritter. State-of-the-art Adsorption and Membrane Separation Processes for Carbon Dioxide Production from Carbon Dioxide Emitting Industries. *Separation Science and Technology* **2009**, *44*, 1273–1421.

[30] D. Ko, R. Siriwardane, L. T. Biegler. Optimization of a Pressure-Swing Adsorption Process Using Zeolite 13X for CO2 Sequestration. *Industrial & Engineering Chemistry Research* **2003**, *42*, 339–348.

[31] P. Xiao, J. Zhang, P. Webley, G. Li, R. Singh, R. Todd. Capture of CO2 from flue gas streams with zeolite 13X byvacuum-pressure swing adsorption. *Adsorption* **2008**, *14*, 575–582.

[32] J. A. McIntyre, A. D. Ebner, J. A. Ritter. Experimental Study of a Dual Reflux Enriching Pressure Swing Adsorption Process for Concentrating Dilute Feed Streams. *Industrial & Engineering Chemistry Research* **2010**, *49*, 1848–1858.

[33] M. Whysall, L. Wagemans, *Very large-scale pressure swing adsorption processes*, **2001**, US Patent 6,210,466. `http://www.google.nl/patents/US6210466`.

[34] J. Chase, M.W., *NIST-JANAF Themochemical Tables, Fourth Edition*, Vol. 9 of *J. Phys. Chem. Ref. Data, Monograph*, **1998**.

[35] T. Sakakura, J.-C. Choi, H. Yasuda. Transformation of Carbon Dioxide. *Chemical Reviews* **2007**, *107*, 2365–2387.

[36] M. Aresta, A. Dibenedetto. Utilisation of CO2 as a chemical feedstock: opportunities and challenges. *Dalton Trans.* **2007**, 2975–2992.

[37] J. H. Meessen, *Urea*, Wiley-VCH Verlag GmbH & Co. KGaA, **2000**.

[38] E. Fiedler, G. Grossmann, D. B. Kersebohm, G. Weiss, C. Witte, *Methanol*, Wiley-VCH Verlag GmbH & Co. KGaA, **2000**.

[39] T. Askgaard, J. Norskov, C. Ovesen, P. Stoltze. A Kinetic Model of Methanol Synthesis. *Journal of Catalysis* **1995**, *156*, 229 – 242.

[40] W.-L. Wong, K.-C. Cheung, P.-H. Chan, Z.-Y. Zhou, K.-H. Lee, K.-Y. Wong. A tricarbonyl rhenium(I) complex with a pendant pyrrolidinium moiety as a robust and recyclable catalyst for chemical fixation of carbon dioxide in ionic liquid. *Chem. Commun.* **2007**, 2175–2177.

[41] J. Wang, J. Wu, N. Tang. Synthesis, characterization of a new bicobalt complex [Co2L2(C2H5OH)2Cl2] and application in cyclic carbonate synthesis. *Inorganic Chemistry Communications* **2007**, *10*, 1493 – 1495.

[42] J. Melendez, M. North, R. Pasquale. Synthesis of Cyclic Carbonates from Atmospheric Pressure Carbon Dioxide Using Exceptionally Active Aluminium(salen) Complexes as Catalysts. *European Journal of Inorganic Chemistry* **2007**, *2007*, 3323–3326.

[43] X.-Y. Dou, J.-Q. Wang, Y. Du, E. Wang, L.-N. He. Guanidinium Salt Functionalized PEG: An Effective and Recyclable Homogeneous Catalyst for the Synthesis of Cyclic Carbonates from CO2 and Epoxides under Solvent-Free Conditions. *Synlett* **2007**, *2007*, 3058–3062.

[44] E.-H. Lee, J.-Y. Ahn, M. M. Dharman, D.-W. Park, S.-W. Park, I. Kim. Synthesis of cyclic carbonate from vinyl cyclohexene

oxide and {CO2} using ionic liquids as catalysts. *Catalysis Today* **2008**, *131*, 130 – 134, Recent advances in catalysis - selected papers from {APCAT} 4 (Singapore, 6-8 December 2006).

[45] T. Sakai, Y. Tsutsumi, T. Ema. Highly active and robust organic-inorganic hybrid catalyst for the synthesis of cyclic carbonates from carbon dioxide and epoxides. *Green Chem.* **2008**, *10*, 337–341.

[46] B. Fan, J. Zhang, R. Li, W. Fan. InSitu Preparation of Functional Heterogeneous Organotin Catalyst Tethered on SBA-15. *Catalysis Letters* **2008**, *121*, 297–302.

[47] Y. Du, L.-N. He, D.-L. Kong. Magnesium-catalyzed synthesis of organic carbonate from 1,2-diol/alcohol and carbon dioxide. *Catalysis Communications* **2008**, *9*, 1754 – 1758.

[48] F. Jutz, J.-D. Grunwaldt, A. Baiker. Mn(III)(salen)-catalyzed synthesis of cyclic organic carbonates from propylene and styrene oxide in supercritical {CO2}. *Journal of Molecular Catalysis A: Chemical* **2008**, *279*, 94 – 103.

[49] T. Sakakura, K. Kohno. The synthesis of organic carbonates from carbon dioxide. *Chem. Commun.* **2009**, 1312–1330.

[50] H. Kolbe. Ueber Synthese der Salicylsäure. *Justus Liebigs Annalen der Chemie* **1860**, *113*, 125–127.

[51] R. Schmitt. Beitrag zur Kenntniss der Kolbe'schen Salicylsäure Synthese. *Journal für Praktische Chemie* **1885**, *31*, 397–411.

[52] A. S. Lindsey, H. Jeskey. The Kolbe-Schmitt Reaction. *Chemical Reviews* **1957**, *57*, 583–620.

[53] O. Boullard, H. Leblanc, B. Besson, *Salicylic Acid*, Wiley-VCH Verlag GmbH & Co. KGaA, **2000**.

[54] C. Song, W. Pan. Tri-reforming of methane: a novel concept for catalytic production of industrially useful synthesis gas with desired H2/CO ratios. *Catalysis Today* **2004**, *98*, 463 – 484.

[55] A. Slagtern, U. Olsbye, R. Blom, I. M. Dahl, H. Fjellvag. In situ {XRD} characterization of LaNiAlO model catalysts for {CO2} reforming of methane. *Applied Catalysis A: General* **1996**, *145*, 375 – 388.

[56] G. Valderrama, M. R. Goldwasser, C. U. de Navarro, J. M. Tatibouët, J. Barrault, C. Batiot-Dupeyrat, F. Martinez. Dry reforming of methane over Ni perovskite type oxides. *Catalysis Today* **2005**, *107â€“108*, 785 – 791, Selected Contributions of the {XIX} Ibero American Catalysis Symposium Selected Contributions of the {XIX} Ibero American Catalysis Symposium.

[57] Y. Hu, E. Ruckenstein. An optimum NiO content in the CO2 reforming of CH4 with NiO/MgO solid solution catalysts. *Catalysis Letters* **1996**, *36*, 145–149.

[58] S. Tsang, J. Claridge, M. Green. Recent advances in the conversion of methane to synthesis gas. *Catalysis Today* **1995**, *23*, 3 – 15, Recent Advances in {C1} Chemistry.

[59] F. Pompeo, N. N. Nichio, M. M. Souza, D. V. Cesar, O. A. Ferretti, M. Schmal. Study of Ni and Pt catalysts supported on a-Al2O3 and ZrO2 applied in methane reforming with {CO2}. *Applied Catalysis A: General* **2007**, *316*, 175 – 183.

[60] C. Gigola, M. Moreno, I. Costilla, M. Sanchez. Characterization of Pd-CeOx interaction on a-Al2O3 support. *Applied Surface Science* **2007**, *254*, 325 – 329, Proceedings of the 13th International Conference on Solid Films and Surfaces {ICSFS} 13.

[61] J. F. Munera, S. Irusta, L. M. Cornaglia, E. A. Lombardo, D. V. Cesar, M. Schmal. Kinetics and reaction pathway of the {CO2} reforming of methane on Rh supported on lanthanum-based solid. *Journal of Catalysis* **2007**, *245*, 25 – 34.

[62] K. Nagaoka, K. Seshan, K.-i. Aika, J. A Lercher. Carbon Deposition during Carbon Dioxide Reforming of Methane-Comparison between Pt/Al2O3 and Pt/ZrO2. *Journal of Catalysis* **2001**, *197*, 34 – 42.

[63] M. M. Barroso Quiroga, A. E. Castro Luna. Kinetic Analysis of Rate Data for Dry Reforming of Methane. *Industrial & Engineering Chemistry Research* **2007**, *46*, 5265–5270.

[64] M. C. J. Bradford, M. A. Vannice. CO2 Reforming of CH4. *Catalysis Reviews* **1999**, *41*, 1–42.

[65] J. R. Rostrup-Nielsen, J. Sehested, *Hydrogen and synthesis gas by steam- and {C02} reforming*, Vol. 47 of *Advances in Catalysis*, Academic Press, **2002**, pp. 65 – 139.

[66] K. Klier, *Methanol Synthesis*, Vol. 31 of *Advances in Catalysis*, H. P. D.D. Eley, P. B. Weisz (Eds.), Academic Press, **1982**, pp. 243 – 313.

[67] J. Bart, R. Sneeden. Copper-zinc oxide-alumina methanol catalysts revisited. *Catalysis Today* **1987**, *2*, 1 – 124.

[68] M. Bowker, R. Hadden, H. Houghton, J. Hyland, K. Waugh. The mechanism of methanol synthesis on copper/zinc oxide/alumina catalysts. *Journal of Catalysis* **1988**, *109*, 263 – 273.

[69] M. A. McNeil, C. J. Schack, R. G. Rinker. Methanol synthesis from hydrogen, carbon monoxide and carbon dioxide over a CuO/ZnO/Al2O3 catalyst: II. Development of a phenomenological rate expression. *Applied Catalysis* **1989**, *50*, 265 – 285.

[70] C. Song, *Introduction to Hydrogen and Syngas Production and Purification Technologies*, John Wiley & Sons, Inc., **2009**, pp. 1–13.

[71] K. Weissermel, H.-J. Arpe, *Basic Products of Industrial Syntheses* in *Industrial Organic Chemistry*, Wiley-VCH Verlag GmbH, **2007**, pp. 13–58.

[72] K. H. Büchel, H.-H. Moretto, P. Woditsch, *Primary Inorganic Materials* in *Industrial Inorganic Chemistry*, Wiley-VCH Verlag GmbH, **2007**, pp. 1–185.

[73] N. M. Laurendeau. Heterogeneous kinetics of coal char gasification and combustion. *Progress in Energy and Combustion Science* **1978**, *4*, 221 – 270.

[74] X. Li, J. Grace, C. Lim, A. Watkinson, H. Chen, J. Kim. Biomass gasification in a circulating fluidized bed. *Biomass and Bioenergy* **2004**, *26*, 171 – 193.

[75] D. Möst, H. Perlwitz. Prospects of gas supply until 2020 in Europe and its relevance for the power sector in the context of emission trading. *Energy* **2009**, *34*, 1510 – 1522, 11th Conference on Process Integration, Modelling and Optimisation for Energy Saving and Pollution Reduction.

[76] H.-H. Rogner. An Assessment of World Hydrocarbon Resources. *Annual Review of Energy and the Environment* **1997**, *22*, 217–262.

[77] R. F. Aguilera. The future of the European natural gas market: A quantitative assessment. *Energy* **2010**, *35*, 3332 – 3339.

[78] K. Liu, G. D. Deluga, A. Bitsch-Larsen, L. D. Schmidt, L. Zhang, *Catalytic Partial Oxidation and Autothermal Reforming*, John Wiley & Sons, Inc., **2009**, pp. 127–155.

[79] R. Reimert, F. Marschner, H.-J. Renner, W. Boll, E. Supp, M. Brejc, W. Liebner, G. Schaub, *Gas Production, 2. Processes*, Wiley-VCH Verlag GmbH & Co. KGaA, **2000**.

[80] W. Boll, G. Hochgesand, C. Higman, E. Supp, P. Kalteier, W.-D. Müller, M. Kriebel, H. Schlichting, H. Tanz, *Gas Production, 3. Gas Treating*, Wiley-VCH Verlag GmbH & Co. KGaA, **2000**.

[81] I. Wender. Reactions of synthesis gas. *Fuel Processing Technology* **1996**, *48*, 189 – 297, Reactions of synthesis gas.

[82] A. P. E. York, T.-c. Xiao, M. L. H. Green, J. B. Claridge. Methane Oxyforming for Synthesis Gas Production. *Catalysis Reviews* **2007**, *49*, 511–560.

[83] V. Subramani, P. Sharma, L. Zhang, K. Liu, *Catalytic Steam Reforming Technology for the Production of Hydrogen and Syngas*, John Wiley & Sons, Inc., **2009**, pp. 14–126.

[84] K. Liu, Z. Cui, T. H. Fletcher, *Coal Gasification*, John Wiley & Sons, Inc., **2009**, pp. 156–218.

[85] X. D. Peng, A. W. Wang, B. A. Toseland, P. J. A. Tijm. Single-Step Syngas-to-Dimethyl Ether Processes for Optimal Productivity, Minimal Emissions, and Natural Gas-Derived Syngas. *Industrial & Engineering Chemistry Research* **1999**, *38*, 4381–4388.

[86] D. H. Gibson. Carbon dioxide coordination chemistry: metal complexes and surface-bound species. What relationships? *Coordination Chemistry Reviews* **1999**, *185-186*, 335 – 355.

[87] I. Tommasi, F. Sorrentino. Utilisation of 1,3-dialkylimidazolium-2-carboxylates as CO2-carriers in the presence of Na+ and K+: application in the synthesis of carboxylates, monomethylcarbonate anions and halogen-free ionic liquids. *Tetrahedron Letters* **2005**, *46*, 2141 – 2145.

[88] H. Hoberg, Y. Peres, C. Krüger, Y.-H. Tsay. A 1-Oxa-2-nickela-5-cyclopentanone from Ethene and Carbon Dioxide: Preparation, Structure, and Reactivity. *Angew. Chem., Int. Ed. Engl.* **1987**, *26*, 771–773.

[89] H. Hoberg, K. Sümmermann, A. Milchereit. CC-Verknüpfung von Alkenen mit Isocyanaten an Ni0-Komplexen - eine neue Synthese von Acrylsäureamiden. *Angew. Chem.* **1985**, *97*, 321–321.

[90] D. Walther, E. Dinjus, J. Sieler, L. Andersen, O. Lindqvist. Aktivierung von kohlendioxid an Übergangsmetallzentren: Metallaringschluss mit dicyclopentadien am elektronenreichen nickel(0)-komplexrumpf als topo- und stereoselektive reaktion. *Journal of Organometallic Chemistry* **1984**, *276*, 99 – 107.

[91] H. Hoberg, D. Schaefer. Nickel(0)-induzierte C - C-verknüpfung zwischen kohlendioxid und ethylen sowie mono- oder di-substituierten alkenen. *J. Organomet. Chem.* **1983**, *251*, C51 – C53.

[92] S. A. Cohen, J. E. Bercaw. Titanacycles derived form reductive coupling of nitriles, alkynes, acetaldehyde, and carbon dioxide with bis(pentamethylcyclopentadienyl)(ethylene)titanium(II). *Organometallics* **1985**, *4*, 1006–1014.

[93] H. Hoberg, K. Jenni, K. Angermund, C. Krüger. CC-Linkages of Ethene with CO2 on an Iron(0) Complex-Synthesis and Crystal Structure Analysis of [(PEt3)2Fe(C2H4)2]. *Angewandte Chemie International Edition in English* **1987**, *26*, 153–155.

[94] R. Alvarez, E. Carmona, D. J. Cole-Hamilton, A. Galindo, E. Gutierrez-Puebla, A. Monge, M. L. Poveda, C. Ruiz. Formation of acrylic acid derivatives from the reaction of carbon dioxide with ethylene complexes of molybdenum and tungsten. *Journal of the American Chemical Society* **1985**, *107*, 5529–5531.

[95] M. Aresta, E. Quaranta. Synthesis, characterization and reactivity of [Rh(bpy)(C2H4)Cl]. A study on the reaction with {C1} molecules (CH2O, CO2) and NaBPh4. *Journal of Organometallic Chemistry* **1993**, *463*, 215 – 221.

[96] Y. Inoue, Y. Itoh, H. Kazama, H. Hashimoto. Reaction of Dialkyl-substituted Alkynes with Carbon Dioxide Catalyzed by Nickel(0) Complexes. Incorporation of Carbon Dioxide in Alkyne Dimers and Novel Cyclotrimerization of the Alkynes. *Bulletin of the Chemical Society of Japan* **1980**, *53*, 3329–3333.

[97] G. Burkhart, H. Hoberg. Oxanickelacyclopentene Derivatives from Nickel(0), Carbon Dioxide, and Alkynes. *Angewandte Chemie International Edition in English* **1982**, *21*, 76–76.

[98] D. Walther, E. Dinjus. Aktivierung von Kohlendioxid an Übergangsmetallzentren; Die Metallaringschlussreaktion zwischen

Kohlendioxid und 1,3-Dienen am elektronenreichen Nickel (0)-Komplexrumpf. *Zeitschrift f ür Chemie* **1982**, *22*, 228–229.

[99] H. Hoberg, B. Oster. Nickel(0)-induzierte C-C-verknüpfung zwischen 1,2-dienen und kohlendioxid. *Journal of Organometallic Chemistry* **1984**, *266*, 321 – 326.

[100] D. Walther, H. Schönberg, E. Dinjus, J. Sieler. Aktivierung von Kohlendioxid an Übergangsmetallzentren: Selektive Cooligomerisation mit Hexin(-3) durch das Katalysatorsystem Acetonitril/Trialkylphosphan/Nickel(0) und Struktur eines Nickel(0)-Komplexes mit side-on gebundenem Acetonitril. *Journal of Organometallic Chemistry* **1987**, *334*, 377 – 388.

[101] Y. Kishimoto, I. Mitani. Solvent-Free Synthesis of 2-Pyrones from Alkynes and Carbon Dioxide Catalyzed by Ni(1,5-cyclooctadiene)2/Trialkylphosphine Catalysts. *Synlett* **2005**, *2005*, 2141–2146.

[102] T. Tsuda, H. Yasukawa, K. Komori. Nickel(0)-Catalyzed Cycloaddition Copolymerization of Ether Diynes with Carbon Dioxide to Poly(2-pyrone)s. *Macromolecules* **1995**, *28*, 1356–1359.

[103] T. Tsuda, H. Yasukawa, H. Hokazono, Y. Kitaike. Nickel(0)-Catalyzed Cycloaddition Copolymerization of Cyclic Diynes with Carbon Dioxide to Ladder Poly(2-pyrone)s. *Macromolecules* **1995**, *28*, 1312–1315.

[104] T. Tsuda, O. Ooi, K. Maruta. Nickel(0)-catalyzed cycloaddition copolymerization involving two diynes and carbon dioxide to poly(2-pyrone). *Macromolecules* **1993**, *26*, 4840–4844.

[105] T. Tsuda, K. Maruta. Nickel(0)-catalyzed alternating copolymerization of 2,6-octadiyne with carbon dioxide to poly(2-pyrone). *Macromolecules* **1992**, *25*, 6102–6105.

[106] T. Tsuda, Y. Kitaike, O. Ooi. Nickel(0)-catalyzed 1:1 cycloaddition copolymerization of 1,3- and 1,4-di(2-hexynyl)benzenes

with carbon dioxide to poly(2-pyrones). *Macromolecules* **1993**, *26*, 4956–4960.

[107] A. Döhring, P. Jolly. The palladium catalyzed reaction of carbon dioxide with allene. *Tetrahedron Letters* **1980**, *21*, 3021 – 3024.

[108] Y. Sasaki, Y. Inoue, H. Hashimoto. Reaction of carbon dioxide with butadiene catalysed by palladium complexes. Synthesis of 2-ethylidenehept-5-en-4-olide. *J. Chem. Soc., Chem. Commun.* **1976**, 605–606.

[109] A. Musco, C. Perego, V. Tartiari. Telomerization reactions of butadiene and {CO2} catalyzed by phosphine Pd(0) complexes: (E)-2-ethylidenehept-6-en-5-olide and octadienyl esters of 2-ethylidenehepta-4,6-dienoic acid. *Inorganica Chimica Acta* **1978**, *28*, L147 – L148.

[110] A. Behr, K.-D. Juszak, W. Keim. Synthese von 2-Ethyliden-6-hepten-5-olid. *Synthesis* **1983**, *1983*, 574–574.

[111] P. Braunstein, D. Matt, D. Nobel. Carbon dioxide activation and catalytic lactone synthesis by telomerization of butadiene and carbon dioxide. *Journal of the American Chemical Society* **1988**, *110*, 3207–3212.

[112] P. Braunstein, D. Matt, D. Nobel. Reactions of carbon dioxide with carbon-carbon bond formation catalyzed by transition-metal complexes. *Chemical Reviews* **1988**, *88*, 747–764.

[113] A. Behr, K.-D. Juszak. Palladium-catalyzed reaction of butadiene and carbon dioxide. *Journal of Organometallic Chemistry* **1983**, *255*, 263 – 268.

[114] A. Musco. Co-oligomerization of butadiene and carbon dioxide catalysed by tertiary phosphine-palladium complexes. *J. Chem. Soc., Perkin Trans. 1* **1980**, 693–698.

[115] A. Behr, M. Heite. Telomerization of Carbon Dioxide and 1,3-Butadiene: Process Development in a Miniplant. *Chemical Engineering & Technology* **2000**, *23*, 952–955.

[116] N. Holzhey, S. Pitter, E. Dinjus. Die heterogen katalysierte Co-oligomerisation von 1,3-Butadien und {CO2} mit immobilisierten Palladiumkomplexen. *Journal of Organometallic Chemistry* **1997**, *541*, 243 – 248.

[117] N. Holzhey, S. Pitter. Selective co-oligomerization of 1,3-butadiene and carbon dioxide with immobilzed catalysts. *Journal of Molecular Catalysis A: Chemical* **1999**, *146*, 25 – 36.

[118] P. Albano, M. Aresta. Some catalytic properties of Rh(diphos)(n-BPh4). *Journal of Organometallic Chemistry* **1980**, *190*, 243 – 246.

[119] A. Behr, E. Herdtweck, W. A. Herrmann, W. Keim, W. Kipshagen. C-C coupling of activated alkanes with carbon dioxide by iridium and rhodium complexes: synthesis and crystallographic characterization of [H2Ir(PMe3)4]+[O2CCH(CN2]-. *J. Chem. Soc., Chem. Commun.* **1986**, 1262–1263.

[120] M. Aresta, A. Dibenedetto, I. Papai, G. Schubert. Unprecedented formal "2+2" addition of allene to {CO2} promoted by [RhCl(C2H4)(PiPr3)]2: direct synthesis of the four membered lactone a-methylene-b-oxiethanone. The intermediacy of [RhH2Cl(PiPr3)]2: theoretical aspects and experiments. *Inorganica Chimica Acta* **2002**, *334*, 294 – 300, Protagonists in Chemistry: Andrew A. Wojcicki.

[121] Y. Yoshida, S. Ishii, M. Watanabe, T. Yamashita. Novel Synthesis of Carbamate Ester from Carbon Dioxide, Amines, and Alkyl Halides. *Bulletin of the Chemical Society of Japan* **1989**, *62*, 1534–1538.

[122] M. Aresta, D. Ballivet-Tkatchenko, D. B. Dell'Amico, M. C. Bonnet, D. Boschi, F. Calderazzo, R. Faure, L. Labella, F. Marchetti. Isolation and structural determination of two derivatives of the elusive carbamic acid. *Chem. Commun.* **2000**, 1099–1100.

[123] W. McGhee, D. Riley, K. Christ, Y. Pan, B. Parnas. Carbon Dioxide as a Phosgene Replacement: Synthesis and Mechanistic Studies of Urethanes from Amines, CO2, and Alkyl Chlorides. *The Journal of Organic Chemistry* **1995**, *60*, 2820–2830.

[124] W. D. McGhee, Y. Pan, D. P. Riley. Highly selective generation of urethanes from amines, carbon dioxide and alkyl chlorides. *J. Chem. Soc., Chem. Commun.* **1994**, 699–700.

[125] M. Shi, Y.-M. Shen. The Reaction of Amines with Benzyl Halides under CO2 Atmosphere. *Helvetica Chimica Acta* **2001**, *84*, 3357–3365.

[126] E. R. Perez, M. Odnicki da Silva, V. C. Costa, U. P. Rodrigues-Filho, D. W. Franco. Efficient and clean synthesis of N-alkyl carbamates by transcarboxylation and O-alkylation coupled reactions using a DBU-CO2 zwitterionic carbamic complex in aprotic polar media. *Tetrahedron Letters* **2002**, *43*, 4091 – 4093.

[127] R. Srivastava, M. Manju, D. Srinivas, P. Ratnasamy. Phosgene-Free Synthesis of Carbamates over Zeolite-Based Catalysts. *Catalysis Letters* **2004**, *97*, 41–47.

[128] R. Srivastava, D. Srinivas, P. Ratnasamy. Zeolite-based organic-inorganic hybrid catalysts for phosgene-free and solvent-free synthesis of cyclic carbonates and carbamates at mild conditions utilizing {CO2}. *Applied Catalysis A: General* **2005**, *289*, 128 – 134.

[129] R. Srivastava, D. Srinivas, P. Ratnasamy. Syntheses of polycarbonate and polyurethane precursors utilizing {CO2} over highly efficient, solid as-synthesized MCM-41 catalyst. *Tetrahedron Letters* **2006**, *47*, 4213 – 4217.

[130] R. Srivastava, D. Srinivas, P. Ratnasamy. {CO2} activation and synthesis of cyclic carbonates and alkyl/aryl carbamates over adenine-modified Ti-SBA-15 solid catalysts. *Journal of Catalysis* **2005**, *233*, 1 – 15.

[131] R. Srivastava, D. Srinivas, P. Ratnasamy. Sites for {CO2} activation over amine-functionalized mesoporous Ti(Al)-SBA-15 catalysts. *Microporous and Mesoporous Materials* **2006**, *90*, 314 – 326, Dedicated to the late Denise Barthomeuf, George Kokotailo and Sergey P. Zhdanov in appreciation of their outstanding contributions to zeolite science.

[132] M. Aresta, E. Quaranta. Role of the macrocyclic polyether in the synthesis of N-alkylcarbamate esters from primary amines, {CO2} and alkyl halides in the presence of crown-ethers. *Tetrahedron* **1992**, *48*, 1515 – 1530.

[133] H. Sugimoto, S. Inoue. Copolymerization of carbon dioxide and epoxide. *Journal of Polymer Science Part A: Polymer Chemistry* **2004**, *42*, 5561–5573.

[134] H. Sugimoto, H. Ohtsuka, S. Inoue, *Alternating Copolymerization of Carbon Dioxide and Epoxide [1]. Aluminum Schiff Base Complex - Quartenary Ammonium Salt Systems as Novel Initiators.* in *Carbon Dioxide Utilization for Global Sustainability Proceedings of 7ththe International Conference on Carbon Dioxide Utilization*, Vol. 153 of *Studies in Surface Science and Catalysis*, J.-S. C. Sang-Eon Park, K.-W. Lee (Eds.), Elsevier, **2004**, pp. 243 – 246.

[135] M. Super, E. Berluche, C. Costello, E. Beckman. Copolymerization of 1,2-Epoxycyclohexane and Carbon Dioxide Using Carbon Dioxide as Both Reactant and Solvent. *Macromolecules* **1997**, *30*, 368–372.

[136] D. J. Darensbourg, M. W. Holtcamp. Catalysts for the reactions of epoxides and carbon dioxide. *Coordination Chemistry Reviews* **1996**, *153*, 155 – 174.

[137] D. J. Darensbourg, M. S. Zimmer. Copolymerization and Terpolymerization of CO2 and Epoxides Using a Soluble Zinc Crotonate Catalyst Precursor. *Macromolecules* **1999**, *32*, 2137–2140.

[138] W.-L. Dai, B. Jin, S.-L. Luo, S.-F. Yin, X.-B. Luo, C.-T. Au. Cross-linked polymer grafted with functionalized ionic liquid as reusable and efficient catalyst for the cycloaddition of carbon dioxide to epoxides. *Journal of {CO2} Utilization* **2013**, *3-4*, 7 – 13.

[139] W.-L. Dai, B. Jin, S.-L. Luo, X.-B. Luo, X.-M. Tu, C.-T. Au. Functionalized phosphonium-based ionic liquids as efficient catalysts for the synthesis of cyclic carbonate from expoxides and carbon dioxide. *Applied Catalysis A: General* **2014**, *470*, 183 – 188.

[140] D. Wei-Li, J. Bi, L. Sheng-Lian, L. Xu-Biao, T. Xin-Man, A. Chak-Tong. Polymers anchored with carboxyl-functionalized di-cation ionic liquids as efficient catalysts for the fixation of CO2 into cyclic carbonates. *Catal. Sci. Technol.* **2014**, *4*, 556–562.

[141] J. Sun, S.-i. Fujita, M. Arai. Development in the green synthesis of cyclic carbonate from carbon dioxide using ionic liquids. *Journal of Organometallic Chemistry* **2005**, *690*, 3490 – 3497, Ionic Liquids Organometallic Chemistry in Ionic Liquids.

[142] Y. N. Lim, C. Lee, H.-Y. Jang. Metal-Free Synthesis of Cyclic and Acyclic Carbonates from CO2 and Alcohols. *European Journal of Organic Chemistry* **2014**.

[143] T. Sakai, N. Kihara, T. Endo. Polymer Reaction of Epoxide and Carbon Dioxide. Incorporation of Carbon Dioxide into Epoxide Polymers. *Macromolecules* **1995**, *28*, 4701–4706.

[144] H. Yasuda, L.-N. He, T. Sakakura, C. Hu. Efficient synthesis of cyclic carbonate from carbon dioxide catalyzed by polyoxometalate: the remarkable effects of metal substitution. *Journal of Catalysis* **2005**, *233*, 119 – 122.

[145] Y. Du, F. Cai, D.-L. Kong, L.-N. He. Organic solvent-free process for the synthesis of propylene carbonate from supercritical carbon dioxide and propylene oxide catalyzed by insoluble ion exchange resins. *Green Chem.* **2005**, *7*, 518–523.

[146] Y. Li, X.-q. Zhao, Y.-j. Wang. Synthesis of dimethyl carbonate from methanol, propylene oxide and carbon dioxide over KOH/4A molecular sieve catalyst. *Applied Catalysis A: General* **2005**, *279*, 205 – 208.

[147] T. Yano, H. Matsui, T. Koike, H. Ishiguro, H. Fujihara, M. Yoshihara, T. Maeshima. Magnesium oxide-catalysed reaction of carbon dioxide with an epoxide with retention of stereochemistry. *Chem. Commun.* **1997**, 1129–1130.

[148] M. Aresta, A. Dibenedetto, L. Gianfrate, C. Pastore. Nb(V) compounds as epoxides carboxylation catalysts: the role of the solvent. *Journal of Molecular Catalysis A: Chemical* **2003**, *204-205*, 245 – 252, In honour of Prof. R. Ugo on the occasion of his 65th. Birthday.

[149] K. Yamaguchi, K. Ebitani, T. Yoshida, H. Yoshida, K. Kaneda. Mg-Al Mixed Oxides as Highly Active Acid-Base Catalysts for Cycloaddition of Carbon Dioxide to Epoxides. *Journal of the American Chemical Society* **1999**, *121*, 4526–4527.

[150] G. Gattow, W. Behrendt. Methyl Hydrogen Carbonate. *Angewandte Chemie International Edition in English* **1972**, *11*, 534–535.

[151] A. Dibenedetto, M. Aresta, P. Giannoccaro, C. Pastore, I. PÃ¡pai, G. Schubert. On the Existence of the Elusive Monomethyl Ester of Carbonic Acid [CH3OC(O)OH] at 300 K: 1H- and 13C NMR Measurements and DFT Calculations. *European Journal of Inorganic Chemistry* **2006**, *2006*, 908–913.

[152] T. Sakakura, Y. Saito, M. Okano, J.-C. Choi, T. Sako. Selective Conversion of Carbon Dioxide to Dimethyl Carbonate by Molecular Catalysis. *The Journal of Organic Chemistry* **1998**, *63*, 7095–7096.

[153] D. Ballivet-Tkatchenko, S. Chambrey, R. Keiski, R. Ligabue, L. Plasseraud, P. Richard, H. Turunen. Direct synthesis of

dimethyl carbonate with supercritical carbon dioxide: Characterization of a key organotin oxide intermediate. *Catalysis Today* **2006**, *115*, 80 – 87, Proceedings of the 8th International Conference on Carbon Dioxide Utilization Dedicated to Professor Michele Aresta.

[154] D. Ballivet-Tkatchenko, T. Jerphagnon, R. Ligabue, L. Plasseraud, D. Poinsot. The role of distannoxanes in the synthesis of dimethyl carbonate from carbon dioxide. *Applied Catalysis A: General* **2003**, *255*, 93 – 99, Catalytic Conversion of Carbon Dioxide.

[155] D. Chaturvedi, A. Kumar, S. Ray. An Efficient One Pot Synthesis of Carbamate Esters through Alcoholic Tosylates. *Synthetic Communications* **2002**, *32*, 2651–2655.

[156] D. Chaturvedi, S. Ray. An Efficient, One-Pot, Basic Resin Catalyzed Novel Synthesis of Carbamate Esters Through Alcoholic Tosylates. *Letters in Organic Chemistry* **2005**, *2*, 742–744.

[157] M. Aresta, A. Dibenedetto, C. Pastore. Synthesis and Characterization of Nb(OR)4[OC(O)OR] (R = Me, Et, Allyl) and Their Reaction with the Parent Alcohol To Afford Organic Carbonates. *Inorganic Chemistry* **2003**, *42*, 3256–3261.

[158] M. Aresta, A. Dibenedetto, C. Pastore, I. Papai, G. Schubert. Reaction mechanism of the direct carboxylation of methanol to dimethylcarbonate: experimental and theoretical studies. *Topics in Catalysis* **2006**, *40*, 71–81.

[159] Y. Ikeda, M. Asadullah, K. Fujimoto, K. Tomishige. Structure of the Active Sites on H3PO4/ZrO2 Catalysts for Dimethyl Carbonate Synthesis from Methanol and Carbon Dioxide. *The Journal of Physical Chemistry B* **2001**, *105*, 10653–10658.

[160] B. M. Bhanage, S.-i. Fujita, Y. Ikushima, M. Arai. Synthesis of dimethyl carbonate and glycols from carbon dioxide, epoxides, and methanol using heterogeneous basic metal oxide catalysts

with high activity and selectivity. *Applied Catalysis A: General* **2001**, *219*, 259 – 266.

[161] V. Eta, P. Maeki-Arvela, E. Salminen, T. Salmi, D. Y. Murzin, J.-P. Mikkola. The Effect of Alkoxide Ionic Liquids on the Synthesis of Dimethyl Carbonate from CO2 and Methanol over ZrO2â€“MgO. *Catalysis Letters* **2011**, *141*, 1254–1261.

[162] H. Wang, S. Shi, Y. Wang, C.-s. Li, J. Sun. CaF2-doped ZrO2: A base catalyst for synthesis of dimethyl carbonate. *Journal of Shanghai University (English Edition)* **2010**, *14*, 281–285.

[163] C. Jiang, Y. Guo, C. Wang, C. Hu, Y. Wu, E. Wang. Synthesis of dimethyl carbonate from methanol and carbon dioxide in the presence of polyoxometalates under mild conditions. *Applied Catalysis A: General* **2003**, *256*, 203 – 212, Heteropoly Acids Special Issue.

[164] K. T. Jung, A. T. Bell. An in Situ Infrared Study of Dimethyl Carbonate Synthesis from Carbon Dioxide and Methanol over Zirconia. *Journal of Catalysis* **2001**, *204*, 339 – 347.

[165] K. Tomishige, Y. Furusawa, Y. Ikeda, M. Asadullah, K. Fujimoto. CeO2-ZrO2 Solid Solution Catalyst for Selective Synthesis of Dimethyl Carbonate from Methanol and Carbon Dioxide. *Catalysis Letters* **2001**, *76*, 71–74.

[166] Y. Yoshida, Y. Arai, S. Kado, K. Kunimori, K. Tomishige. Direct synthesis of organic carbonates from the reaction of {CO2} with methanol and ethanol over CeO2 catalysts. *Catalysis Today* **2006**, *115*, 95 – 101, Proceedings of the 8th International Conference on Carbon Dioxide Utilization Dedicated to Professor Michele Aresta.

[167] K. Tomishige, K. Kunimori. Catalytic and direct synthesis of dimethyl carbonate starting from carbon dioxide using CeO2-ZrO2 solid solution heterogeneous catalyst: effect of {H2O} removal from the reaction system. *Applied Catalysis A: General* **2002**, *237*, 103 – 109.

[168] J. Hagen, *Introduction*, Wiley-VCH Verlag GmbH & Co. KGaA, **2006**, pp. 1–14.

[169] B. Cornils, W. A. Herrmann, *Introduction*, Wiley-VCH Verlag GmbH, **2008**, pp. 1–27.

[170] J. Hagen, *Homogeneously Catalyzed Industrial Processes*, Wiley-VCH Verlag GmbH & Co. KGaA, **2006**, pp. 59–82.

[171] F. Calderazzo, D. Carmona, M. Catellani, H. Brintzinger, M. G. Clerici, C. Dwyer, G. Fink, J. Fraile, A. Haynes, P. Howard, G. Morris, L. A. Oro, M. Ricci, G. Strukul, G. Sunley, *Metal-catalysis in Industrial Organic Processes*, G. P. Chiusoli, P. M. Maitlis (Eds.), The Royal Society of Chemistry, **2007**.

[172] T. V. RajanBabu, N. Nomura, J. Jin, B. Radetich, H. Park, M. Nandi. Hydrovinylation and Related Reactions: New Protocols and Control Elements in Search of Greater Synthetic Efficiency and Selectivity. *Chemistry - A European Journal* **1999**, *5*, 1963 –1968.

[173] *Dimerisation-Polymerisation* in *Metal Catalysed Reactions in Ionic Liquids*, Vol. 29 of *Catalysis by Metal Complexes*, Springer Netherlands, **2005**, pp. 167–186.

[174] R. Mason, **1972**.

[175] R. Mason, **1972**.

[176] A. Shamiri, M. H. Chakrabarti, S. Jahan, M. A. Hussain, W. Kaminsky, P. V. Aravind, W. A. Yehye. The Influence of Ziegler-Natta and Metallocene Catalysts on Polyolefin Structure, Properties, and Processing Ability. *Materials* **2014**, *7*, 5069–5108.

[177] C. M. Thomas, G. Suss-Fink. Ligand effects in the rhodium-catalyzed carbonylation of methanol. *Coordination Chemistry Reviews* **2003**, *243*, 125 – 142.

[178] P. W. Leeuwen, *Rhodium Catalysed Hydroformylation* in *Homogeneous Catalysis*, Springer Netherlands, **2004**, pp. 139–174.

[179] T. V. B. Rajanbabu, *Hydrocyanation of Alkenes and Alkynes*, John Wiley & Sons, Inc., **2004**.

[180] A. P. V. Gothlich, M. Tensfeldt, H. Rothfuss, M. E. Tauchert, D. Haap, F. Rominger, P. Hofmann. Novel Chelating Phosphonite Ligands: Syntheses, Structures, and Nickel-Catalyzed Hydrocyanation of Olefins. *Organometallics* **2008**, *27*, 2189–2200.

[181] S.-I. Murahashi, N. Komiya, *Oxidation Reactions*, Wiley-VCH Verlag GmbH & Co. KGaA, **2005**, pp. 53–93.

[182] W. Zhou, B. Hu, Z. Liu. Metallo-deuteroporphyrin complexes derived from heme: A homogeneous catalyst for cyclohexane oxidation. *Applied Catalysis A: General* **2009**, *358*, 136 – 140.

[183] M. Ghanta, B. Subramaniam, H.-J. Lee, D. H. Busch. Highly selective homogeneous ethylene epoxidation in gas (ethylene)-expanded liquid: Transport and kinetic studies. *AIChE Journal* **2013**, *59*, 180–187.

[184] J. H. Grate, D. R. Hamm, S. Mahajan. Palladium and phosphomolybdovanadate catalyzed olefin oxidation to carbonyls. *Molecular Engineering* **1993**, *3*, 205–229.

[185] J. Reimers, *Process for production of 3,4-dichlorobutene-1*, **2011**.

[186] T. Rostovshchikova, M. Korobov, D. Pankratov, G. Yurkov, S. Gubin. Catalytic conversions of chloroolefins over iron oxide nanoparticles 2. Isomerization of dichlorobutenes over iron oxide nanoparticles stabilized on the surface of ultradispersed poly(tetrafluoroethylene). *Russian Chemical Bulletin* **2005**, *54*, 1425–1432.

[187] K. Weiss, M. Thuering, *ROMP and ADMET Polymerisation with Carbyne Complexes as Catalysts* in *Ring Opening Metathesis*

Polymerisation and Related Chemistry, Vol. 56 of *NATO Science Series*, E. Khosravi, T. Szymanska-Buzar (Eds.), Springer Netherlands, **2002**, pp. 321–330.

[188] H.-U. Blaser, A. Indolese, A. Schnyder. Applied homogeneous cataysis by organometallic complexes. *Current Science* **2000**, *78*, 1336.

[189] R. H. Crabtree, *General Properties of Organometallic Complexes*, John Wiley & Sons, Inc., **2005**, pp. 29–52.

[190] A. Behr, *Catalysis, Homogeneous*, Wiley-VCH Verlag GmbH & Co. KGaA, **2000**.

[191] S. Bhaduri, D. Mukesh, *Basic Chemical Concepts*, John Wiley & Sons, Inc., **2002**, pp. 13–36.

[192] J. A. Dumesic, G. W. Huber, M. Boudart, *Principles of Heterogeneous Catalysis* in *Handbook of Heterogeneous Catalysis*, G. Ertl, H. Knözinger, F. Schüth, J. Weitkamp (Eds.), Wiley-VCH Verlag GmbH & Co. KGaA, **2008**.

[193] H. S. Taylor. A Theory of the Catalytic Surface. *Proceedings of the Royal Society of London. Series A* **1925**, *108*, 105–111.

[194] H. Hoberg, Y. Peres, C. Krüger, Y.-H. Tsay. Ein 1-Oxa-2-nickela-5-cyclopentanon aus Ethen und Kohlendioxid; Herstellung, Struktur und Reaktivitä. *Angew. Chem.* **1987**, *99*, 799–800.

[195] R. Fischer, D. Walther, G. Braunlich, B. Undeutsch, W. Ludwig, H. Bandmann. Nickelalactone als Synthesebausteine: Sonochemische und Bimetallaktivierung der Kreuzkopplungsreaktion mit Alkyl-halogeniden. *J. Organomet. Chem.* **1992**, *427*, 395 – 407.

[196] C. M. Williams, J. B. Johnson, T. Rovis. Nickel-Catalyzed Reductive Carboxylation of Styrenes Using CO2. *J. Am. Chem. Soc.* **2008**, *130*, 14936–14937.

[197] C. Bruckmeier, M. W. Lehenmeier, R. Reichardt, S. Vagin, B. Rieger. Formation of Methyl Acrylate from CO2 and Ethylene via Methylation of Nickelalactones. *Organometallics* **2010**, *29*, 2199–2202.

[198] S. Y. T. Lee, M. Cokoja, M. Drees, Y. Li, J. Mink, W. A. Herrmann, F. E. Kühn. Transformation of Nickelalactones to Methyl Acrylate: On the Way to a Catalytic Conversion of Carbon Dioxide. *ChemSusChem* **2011**, *4*, 1275–1279.

[199] R. Fischer, B. Nestler, H. Schütz. Zur Synthese und Charakterisierung von N,N'-Tetramethylethylendiaminnickelacyclopropionat. *Zeitschrift für anorganische und allgemeine Chemie* **1989**, *577*, 111–114.

[200] R. Fischer, J. Langer, A. Malassa, D. Walther, H. Gorls, G. Vaughan. A key step in the formation of acrylic acid from CO2 and ethylene: the transformation of a nickelalactone into a nickel-acrylate complex. *Chem. Commun.* **2006**, *0*, 2510–2512.

[201] S. Y. T. Lee, A. A. Ghani, V. D'Elia, M. Cokoja, W. A. Herrmann, J.-M. Basset, F. E. Kuhn. Liberation of methyl acrylate from metallalactone complexes via M-O ring opening (M = Ni, Pd) with methylation agents. *New J. Chem.* **2013**, *37*, 3512–3517.

[202] D. Jin, T. J. Schmeier, P. G. Williard, N. Hazari, W. H. Bernskoetter. Lewis Acid Induced ß-Elimination from a Nickelalactone: Efforts toward Acrylate Production from CO2 and Ethylene. *Organometallics* **2013**, *32*, 2152–2159.

[203] M. L. Lejkowski, R. Lindner, T. Kageyama, G. Bódizs, P. N. Plessow, I. B. Müller, A. Schäfer, F. Rominger, P. Hofmann, C. Futter, S. A. Schunk, M. Limbach. The First Catalytic Synthesis of an Acrylate from CO2 and an Alkene - A Rational Approach. *Chem.–Eur. J.* **2012**, *18*, 14017–14025.

[204] M. Limbach, J. Miller, S. Schunk, *Preparation of ethylenically unsaturated carboxylic salts by carboxylation of alkenes*,

2011, US Patent App. 13/040,043. http://www.google.com/patents/US20110218359.

[205] W. Huiyuan, X. Songlin. Separation of tert-Butyl Alcohol-Water Mixtures by a Heterogeneous Azeotropic Batch Distillation Process. *Chemical Engineering & Technology* **2006**, *29*, 113–118.

[206] W. Behrendt, G. Gattow, M. Dräger. Über Chalkogenolate. LXI. Untersuchungen über Halbester der Kohlensäure. 1. Darstellung und Eigenschaften von Monomethyl- und Monoäthylcarbonaten. *Zeitschrift für anorganische und allgemeine Chemie* **1973**, *397*, 237–246.

[207] E. F. V. Scriven, R. Murugan, *Pyridine and Pyridine Derivatives*, John Wiley & Sons, Inc., **2000**.

[208] M. B. Smith, *Chapter 2 - Acids, Bases and Functional Group Exchange Reactions* in *Organic Synthesis (Third Edition) third edition ed.*, M. B. Smith (Ed.), Academic Press, Oxford, **2010**, pp. 77 – 217.

[209] Y. Kondo, *Phosphazene: Preparation, Reaction and Catalytic Role*, John Wiley & Sons, Ltd, **2009**, pp. 145–185.

[210] N. Huguet, I. Jevtovikj, A. Gordillo, M. L. Lejkowski, R. Lindner, M. Bru, A. Y. Khalimon, F. Rominger, S. A. Schunk, P. Hofmann, M. Limbach. Nickel catalyzed carboxylation of olefins with CO2: one-pot synthesis of a,b-unsaturated carboxylic acid salts. *Angewandte Communications* **2014**.

[211] C. Villiers, J.-P. Dognon, R. Pollet, P. Thuery, M. Ephritikhine. An Isolated CO2 Adduct of a Nitrogen Base: Crystal and Electronic Structures. *Angewandte Chemie International Edition* **2010**, *49*, 3465–3468.

[212] http://www.dguv.de/ifa/Gefahrstoffdatenbanken/GESTIS-Stoffdatenbank/index-2.jsp.

[213] D. Jin, P. G. Williard, N. Hazari, W. H. Bernskoetter. Effect of Sodium Cation on Metallacycle b-Hydride Elimination in CO2-Ethylene Coupling to Acrylates. *Chemistry - A European Journal* **2014**, n/a–n/a.

[214] A. Ganguly, *Fundamentals of Inorganic Chemistry for competitive examinations*, S. Sharma, K. S. Khosa (Eds.), Pearson, **2012**.

[215] J. Langer, R. Fischer, H. Görls, D. Walther. A new set of nickelacyclic carboxylates ("nickelalactones") containing pyridine as supporting ligand: synthesis, structures and application in C-C- and C-S- linkage reactions. *Journal of Organometallic Chemistry* **2004**, *689*, 2952 – 2962.

[216] G. Dümbgen, D. Neubauer. Grosstechnische Herstellung von Oxo-Alkoholen aus Propylen in der BASF. *Chemie Ingenieur Technik* **1969**, *41*, 974–980.

[217] G. V. Smith, F. Notheisz, *Chapter 7 - Immobilized Homogeneous Catalysts* in *Heterogeneous Catalysis in Organic Chemistry*, Academic Press, San Diego, **1999**, pp. 247 – 289.

[218] A. P. Wight, M. E. Davis. Design and Preparation of Organic - Inorganic Hybrid Catalysts. *Chemical Reviews* **2002**, *102*, 3589–3614, PMID: 12371895.

[219] P. McMorn, G. J. Hutchings. Heterogeneous enantioselective catalysts: strategies for the immobilisation of homogeneous catalysts. *Chem. Soc. Rev.* **2004**, *33*, 108–122.

[220] Z. Wang, K. Ding, Y. Uozumi, *An Overview of Heterogeneous Asymmetric Catalysis* in *Handbook of Asymmetric Heterogeneous Catalysis*, K. Ding, Y. Uozumi (Eds.), Wiley-VCH Verlag GmbH & Co. KGaA, **2008**, pp. 1–24.

[221] R. Anwander, *Immobilization of Molecular Catalysts* in *Handbook of Heterogeneous Catalysis*, G. Ertl, H. Knözinger, F. Schüth, J. Weitkamp (Eds.), Wiley-VCH Verlag GmbH & Co. KGaA, **2008**.

[222] F. Averseng, M. Vennat, M. Che, *Grafting and Anchoring of Transition Metal Complexes to Inorganic Oxides* in *Handbook of Heterogeneous Catalysis*, G. Ertl, H. Knözinger, F. Schüth, J. Weitkamp (Eds.), Wiley-VCH Verlag GmbH & Co. KGaA, **2008**.

[223] R. B. Merrifield. Solid Phase Peptide Synthesis. I. The Synthesis of a Tetrapeptide. *Journal of the American Chemical Society* **1963**, *85*, 2149–2154.

[224] L. Nicole, C. Boissiere, D. Grosso, A. Quach, C. Sanchez. Mesostructured hybrid organic-inorganic thin films. *J. Mater. Chem.* **2005**, *15*, 3598–3627.

[225] P. C. Angelome, G. J. d. A. A. Soler-Illia. Ordered mesoporous hybrid thin films with double organic functionality and mixed oxide framework. *J. Mater. Chem.* **2005**, *15*, 3903–3912.

[226] N. Liu, R. A. Assink, B. Smarsly, C. J. Brinker. Synthesis and characterization of highly ordered functional mesoporous silica thin films with positively chargeable -NH2 groups. *Chem. Commun.* **2003**, 1146–1147.

[227] C. Sanchez, C. Boissiere, D. Grosso, C. Laberty, L. Nicole. Design, Synthesis, and Properties of Inorganic and Hybrid Thin Films Having Periodically Organized Nanoporosityâ€. *Chemistry of Materials* **2008**, *20*, 682–737.

[228] A. Vinu, K. Z. Hossain, K. Ariga. Recent Advances in Functionalization of Mesoporous Silica. *Journal of Nanoscience and Nanotechnology* **2005**, *5*, 347–371.

[229] C. Merckle, J. Blümel. Bifunctional Phosphines Immobilized on Inorganic Oxides. *Chemistry of Materials* **2001**, *13*, 3617–3623.

[230] M. E. McGovern, K. M. R. Kallury, M. Thompson. Role of Solvent on the Silanization of Glass with Octadecyltrichlorosilane. *Langmuir* **1994**, *10*, 3607–3614.

[231] E. T. Vandenberg, L. Bertilsson, B. Liedberg, K. Uvdal, R. Erlandsson, H. Elwing, I. Lundstrom. Structure of 3-aminopropyl triethoxy silane on silicon oxide. *Journal of Colloid and Interface Science* **1991**, *147*, 103 – 118.

[232] K. K. Sharma, A. Anan, R. P. Buckley, W. Ouellette, T. Asefa. Toward Efficient Nanoporous Catalysts: Controlling Site-Isolation and Concentration of Grafted Catalytic Sites on Nanoporous Materials with Solvents and Colorimetric Elucidation of Their Site-Isolation. *Journal of the American Chemical Society* **2008**, *130*, 218–228.

[233] S. L. Brandow, M.-S. Chen, R. Aggarwal, C. S. Dulcey, J. M. Calvert, W. J. Dressick. Fabrication of Patterned Amine Reactivity Templates Using 4-Chloromethylphenylsiloxane Self-Assembled Monolayer Films. *Langmuir* **1999**, *15*, 5429–5432.

[234] E. Asenath Smith, W. Chen. How To Prevent the Loss of Surface Functionality Derived from Aminosilanes. *Langmuir* **2008**, *24*, 12405–12409.

[235] R. M. Pasternack, S. Rivillon Amy, Y. J. Chabal. Attachment of 3-(Aminopropyl)triethoxysilane on Silicon Oxide Surfaces: Dependence on Solution Temperature. *Langmuir* **2008**, *24*, 12963–12971.

[236] J. A. Howarter, J. P. Youngblood. Optimization of Silica Silanization by 3-Aminopropyltriethoxysilane. *Langmuir* **2006**, *22*, 11142–11147.

[237] F. Zhang, M. P. Srinivasan. Self-Assembled Molecular Films of Aminosilanes and Their Immobilization Capacities. *Langmuir* **2004**, *20*, 2309–2314.

[238] J. Kim, G. J. Holinga, G. A. Somorjai. Curing Induced Structural Reorganization and Enhanced Reactivity of Amino-Terminated Organic Thin Films on Solid Substrates: Observations of Two Types of Chemically and Structurally Unique Amino Groups on the Surface. *Langmuir* **2011**, *27*, 5171–5175.

[239] E. Metwalli, D. Haines, O. Becker, S. Conzone, C. Pantano. Surface characterizations of mono-, di-, and tri-aminosilane treated glass substrates. *Journal of Colloid and Interface Science* **2006**, *298*, 825 – 831.

[240] J. H. Moon, J. W. Shin, S. Y. Kim, J. W. Park. Formation of Uniform Aminosilane Thin Layers: An Imine Formation To Measure Relative Surface Density of the Amine Group. *Langmuir* **1996**, *12*, 4621–4624.

[241] T. G. Waddell, D. E. Leyden, M. T. DeBello. The nature of organosilane to silica-surface bonding. *Journal of the American Chemical Society* **1981**, *103*, 5303–5307.

[242] M. Zhu, M. Z. Lerum, W. Chen. How To Prepare Reproducible, Homogeneous, and Hydrolytically Stable Aminosilane-Derived Layers on Silica. *Langmuir* **2012**, *28*, 416–423.

[243] J. Blümel. Linkers and catalysts immobilized on oxide supports: New insights by solid-state {NMR} spectroscopy. *Coordination Chemistry Reviews* **2008**, *252*, 2410 – 2423, Applications of {NMR} to Inorganic and Organometallic Chemistry.

[244] S. Gauthier, J. P. Aime, T. Bouhacina, A. J. Attias, B. Desbat. Study of Grafted Silane Molecules on Silica Surface with an Atomic Force Microscope. *Langmuir* **1996**, *12*, 5126–5137.

[245] D. F. Siqueira Petri, G. Wenz, P. Schunk, T. Schimmel. An Improved Method for the Assembly of Amino-Terminated Monolayers on SiO2 and the Vapor Deposition of Gold Layers. *Langmuir* **1999**, *15*, 4520–4523.

[246] J. Blümel. Reactions of Ethoxysilanes with Silica: A Solid-State NMR Study. *Journal of the American Chemical Society* **1995**, *117*, 2112–2113.

[247] A. Simon, T. Cohen-Bouhacina, M. Porte, J. P. Aime, C. Baquey. Study of Two Grafting Methods for Obtaining a 3-Aminopropyltriethoxysilane Monolayer on Silica Surface. *Journal of Colloid and Interface Science* **2002**, *251*, 278 – 283.

[248] J. Goodwin, R. Harbron, P. Reynolds. Functionalization of colloidal silica and silica surfaces via silylation reactions. *Colloid and Polymer Science* **1990**, *268*, 766–777.

[249] M. B. Smith, J. March, *March's Advanced Organic Chemistry: Reactions, Mechanisms, and Structure*, John Wiley & Sons, Inc., **2007**.

[250] M. Ohff, J. Holz, M. Quirmbach, A. Börner. Borane Complexes of Trivalent Organophosphorus Compounds. Versatile Precursors for the Synthesis of Chiral Phosphine Ligands for Asymmetric Catalysis. *Synthesis* **1998**, *1998*, 1391–1415.

[251] T. Imamoto, T. Kusumoto, N. Suzuki, K. Sato. Phosphine oxides and lithium aluminum hydride-sodium borohydride-cerium(III) chloride: synthesis and reactions of phosphine-boranes. *Journal of the American Chemical Society* **1985**, *107*, 5301–5303.

[252] J. M. Brunel, B. Faure, M. Maffei. Phosphane-boranes: synthesis, characterization and synthetic applications. *Coordination Chemistry Reviews* **1998**, *178-180*, 665 – 698.

[253] B. Carboni, L. Monnier. Recent developments in the chemistry of amine- and phosphine-boranes. *Tetrahedron* **1999**, *55*, 1197 – 1248.

[254] A. H. Cowley, M. C. Damasco. Donor-acceptor bond in phosphine-borane complexes. *Journal of the American Chemical Society* **1971**, *93*, 6815–6821.

[255] H. Brisset, Y. Gourdel, P. Pellon, M. Le Corre. Phosphine-borane complexes; direct use in asymmetric catalysis. *Tetrahedron Letters* **1993**, *34*, 4523 – 4526, The International Journal for the Rapid Publication of Preliminary.

[256] H. Yang, N. Lugan, R. Mathieu. Study of the Bonding Properties of the New Ligands C5H3N(2-R')(6-CH2PPhR) toward Rhodium(I). Evidence for a Dynamic Competition for Bonding between O- and N-Donor Centers When R = o-Anisyl, R' = Me. *Organometallics* **1997**, *16*, 2089–2095.

[257] B. Mohr, D. M. Lynn, R. H. Grubbs. Synthesis of Water-Soluble, Aliphatic Phosphines and Their Application to Well-Defined Ruthenium Olefin Metathesis Catalysts. *Organometallics* **1996**, *15*, 4317–4325.

[258] G. Knuhl, P. Sennhenn, G. Helmchen. New chiral [small beta]-phosphinocarboxylic acids and their application in palladium-catalysed asymmetric allylic alkylations. *J. Chem. Soc., Chem. Commun.* **1995**, 1845–1846.

[259] L. McKinstry, J. J. Overberg, C. Soubra-Ghaoui, D. S. Walsh, K. A. Robins, T. T. Toto, J. L. Toto. Acid Mediated Phosphine-Borane Decomplexation:A Model for Characterizing Short-Lived Intermediates with Experimental and ab Initio NMR Data. *The Journal of Organic Chemistry* **2000**, *65*, 2261–2263.

[260] D. Moulin, S. Bago, C. Bauduin, C. Darcel, S. Juge. Asymmetric synthesis of P-stereogenic o-hydroxyaryl-phosphine (borane) and phosphine-phosphinite ligands. *Tetrahedron: Asymmetry* **2000**, *11*, 3939 – 3956.

[261] M. Schröder, K. Nozaki, T. Hiyama. A Novel Mild Deprotection Method for Phosphine-Boranes. *Bulletin of the Chemical Society of Japan* **2004**, *77*, 1931–1932.

[262] M. Van Overschelde, E. Vervecken, S. G. Modha, S. Cogen, E. Van der Eycken, J. Van der Eycken. Catalyst-free alcoholysis of phosphane-boranes: a smooth, cheap, and efficient deprotection procedure. *Tetrahedron* **2009**, *65*, 6410 – 6415.

[263] A. Pelter, R. Rosser, S. Mills. New uses for old complexes. Hydroborations involving nitrogen and phosphorus complexes of borane. *J. Chem. Soc., Chem. Commun.* **1981**, 1014–1015.

[264] N. Iranpoor, H. Firouzabadi, R. Azadi, F. Ebrahimzadeh. Regioselective synthesis of vic-halo alcohols and symmetrical or unsymmetrical vic-dihalides from epoxides using triphenylphosphine Â– N-halo imides. *Canadian Journal of Chemistry* **2006**, *84*, 69–75.

[265] G. Aghapour, A. Afzali. Solvent-Free, Efficient, and High Regioselective Conversion of Epoxides to Symmetrical and Unsymmetrical vic-Dihalides Using Chlorodiphenylphosphine and N-Halosuccinimides. *Phosphorus, Sulfur, and Silicon and the Related Elements* **2011**, *186*, 598–605.

[266] A. J. Chalk, J. F. Harrod. Homogeneous Catalysis. II. The Mechanism of the Hydrosilation of Olefins Catalyzed by Group VIII Metal Complexes1. *Journal of the American Chemical Society* **1965**, *87*, 16–21.

[267] S. Acharya, *Synthesis and Catalytic Applications of Platinum(II) and Palladium(II)-PTA and DAPTA Complexes*, Ph.D. thesis, University of Missouri - Saint Louis, **2012**.

[268] F. Guillier, D. Orain, M. Bradley. Linkers and Cleavage Strategies in Solid-Phase Organic Synthesis and Combinatorial Chemistry. *Chemical Reviews* **2000**, *100*, 2091–2158, PMID: 11749285.

[269] A. J. Wills, S. Balasubramanian. Recent developments in linker design and application. *Current Opinion in Chemical Biology* **2003**, *7*, 346 – 352.

[270] J. Frey, Y. S. Ooi, B. Thomas, V. R. R. Marthala, A. Bressel, T. Schölkopf, T. Schleid, M. Hunger. Vanadium phosphates on mesoporous supports: model catalysts for solid-state {NMR} studies of the selective oxidation of n-butane. *Solid State Nuclear Magnetic Resonance* **2009**, *35*, 130 – 137, <ce:title>Solid State {NMR} in Catalysis</ce:title> <ce:subtitle>NMR in Catalysis</ce:subtitle>.

[271] F. J. Fananas, R. Sanz, *Intramolecular Carbolithiation Reactions*, John Wiley & Sons, Ltd, **2006**, pp. 295–379.

[272] D. C. Graham, C. Mitchell, M. I. Bruce, G. F. Metha, J. H. Bowie, M. A. Buntine. Production of Acrylic Acid through Nickel-Mediated Coupling of Ethylene and Carbon Dioxide A DFT Study. *Organometallics* **2007**, *26*, 6784–6792.

[273] E. Klemm, *Heterogeneous Catalysis Engineering* in *Workshop Catalysis Stuttgart 2011*.

[274] G. Liu, B. Huang, M. Cai. Synthesis of a novel fumed silica-supported poly-4-oxa-6,7-bis(diphenylarsino)heptylsiloxane platinum complex and its catalytic behavior in the hydrosilylation of olefins with triethoxysilane. *Reactive and Functional Polymers* **2007**, *67*, 294 – 298.

[275] M. Cai, Y. Huang, H. Zhao, C. Song. Silica-supported bidentate arsine palladium(0) complex: a highly active and stereoselective catalyst for arylation of conjugated alkenes. *Journal of Organometallic Chemistry* **2003**, *682*, 20 – 25.

[276] X. Lu, Z. Zhong, Y. Chen. Synthesis of Poly-4-oxa-6,7-bis(diphenylphosphino) heptyl Siloxanc Rhodium Complex and Its Catalytic Hydrosilylation Behavior. *Chemical Journal of Chinese Universities* **1990**, *11*, 561 (3 pages).

[277] N. A. Bumagin, E. V. Luzikova. Palladium catalyzed cross-coupling reaction of Grignard reagents with halobenzoic acids, halophenols and haloanilines. *Journal of Organometallic Chemistry* **1997**, *532*, 271 – 273.